Long-term morphodynamics of the Western Scheldt estuary

A modeling and data study

Dam, G.

DOI
10.4233/uuid:5d2645cc-68dd-4465-8777-a93772b5d5ea

Publication date
2025

Document Version
Final published version

Citation (APA)
Dam, G. (2025). *Long-term morphodynamics of the Western Scheldt estuary: A modeling and data study*. [Dissertation (TU Delft), Delft University of Technology]. https://doi.org/10.4233/uuid:5d2645cc-68dd-4465-8777-a93772b5d5ea

Important note
To cite this publication, please use the final published version (if applicable).
Please check the document version above.

Long-Term Morphodynamics of the Western Scheldt Estuary

A Modelling and Data Study

Gerard Dam

LONG-TERM MORPHODYNAMICS OF THE WESTERN SCHELDT ESTUARY

A MODELING AND DATA STUDY

Gerrit Dam

LONG-TERM MORPHODYNAMICS OF THE WESTERN SCHELDT ESTUARY

A MODELING AND DATA STUDY

DISSERTATION

for the purpose of obtaining the degree of doctor
at Delft University of Technology
by the authority of the Rector Magnificus Prof.dr.ir. T.H.J.J. van der Hagen,
chair of the Board for Doctorates
and
in fulfilment of the requirement of the Rector of IHE Delft
Institute for Water Education, Prof.dr. E.J. Moors,
to be defended in public on
Friday 4 April, 2025 at 12:30 hours

by

Gerrit DAM

This dissertation has been approved by the (co)promotor

Composition of the doctoral committee:

Rector Magnificus TU Delft	chairperson
Rector IHE Delft	vice-chairperson
Prof.dr.ir. J.A. Roelvink	TU Delft / IHE-Delft, promotor
Dr.ir. M. van der Wegen	IHE Delft, copromotor
Independent members:	
Prof.dr.ir. Z.B. Wang	TU Delft
Prof.dr. C. Winter	Kiel University, Germany
Prof.dr. S. Temmerman	University of Antwerp, Belgium
Prof.dr. M.G. Kleinhans	Utrecht University
Prof.dr. I.I. Popescu	TU Delft / IHE-Delft, reserve member

Cover image: Historical chart of the Scheldt of 1654, Visscher (Public domain)

Published by IHE Delft Institute for Water Education
www.un-ihe.org
ISBN 978-90-73445-72-7

A river cuts through rock, not because of its power, but because of its persistence

Jim Watkins

CONTENTS

SUMMARY

ESTUARIES are coastal environments where freshwater from the river and saltwater from the sea come together. Tidal flats in estuaries provide feeding grounds, breeding sites, and shelter for numerous species, including migratory birds and fish. They are known for their high productivity and support diverse food webs, thereby contributing to the overall biodiversity and ecological functioning of estuaries. Further, estuaries are important navigational gateways to ports and rivers further upstream, whereby maintenance dredging of the navigational channel is often required to maintain port access.

Estuaries face several future challenges. One significant challenge is the morphological changes occurring in estuaries due to both natural and human-induced factors. Human activities, such as land reclamation and dredging, can exacerbate morphological changes, leading to potential habitat loss and potential disruptions to estuarine ecosystems. Another challenge is projected sea-level rise, which poses a threat to tidal flats and estuaries as a whole. Rising sea levels can result in the inundation and submergence of tidal flats, leading to habitat loss and a decline in biodiversity. The effects of such changes can last decades.

To address these challenges, integrated and sustainable management strategies are necessary. A tool that can help understand consequences of natural and human impacts is a process-based morphological model. These morphodynamic models have become widely available in the last decades and are usually applied for shorter time time periods, yet it is not known if these models give useful long-term predictions.

The main objective of this research is to investigate the model skill of a process-based numerical morphological model (FINEL2d) over a centennial time scale. This research shows that a morphological hindcast of the Western Scheldt for the period 1860-1970 shows excellent skill after 110 years. This is attributed to the self-organization of the morphological system which is reproduced correctly by the numerical model. On time scales exceeding decades, the interaction between the major tidal forcing and the confinement of the estuary overrules other uncertainties. Both measured and modeled bathymetries reflect a trend of decreasing energy dissipation, less morphodynamic activity, and thus a more stable morphology over time, albeit that the estuarine adaptation time is long (approximately centuries).

Further, the long-term behaviour of sand in mud in the Western Scheldt is investigated.

Bathymetric data of the Western Scheldt from 1860 onwards was combined with a three-dimensional underground model ('GeoTop') in order to create a long-term sediment budget study. Since data of an underground model was taken into account a differentiation between sand and mud could be made. This research showed that the estuary narrowed and deepened, while the estuary exported sand (1.5-2.5 million m^3/year) and imported mud (0.5-1.5 million m^3/year) over the 1860-1955 period. The eroded sand originated from the eroding channels in the seaward part of the estuary and transported towards the sea, the inner part and in the side branches. The imported marine mud deposited permanently in shoal areas and the side branches, which were gradually reclaimed over time. Being able to differentiate between sand and mud in this sediment budget study it is shown that different sediment types can react differently to the same forcing conditions and even can have opposite net directions. By extending the morphodynamic sand model with a sand-mud module, a reproduction of the sand and mud fluxes are carried out for the 1860-1955 period, explaining the underlying transport mechanisms of sand and mud.

The model results show that the observed sand export and mud import of the 1860-1955 period is reproduced by the sand-mud model. Furthermore, the observed erosion/ sedimentation pattern is (still) skillfully reproduced, together with the observed increase in tidal range over this period. The marine mud import in the mouth of the estuary changes into a mud export when the simulation is extended to 250 years. Accommodation space for mud settlement becomes exhausted over long timescales and fluvial mud will be flushed to the sea. Since mud settlement becomes less over time mud concentrations are increasing according to model results. The observed sand export is reproduced by the morphodynamic sand-mud model. Even tough the tide is hydrodynamically flood dominant, there is a clear sand export due to longer ebb times. Extending the model simulation towards 250 years the sand export eventually approaches zero. These model results indicate that the estuary evolves towards an equilibrium state. These model simulations are performed without dredging of the navigational channel that really took off in the 1970's. In reality, the import/export of sediment during more recent periods (after 1970's) are likely to have been affected by anthropogenic influences.

Land reclamations from 1860 onwards have increased the tidal range with about 10 cm over a 100-year period according to model scenarios. Reclamation was mostly done after the secondary basin had already filled inn with sediment. Closing off an area with dikes (the actual reclamation) was merely strengthening of an ongoing trend. However, the final state of the estuary is different over long timescales. Noticeable is that the sediment amount in the total estuary differs due to reclamation. Reclamation leads to less tidal prism (i.e., the amount of water that enters and empties the estuary each tide), slightly less tidal velocities, and deceleration of the morphodynamic trend. The export of sand is noticeably slower due to reclamation. Furthermore, the net import of mud over long time scales is less due to less accommodation space for the mud to settle in the reclaimed side branches. Dredging

and dumping has significantly altered the morphodynamics in the Western Scheldt estuary over long time scales. Scenario runs with and without dredging over the 1965-2002 show that not only the navigational channel has become deeper, but the secondary channel has become shallower. Especially the morphology of the eastern (landward) part of the estuary has been affected greatly. Dredging and dumping has led to increased tidal ranges over time and a faster celerity of the tidal wave into the estuary. Model results are compared to measured tidal range increase and celerity and show good comparisons. An extreme (unrealistic) sand mining scenario show that the tidal wave can increase further if there is less sediment available in the estuary.

SAMENVATTING

ESTUARIES zijn kustomgevingen waar zoetwater uit de rivier en zeewater uit de zee samenkomen. Getijdeplaten in estuaria bieden voedselgronden, broedplaatsen en schuilplaatsen voor talrijke soorten, waaronder trekvogels en vissen. Ze staan bekend om hun hoge productiviteit en ondersteunen diverse voedselketens, waardoor ze bijdragen aan de algehele biodiversiteit en ecologische werking van estuaria. Bovendien zijn estuaria belangrijke navigatiepoorten naar havens en rivieren stroomopwaarts, waarbij vaak onderhoudsbaggerwerkzaamheden in het vaargebied nodig zijn om de toegang tot de haven te behouden.

Estuaria staan voor diverse toekomstige uitdagingen. Een belangrijke uitdaging is de morfologische veranderingen die optreden in estuaria als gevolg van zowel natuurlijke als door de mens veroorzaakte factoren. Menselijke activiteiten, zoals landwinning en baggerwerk, kunnen morfologische veranderingen verergeren, wat kan leiden tot habitatverlies en verstoringen van estuariene ecosystemen. Een andere uitdaging is de voorspelde zeespiegelstijging, die een bedreiging vormt voor getijdenplaten en estuaria als geheel. Stijgende zeeniveaus kunnen leiden tot overstroming en onderdompeling van getijdeplaten, wat resulteert in habitatverlies en afname van biodiversiteit. De effecten van dergelijke veranderingen kunnen tientallen jaren duren.

Om deze uitdagingen aan te pakken, zijn geïntegreerde en duurzame beheerstrategieën noodzakelijk. Een hulpmiddel dat kan helpen bij het begrijpen van de gevolgen van natuurlijke en menselijke invloeden is een proces gebaseerd morfologisch model. Deze modellen zijn de afgelopen decennia wijdverspreid beschikbaar geworden en worden doorgaans toegepast voor kortere tijdsperioden, maar het is niet bekend of deze modellen nuttige langetermijnvoorspellingen geven.

Het hoofddoel van dit onderzoek is het onderzoeken van de modelvaardigheid van een op proces gebaseerd numeriek morfologisch model (FINEL2d) over een tijdsbestek van een eeuw. Dit onderzoek toont aan dat een morfologische reconstructie van de Westerschelde voor de periode 1860-1970 na 110 jaar uitstekende 'skill' vertoont. Dit wordt toegeschreven aan de zelforganisatie van het morfologische systeem die correct wordt gereproduceerd door het numerieke model. Op tijdschalen van enkele decennia overtreft de interactie tussen het dominante getij en de begrenzing van het estuarium andere onzekerheden. Zowel gemeten als gemodelleerde diepteprofielen tonen een trend van afnemende energiedissi-

patie, minder morfodynamische activiteit en daardoor een stabielere morfologie in de loop van de tijd, hoewel de aanpassingstijd van het estuarium lang is (ongeveer eeuwen).

Verder wordt het langetermijngedrag van zand en slib in de Westerschelde onderzocht. Bathymetrische gegevens van de Westerschelde vanaf 1860 werden gecombineerd met een driedimensionaal ondergronds model ('GeoTop') om een langetermijn-studie van het sedimentbudget uit te voeren. Aangezien er rekening werd gehouden met gegevens van een ondergronds model, kon er onderscheid gemaakt worden tussen zand en slib. Dit onderzoek toonde aan dat het estuarium smaller en dieper werd, terwijl het zand exporteerde (1,5-2,5 miljoen m^3/jaar) en slib importeerde (0,5-1,5 miljoen m^3/jaar) gedurende de periode 1860-1955. Het geërodeerde zand komt voornamelijk uit de eroderende geulen in het zeegebied van het estuarium en wordt getransporteerd naar de zee, het binnenste deel en de zijtakken. Het geïmporteerde mariene slib wordt permanent afgezet in zandbankgebieden en zijtakken, die in de loop van de tijd geleidelijk zijn ingepolderd. Door onderscheid te kunnen maken tussen zand en slib in deze sedimentbudgetstudie wordt aangetoond dat verschillende sedimenttypen verschillend kunnen reageren op dezelfde omstandigheden en zelfs tegengestelde netto richtingen kunnen hebben. Door het morfodynamische zandmodel uit te breiden met een zand-slibmodule worden zand- en slibstromen gereproduceerd voor de periode 1860-1955, waarbij de onderliggende transportmechanismen van zand en slib worden verklaard.

De modelresultaten tonen aan dat de waargenomen export van zand en import van slib in de periode 1860-1955 worden gereproduceerd door het zand-slibmodel. Bovendien wordt het waargenomen erosie/sedimentatiepatroon (nog steeds) goed gereproduceerd, samen met de waargenomen toename van de getijslag in deze periode. De import van marien slib in de monding van het estuarium verandert in een export van slib wanneer de simulatie wordt verlengd tot 250 jaar. De ruimte voor slibafzetting raakt uitgeput op lange tijdschalen en fluviaal slib wordt naar zee gespoeld. Aangezien slibafzetting in de loop van de tijd afneemt, nemen de slibconcentraties toe volgens de modelresultaten. De waargenomen export van zand wordt gereproduceerd door het morfodynamische zand-slibmodel. Hoewel het getij hydrodynamisch vloeddominant is, is er een duidelijke export van zand door langere ebgetijden. De verlenging van de model simulatie tot 250 jaar nadert uiteindelijk een nul-export van zand. Deze modelresultaten geven aan dat het estuarium evolueert naar een evenwichtstoestand. Deze model simulaties zijn uitgevoerd zonder baggeren van de geulen dat pas in de jaren 1970 echt op gang kwam. In werkelijkheid zijn de import/export van sediment tijdens meer recente perioden (na de jaren 1970) waarschijnlijk beïnvloed door antropogene invloeden.

Inpolderingen vanaf 1860 hebben de getijslag met ongeveer 10 cm vergroot over een periode van 100 jaar volgens modelscenario's. Landwinning werd voornamelijk uitgevoerd nadat het secundaire bekken al met sediment was gevuld. Het afsluiten van een gebied

met dijken (de eigenlijke landwinning) was slechts een versterking van een voortdurende trend. De uiteindelijke toestand van het estuarium verschilt echter op lange tijdschalen. Merkbaar is dat de hoeveelheid sediment in het totale estuarium verschilt door inpolderingen. Landwinning leidt tot een kleinere getijprisma (dat wil zeggen de hoeveelheid water die bij elke tij binnen- en uitstroomt), iets lagere getijdenstromingen en vertraging van de morfodynamische trend. De export van zand verloopt merkbaar langzamer door landwinning. Bovendien is de netto import van slib op lange tijdschalen minder vanwege de verminderde ruimte voor slibafzetting in de gereclameerde zijtakken. Baggeren en storten hebben de morfodynamica in het Westerschelde estuarium op lange tijdschalen aanzienlijk veranderd. Scenario's met en zonder baggeren voor de periode 1965-2002 laten zien dat niet alleen het vaarwater dieper is geworden, maar ook de secundaire geul ondieper is geworden. Met name de morfologie van het oostelijke (landinwaartse) deel van het estuarium is sterk beïnvloed door het baggeren. Baggeren en storten hebben geleid tot een toename van de getijslag in de loop van de tijd en een snellere voortplantingssnelheid van de getijgolf in het estuarium. De modelresultaten zijn vergeleken met een gemeten toename van de getijslag en voortplantingssnelheid en laten goede overeenkomsten zien. Een extreem (onrealistisch) scenario van zandwinning laat zien dat de getijgolf verder kan toenemen als er minder sediment beschikbaar is in het estuarium.

1

INTRODUCTION

1.1. GENERAL

ESTUARIES are typically bordered between the river and the sea. Estuaries are important navigational gateways to ports and rivers further upstream in often densily populated areas. Estuaries have also important ecological functions like breeding ground for fish (Figure 1.1 and 1.2).

Tides, river discharge and waves are natural forces that shape the morphology of estuaries. The morphology of the estuary is further modified by human impacts. For example dredging and land reclamation have influenced the eco-morphology of the Western Scheldt and Yangste estuary (De Vriend et al., 2011). Bale et al. (2007) has investigated the impact of dredging activity in the Tamar estuary in southwest England. In the closed-off Dechutes estuary (USA) the morphological response is investigated when the tide is restored (George et al., 2012). In the Humber estuary safety against flooding is promoted by stimulating sedimentation of inter tidal areas as a natural defense (Winn et al., 2003). Tönis et al. (2002) investigates the morphological response of the Haringvliet estuary in the Netherlands after closure in 1970. Thomas et al. (2002) and Blott et al. (2006) identified the building of training walls in the Mersey estuary (UK) as an important factor for the morphological change in the estuary. In the Seine estuary the impact of human activities like the construction of dykes, a bridge and a port is thought to be responsible for the loss of a large portion of a tidal mudflat. (Cuvilliez et al., 2009). Wang et al. (2010) identifies the building of large reservoirs and soil conservation practices in the Yellow River (China) to be the cause of a 90 percent sediment reduction to the estuary, causing erosion in the downstream channels. Embankment construction, land reclamation and construction and maintenance of a navigational channel were identified by Van der Wal et al. (2002) as causes for morphological

Figure 1.1: Photo of the Scheldt estuary, view on nature area Saeftinghe and industrial complex Doel. Source: https://beeldbank.rws.nl, Rijkswaterstaat / Joop van Houdt

Figure 1.2: Areal photo of the Western Scheldt, view on nature area Saeftinghe and industrial complex Doel, together with the navigational channel to the port of Antwerp. Source: https://beeldbank.rws.nl, Rijkswaterstaat / Harry van Reeken

changes in the Ribble Estuary (UK).

Understanding the morphodynamics of estuaries and being able to predict human effects on the morphology is important for policy and decision-making processes. It may be that for this reason that there has been a long history of research in this field (Bakker and De Vriend, 1995). Starting from purely empirical work (O'Brien, 1931, 1969) and classification (Pritchard, 1967), via mathematical analyses (Escoffier, 1940) and semi-empirical models (e.g. Stive and Wang, 2003) to highly sophisticated 3D morphodynamic simulation models (Lesser et al., 2004a).

1.2. RELEVANCE OF THIS RESEARCH

THE morphological changes in an estuary are complex. The bed of an estuary usually consists of non-cohesive sediments (sand) and cohesive sediments (mud). The sediment is eroded when large forces act on the sediment due to tidal flow and or waves. Advective and diffusive processes transport the sediment and it gets deposited at places where the shear stress is low. In this way patterns emerge (e.g. ripples, bars, channels) that can in return also influence the water motion. So the water motion, sediment transport and bed evolution form a coupled system. This coupled system forms the basis of process-based models that are used extensively for research and engineering purposes. In the last decades these process-based models have been developed to predict the morphological developments in all kinds of coastal systems. The use of these models has seen a large increase in both science and engineering in the last years. Forecast periods of more than a few years with these models are scarce because of the large computational time involved and because it is believed that these models are not able to accurately predict morphological change over longer time-scales (more than a few years). However the morphological time scales involved in management issues are much larger (decades to centuries).

The ecological valuable inter tidal areas in estuaries often consists of mudflats and salt marshes, which are dominated by the mud fraction. Most research on morphological change in estuaries have focused on the sand fraction only for simplicity and computational reasons. To model any potential impact on these inter tidal areas it is also required to model the mud fraction. Since the modelling of mud involves other sediment transport formula than the sand fraction, the modelling of mud usually is carried out using a different model and on a short timescale without a bed update. Morphological modelling of both sand and mud involves a multiple fraction model in which both fractions interact with each other. Since most estuaries consists of both sand and mud it is therefore useful to look at the long-term behaviour of sand and mud.

Summarising, the questions that need to be answered using morphological models requires longer time scales and more processes (e.g. both the sand and mud fraction). It

is therefore important to know if these models are able to predict realistic morphological changes over decades to centuries. Hindcasting [1] morphological models on historical morphological changes over decades to a century scale however is scarce for two reasons:

- Bathymetrical data of estuaries over decades to a century scale with sufficient quality is scarce;
- Computational resources were limited until recently.

It is for this reason that it is not known how well process-based morphological models can perform on long time scales. Therefore the main goal of this research is to test these models on long-term bathymetrical changes in estuaries and to see how good these models can perform on these long time scales. In this PhD research a process-based morphological model is used to hindcast morphological changes over decades to a century scale and to show the effect of a combination of sand and mud on the long-term behaviour of estuaries. The Western Scheldt estuary is used as primary case study and is described in the next section.

1.3. PHENOMENOLOGICAL DESCRIPTION

A phenomenological description of the morphology of estuaries is the starting point for our knowledge of these systems. Here we describe the research that is most useful for this research.

Van Veen (1950) describes the existence of different ebb- and flood channels as they occur in for example the Western Scheldt estuary. Ebb channels are usually the deeper channels as the ebb flow usually occurs at lower water levels. The ebb channels tend to migrate until they reach the outer bend. Flood channels are more straight and shallow. Ahnert (1960) also noted the existence of different ebb- and flood channels in a tidal environment.

Pillsbury (1956) suggested the concept of an ideal estuary, in which the morphology of an estuary is going to an equilibrium state. In this ideal state no gradients in tidal water level and velocity amplitudes exists anymore, leading to zero bed shear stresses and sediment transport. Pethick (1994) describes how the trumpet shape of the estuary is formed: flow rates at the estuary head will be a minimum and at the estuary mouth will be maximum due to resonance of the basin. As a consequence inter-tidal deposition rates will be increased further landwards into the estuary, resulting in the exponential plan form of the estuary. The decreasing landward depth results in an increasing friction of the channel, resulting in a long-term steady state between morphology and tidal energy.

[1] Hindcasting is a way of testing the model against reality. A past event is modelled to see if the model output matches the known results

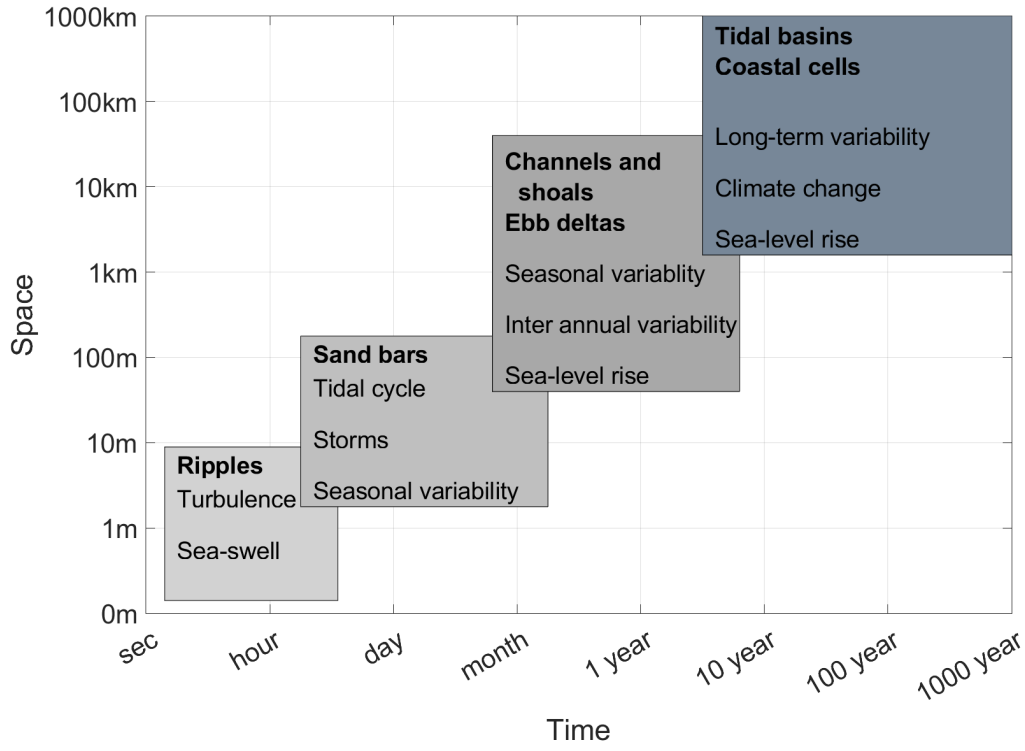

Figure 1.3: Different time and length scales involved in morphology (After De Vriend, 1991)

1.4. LENGTH AND TIME SCALES

ONE of the major problems in morphological modelling is the wide range of different length and time scales involved (De Vriend, 1991). Local ripples are formed within hours, while channel and shoal patterns take years to develop on a scale of kilometers. The change of a complete estuary due to for example climate change can take decades to hundreds of years. The different time and length scales are illustrated in Figure 1.3.

In this research the focus is on long-term morphology. Long-term is here defined as decadal to a century scale, i.e. this is associated with the adaptation time of a complete estuary.

1.5. TYPES OF MORPHOLOGICAL MODELS

DIFFERENT morphological models have been created to describe physical processes on different time and spatial scales. Each model has its own advantages and disadvantages. A classification is made between types of models based on De Vriend et al. (1993) and De Vriend (1996):

- Behaviour oriented models: In these kind of models the underlying processes are ignored and modelling is based on observed data. The following classes of models exits De Vriend (1996):

  - Data based models: Data based models focuses on empirical relations between different types of coastal parameters without describing the underlying physical processes. Data based models use observations and statistical techniques for prediction purposes, i.e. take an observed trend and extrapolate this trend into the future. Data based models typically concern macroscale phenomena (De Vriend, 1996).
  - Empirical relationships: Early research in the field of estuaries and tidal inlets concerned the well known empirical relationship between tidal prism and cross-sectional area. O'Brien (1931, 1969). Prediction of erosion or sedimentation is then defined as a deviation from this equilibrium relationship.
  - Semi-empirical, long-term models: Semi-empirical models for long-term morphological modelling of estuaries have been developed that combines empirical relationships with process-based modelling (Stive and Wang, 2003; Wang et al., 1999). Since these type of models do not require a lot of computational effort this has been a popular way to model long-term changes in estuaries. The problem with these semi-empirical models is twofold: First, it is often very difficult to define the morphodynamic equilibrium, especially after a large human interference. Second, the location of the morphological units is assumed stationary or irrelevant: the models merely describe the evolution of variables such as the mean depth De Vriend et al. (1993).

- Process-based models: Process-based (or bottom-up) models are based on physical principles (e.g. mass conservation) and use mathematical equations to describe water motion, sediment transport and bottom change. The last decades these models have developed rapidly and are becoming robust tools to calculate morphological changes (Van der Wegen and Roelvink, 2012).

  A process-based model describes the water motion with a typical time step of seconds to minutes for numerical stability. Using an empirical sediment transport formula (e.g. Engelund and Hansen, 1967) sediment transport is calculated within this time step. The next step is to calculate bottom changes, which are fed back into the water motion the following time step. Since the desired morphological scale is much larger than the hydrodynamic time step these morphological computations typically require a large computational effort. To speed up the computation the bottom change is usually multiplied by a factor: the so called morphological acceleration factor or morfac (Roelvink, 2006).

In the range of available morphological models process-based models have the advantage of systematically turning on and off processes to gain insight in how the system works. Therefore process-based models are widely used in science and engineering (Roelvink and Reiniers, 2011).

- Combination of behaviour oriented and process-based models:
  - Formally integrated long-term models or idealised models: these type of models are derived from process-based models by formal integration over time (and space), with empirical or parametric closure relationships. The models are idealised, meaning that they only consider simple geometries or simplifying assumptions (Schuttelaars, 1997). For example the formation of bars in tidal channels have been investigated (Schuttelaars and de Swart, 1999; Seminara and Turbino, 2001; Schramkowski et al., 2003) and the equilibria of tidal embayments (Schuttelaars and de Swart, 2000). The advantage of these models is that they offer fundamental knowledge on the physical mechanisms for morphological changes. Drawback is that they cannot be used in a real geometry to give predictions of the morphology over a determined timescale.
  - Inverse methodology: The idea of inverse modeling is that available data is used to determine unknown parameters or functions in the the governing equations (of process-based models). The drawback is that long-term bathymetric data should be available. Karunarathna et al. (2008) used 150 year data of the Humber estuary to discriminate between diffusive and non-diffusive processes.

The focus point of this research is on process-based models. The reason is that in the range of available models potentially it is the only model that is able to describe morphological changes in a real case study with sufficient spatial detail. The ability of long-term modelling using process-based models is described in the next section.

1.6. EXAMPLE: THE WESTERN SCHELDT ESTUARY

THE Scheldt estuary is one of the major estuaries of North-West Europe. The estuary is approximately 160 km long and is located both on Dutch and Belgian territory. The down-estuarine part (last 60 km) is called the Western Scheldt (Figure 1.4) and is characterised by a width of almost 5 km near the mouth and 1 km near the Dutch-Belgian border. The mean tidal range increases from 3.8m at the mouth to over 5.0m near Temse, almost 100 km from the mouth of the estuary. The morphological changes in the Scheldt estuary are dominated by the tidal motion. The river discharge is of minor importance since the fresh water discharge, on average 120 m^3/s, is only 0.6% of the tidal prism at the mouth (Van der Spek, 1997). The estuary is well-mixed.

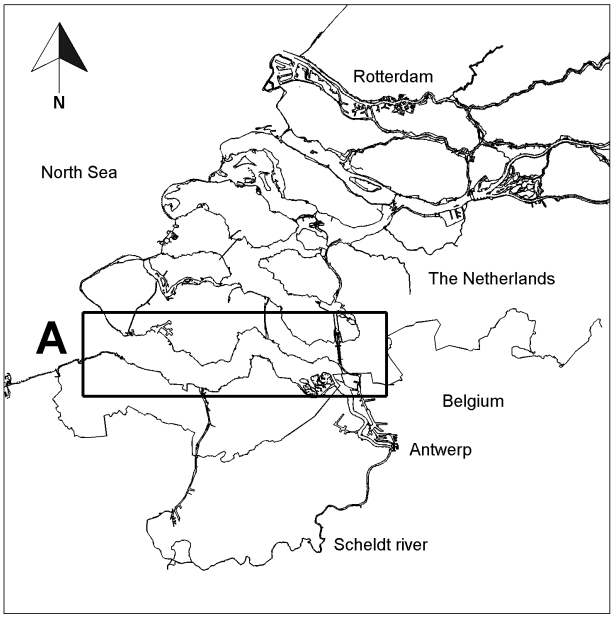

Figure 1.4: Location of the Western Scheldt estuary

The Western Scheldt incorporates large extents of tidal flats and salt marshes. Nature is therefore an important function and stringent EU and national legislation is maintained to safeguard its natural values. Equally important are the functions of the estuary in the safety against flooding and the access to the Port of Antwerp.

The Western Scheldt is a multiple channel system, see figure 1.5. Ebb and flood channels show an evasive character separated by inter tidal shoals (Van Veen, 1950). The ebb channel shows a meandering character, while the flood channel is straighter. The ebb flow reaches it maximum velocity near mean sea level (MSL), while the flood flow reaches its peak one hour before high water (Van Den Berg et al., 1996). As a consequence the ebb flow is more concentrated in the channels, resulting in deeper ebb channels. The ebb channel is therefore generally designated as the navigational channel in the Western Scheldt.

The tidal flats and surrounding ebb and flood channels form morphological macro cells Winterwerp et al. (2001). At the locations where the cells coincide, sills develop, which block the fairway to the port of Antwerp and therefore require maintenance dredging (Meerschout et al., 2004). Several million m^3 are dredged annually to maintain the navigational channel to the Port of Antwerp. This material is distributed back in the estuary. In addition yearly 2 million m^3 of sand is mined from the Western Scheldt.

In the 1970's and 1990's a deepening of the navigational channel has been carried out to allow vessels with greater draught to enter the port of Antwerp. Just recently a third deepening has been completed. Most of the dredging had to be done at the sills. The annual dredging volumes (maintenance plus deepening) range from 5 million m^3 in 1968 to 14

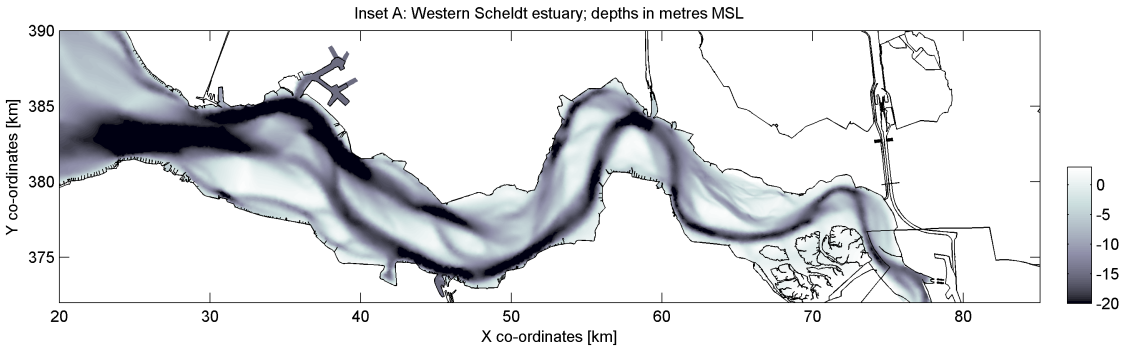

Figure 1.5: Depth of the Western Scheldt estuary

million m^3 during the second deepening. After the second deepening the volumes seem to establish around 7 to 8 million m^3 per year. The dredged material is deposited back into the estuary in designated areas, usually in the secondary branches. During the last enlargement of the navigation channel (2010) a new disposal strategy was used (Plancke et al., 2010). Within this strategy dredged sediments are being used to reshape sandbars and create ecological valuable habitats.

In the past centuries land reclamations has narrowed the Western Scheldt estuary. The largest surface area was in the 16th century (Figure 1.6). In the centuries after, the side branches silted up and were bit by bit reclaimed (Figure 1.7, Figure 1.8 and Figure 1.5), resulting in increasing tidal levels. The tidal amplitude and celerity also increased during the last decades, but this is believed to be due to the dredging works (Taal et al., 2013; Dam et al., 2013). The tide is important for all functions related to the Scheldt estuary: safety, accessibility and nature.

- Safety against flooding is directly affected by a change in the tidal propagation.
- Accessibility is dependent on the bed level of the navigational channel. The tide further determines accessibility because of tidal windows and tidal (cross-current) flow.
- The time that an inter tidal area is dry is important for its ecological value; a change in the tide has thus an effect on the ecology. Furthermore an increase in tidal velocities generally reduces the ecological richness of the bed.

1.7. RESEARCH QUESTIONS

FOR a better understanding of the performance of process-based morphological models on longer timescales it is necessary to carry out long-term hindcasts and determine the

Figure 1.6: Historical chart of the Scheldt of 1560, Jacob van Deventer (Public domain)

Figure 1.7: Historical chart of the Scheldt of 1654, Visscher (Public domain)

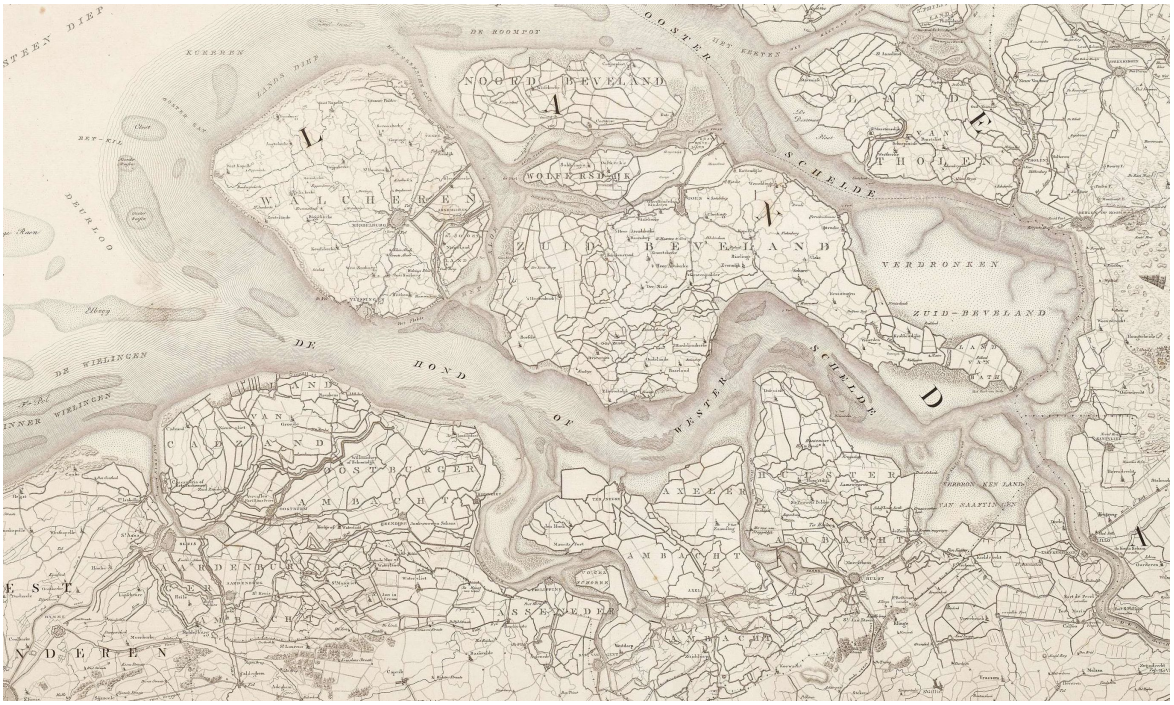

Figure 1.8: Historical chart of the Scheldt of 1829, Krayenhoff (Public domain)

value of these models over these time scales (decades-centuries). Therefore the following main research question is formulated:

Q1: What is the skill of process-based models in long-term morphological hindcasts of estuaries?

Further, the following research questions are formulated:

Q2: What is the long-term behaviour of sand and mud in estuaries?

Q3: What are the long-term effects on the estuarine morphology and tides of historic anthropogenic interventions, such as land reclamations, dredging and sandmining

1.8. METHODOLOGY

This study focuses on the Western Scheldt because there is ample of historic data available for model validation and calibration. Furthermore the Western Scheldt is a relative simple

estuary because of limited river discharge.

Central in this thesis is the use of a process-based morphological model called FINEL2d that solves the Navier-Stokes equations, calculates the sediment transport and derives the morphodynamic development based on divergence of the sediment transport fields on a high resolution grid covering centenial time-scales. This allows for close analysis of processes and the impact of human interventions. The principal equations are described in Appendix A.

We first look at long-term model skill on a morphodynamic hindcast that reproduce a unique historic dataset of erosion and sedimentation patterns between the 1860-1970 period (Chapter 2).

A second performance test relates to sediment fluxes. We derive historic sand and mud budgets based on an historic bathymetric data and subbottom sediment composition (Chapter 3). These derived sand and mud fluxes are used to validate the morphodynamic model in a hindcast study. To assess the long-term impact of historic land reclamations in addition a forecast is carried out (Chapter 4).

Finally we run morphodynamic simulations from 1964 to 2002 with and without dredging and sand mining (Chapter 5). We compare the results and we draw conclusions about these human impacts on the estuary.

2

MODELING CENTURIES OF ESTUARINE MORPHODYNAMICS IN THE WESTERN SCHELDT ESTUARY

We hindcast a 110 year period (1860-1970) of morphodynamic behavior of the Western Scheldt estuary by means of a 2D, high resolution, process-based model and compare results to a historically unique bathymetric dataset. Initially the model skill decreases for a few decades. Against common perception, the model skill increases after that to become excellent after 110 years. We attribute this to the self-organization of the morphological system which is reproduced correctly by the numerical model. On time scales exceeding decades, the interaction between the major tidal forcing and the confinement of the estuary overrules other uncertainties. Both measured and modeled bathymetries reflect a trend of decreasing energy dissipation, less morphodynamic activity and thus a more stable morphology over time, albeit that the estuarine adaptation time is long (~centuries). Process-based models applied in confined environments and under constant forcing conditions may perform well especially on long (> decades) time scales.

Dam, G, Van der Wegen M., Labeur, R.J., and J. A. Roelvink (2016), Modeling centuries of estuarine morphodynamamics in the Western Scheldt Estuary, Geophysical Research Letters, 43, 3839-3847, doi:10.1002/2015GL066725.

2.1. INTRODUCTION

ESTUARINE morphology and its development over time have been the subject of research ever since estuaries became important navigational gateways to ports and their hinterland (Reynolds, 1887; LeConte, 1905). Estuaries are unique ecosystems with important ecological functions like breeding ground for fish or feeding areas for migratory birds (Gill et al., 2001; Barbier et al., 2011). Estuaries are put under increasing pressure by human activities (dredging of navigational channels, land reclamation works) and climate change (Barbier et al., 2011). Understanding and forecasting estuarine morphodynamics is essential for adequate estuarine management and policy-making.

Exploring morphological dynamics raises questions on the existence and character of morphological equilibrium. Dronkers (1986) states that external conditions in reality change continuously so that equilibrium conditions cannot be reached. 1D and 2D modeling approaches find equilibrium conditions under highly schematized settings (e.g. Schuttelaars and de Swart, 2000; Lanzoni and Seminara, 2002; Hibma et al., 2004). Equilibrium can exist at smaller scales of channel-shoal patterns while larger scales (at basin size) have century long adaptation time scales (Van der Wegen and Roelvink, 2008; Van der Wegen et al., 2008). At the same time, equilibrium can be dynamic due to cyclic behavior of channels and shoals or can be reached only by approximation due to long adaptation timescales.

Morphodynamic development may be investigated by empirical relationships (e.g. O'Brien, 1969) laboratory scale tests (Reynolds, 1887; Tambroni et al., 2005), or numerical models ranging from highly schematized to fully process-based (De Vriend et al., 1993; Murray, 2003). Schematized (or reduced complexity) modeling efforts have an inductive character by assuming (empirical) equilibrium relationships between forcing and elements of the estuarine morphodynamic system (Kragtwijk et al., 2004). Any disturbance of the system will eventually strive towards equilibrium conditions. In contrast, process-based models have a strong deductive character by taking physical processes as a starting point without defining equilibrium conditions a-priori.

Process-based models are widely used in the science and engineering community (Lesser et al., 2004b; Hervouet, 2000; Shchepetkin and McWilliams, 2005). In this paper we apply a 2 dimensional depth-averaged process-based model in the horizontal plane (Dam et al., 2007; Dam and Bliek, 2013) to predict centennial time scale morphodynamics.

Many process-based models were originally developed to address the short-term morphological impact of engineering works (Roelvink and Reiniers, 2011). The essential part of these morphodynamic models is the feedback loop between topography, fluid dynamics and sediment transport, the gradients of which result in morphodynamic change. The feedback can either be positive or negative. Positive feedback occurs when instabilities grow. Negative feedback is attributed to damping of the system. Switches between these

states mark thresholds in morphodynamic behavior (Cowell and Thom, 1996).

By increasing computational power and clever morphological updating techniques the models have evolved into scientific tools that are potentially able to calculate high resolution (~100m) morphological change over decades to millennia in large (~100 km) domains with a computation time of days to weeks on a standard PC. Numerous process-based studies describe stable centennial to millennial time scale morphodynamic development in highly schematized tidal basins under constant forcing conditions (e.g. Hibma et al., 2003b; Maanen et al., 2013; Bertin et al., 2005; Zhou et al., 2014).

The potential for successful predictions in more realistic environments remains however questionable (De Vriend et al., 1993; Haff, 1996, 2013; Stive and Wang, 2003). Small errors in prediction, coupled with non-linear interactions that are chaotic in nature, may eventually lead to unrealistic developments. Apart from numerical shortcomings, sources of uncertainty or error that may arise include (Haff, 1996):

- Model imperfection: e.g. application of an empirical sediment transport formula derived in a laboratory on a large morphodynamic scale;
- Omission of known and unknown processes: e.g. wave action plays a role in morphodynamics of shoals, but is often ignored in long-term morphodynamic simulations of estuaries;
- Lack of knowledge of initial conditions: e.g. distribution of sediment characteristics over the domain and in the bed;
- Sensitivity to initial conditions: If estuarine morphology behaves chaotically long-term morphodynamic prediction is not possible (Philips, 1992);
- Unresolved, sub-grid heterogeneity;
- Unknown external forcing.

However, using a similar type of process-based model as we apply in the current study successful decadal time scale hindcasts in complex estuarine environment of San Francisco Bay sub-embayments are possible, given a strong disturbance by excessive sediment supply gradients (Ganju et al., 2009a; Van der Wegen and Jaffe, 2013).

Thus far the centennial timescale performance of morphodynamic process-based models in relatively undisturbed systems has been unclear. An important reason is that bathymetric data for model validation covering typical morphological time scales of decades to centuries are scarce.

For that reason we explore the skill of a process-based model in hindcasting morphodynamic development in the Western Scheldt estuary in the Netherlands. Model validation is based on a unique 110 year long bathymetric dataset starting in 1860 and continuing with intervals ranging from 5 to 25 years. As a final step we extend the simulation to 250 years and analyze energy dissipation and morphodynamic activity.

2.2. THE MODEL APPROACH

2.2.1. INTRODUCTION

We apply a 2 dimensional process-based model called FINEL2d (Dam et al., 2007; Dam and Bliek, 2013) that is based on the finite element method that solves the 2-dimensional shallow water equations employing a Riemann solver (Glaister, 1993), a sediment transport formulation, followed by a bed update method based on the 'online approach' (Roelvink, 2006). See Appendix A for more information.

FINEL2d uses an unstructured triangular mesh. The advantage of such a mesh in comparison to for example a finite difference grid is the flexible mesh generation. In FINEL2d no nesting techniques are required in regions of specific interest, where a higher degree of resolution is needed. Arbitrary coastlines and complex geometries can be resolved accurately.

The seaward boundaries of the computational mesh of the Western Scheldt are situated approximately 40 km away from the coastline and coincide with the boundaries of existing models covering the North Sea (Figure 2.1). The latter can be used to obtain the corresponding boundary conditions. The major part of the Scheldt-estuary in Belgium is also included in the schematization (Figure 2.1a). In the area of interest, the Western Scheldt, the average grid size is approximately 1.1 ha (Figure 2.1b). Near the seaward boundaries the grid size is approximately 2.5 km^2. The total number of elements (triangles) of the mesh is 59,937. The resulting simulation time of the 110 year hindcast is 4.7 days on a 2.6 GHz machine using 16 CPU's.

On the river side constant (yearly averaged values) river discharges are assumed. The average discharge of the Scheldt river and tributaries is around 100 m^3/s. The discharge fluctuates between 50 m^3/s during summer and 180 m^3/s during winter periods.

On the seaward side of the grid 60 astronomical tidal boundary conditions are given. The sea level rise in the 110 year period is approximately 15 cm and is included in the simulation. Only the influence of the tidal action on the morphology is taken into account. Wave action is ignored for simplicity reasons, although intertidal areas can be influenced by wave action.

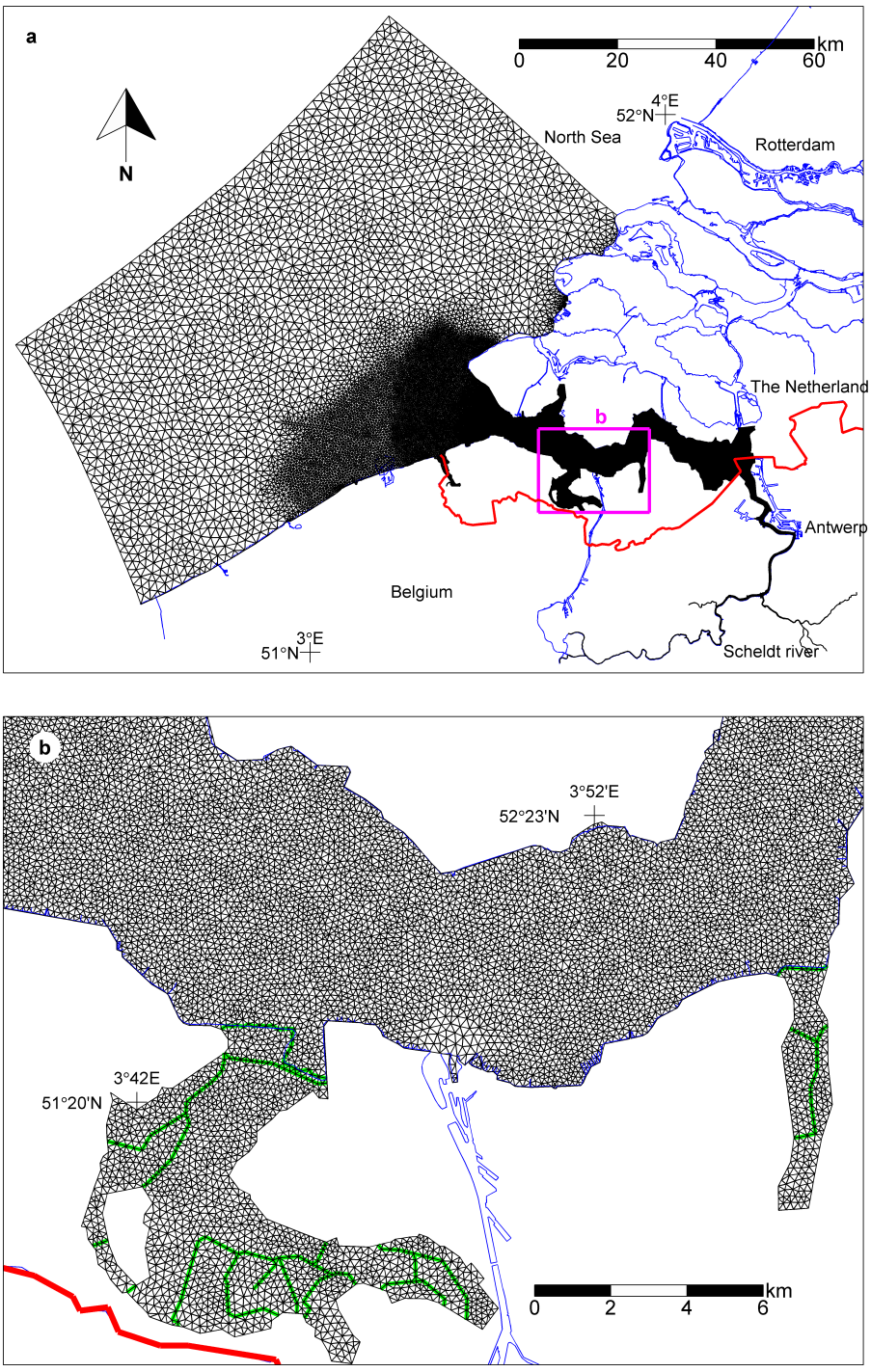

Figure 2.1: Computational grid (black lines). (a) Complete computational grid (b) Detail of the grid inside the estuary. Blue line indicates the land boundary; red line indicates the border between Netherlands and Belgium. Green line indicates the land reclamations in figure b.

The computational domain follows the exact outline of the estuary in 1860. Since then land reclamations have decreased the surface area of the estuary from 410 km^2 to 323 km^2. The land reclamations are taken into account in the computation. The borders of the land reclamations coincide with the computational mesh. At the year of closure a weir is implemented in the model, so that this section is closed off from the tidal influence and morphodynamic activity in the closed-off section stops.

2.2.2. BRIER-SKILL SCORE

To objectively compare measured and modeled bed changes, we use the Brier-Skill Score (BSS), see equation 2.1 (Sutherland et al., 2004).

$$BSS = 1 - \frac{\langle (Y - X)^2 \rangle}{\langle (B - X)^2 \rangle} \tag{2.1}$$

Where:
BSS = Brier-skill score [$-$]
X = Measured bed level [m]
Y = Modeled bed level [m]
B = Initial bed level [m]
$\langle\rangle$ Arithmetic mean

The second term of equation 2.1 can be split in the numerator and the denominator, which we define as error (equation 2.2) and signal (equation 2.3):

$$Error = \langle (|Y - X|) \rangle \tag{2.2}$$

$$Signal = \langle (|B - X|) \rangle \tag{2.3}$$

The error is the difference between model and measurement in meters, the signal is the change in measured bed level since start of computation in meters, both averaged over the model domain.

The following rating of the BSS for morphological models is used (Sutherland et al., 2004):
Bad : <0;
Poor : 0.0 – 0.1;
Reasonable/fair : 0.1 – 0.3;
Good : 0.3 - 0.5;
Excellent : 0.5 – 1.0.

As a reference, weather forecasting considers a BSS over 0.2 to be a useful prediction (Murphy and Epstein, 1989).

2.2.3. MODEL SETTINGS

THE settings of the parameters are the result of calibration (with a maximum BSS) and are as follows: A morphological acceleration factor of 24.75 is applied. This factor is used to multiply the computed bed level changes. Since the morphological changes are small per tidal cycle this approach is allowed (Roelvink, 2006). A sensitivity run for the 1860-1970 period with a morphological acceleration factor of 12.375 shows no significant changes in bed level and BSS values.

In the model we use a hydraulic roughness and a morphological roughness. For both the hydraulic and morphological roughness a value of 1 cm is applied over the domain and time. The constant hydraulic roughness value is the result of calibration of the response of the estuary to the tide.

The morphological roughness is used to calculate the Chézy coefficient in the Engelund-Hansen sediment transport formula. This roughness is one of the factors that controls the amount sediment transport in the model, so it controls the morphological time scale. A uniform and constant value of 1 cm resulted in the highest BSS at the end of the simulation. Sensitivity runs with a higher constant morphological roughness show the same positive trend of the BSS over time with a minimum value of 0.3 (good) for the 1860-1970 run.

We are aware of the fact that in some areas with large bed forms the hydraulic (and morphological) roughness can be higher. At this moment we think it is too ambitious to estimate a spatial and time varying roughness over a morphological period of 110 years and we accept our approach possibly introduces local errors in the roughness field.

One sand fraction is used, although a spatially varying grain size is used to calculate the equilibrium sand concentration. Field data shows that the grain size varies spatially and generally is coarser in the western part than in the eastern part (McClaren, 1994). To compensate for this we apply an average grain size (d_{50}) of 300 μm in the western part, linearly decreasing in landward direction to 150 μm to the eastern part of the estuary. The d_{50} is an input for the Engelund-Hansen sediment transport formula that computes the equilibrium concentration ce. The model concentration c is lagging behind this equilibrium concentration (see previous section). The model concentration is the actual concentration that calculates the bed level changes and sediment transport and is not further dependant on the d_{50}. So the spatial varying d_{50} implies a larger transport in the eastern part of the estuary under equal circumstances. Sensitivity runs with a constant d_{50} show the same positive trend of the BSS over time with a minimum value of 0.32 (good) for the 1860-1970

run, instead of 0.52 for the presented simulation.

Erosion resistant layers are included in the simulation and are based on core sample data throughout the estuary (Gruijters et al., 2004; Dam, 2013), see Figure 2.3. A simulation without erosion resistant layer results in a BSS of 0.4 for the 1860-1970 period. This means that the erosion resistant layer increases the skill of the model, but the effect is not so strong that the model skill is seriously affected. The erosion resistant layer has the largest effect on the morphology in the eastern part of the estuary (not shown).

2.3. THE WESTERN SCHELDT ESTUARY

THE Scheldt estuary is located in the southwest of the Netherlands and Belgium (51°25'N, 4°E). The Western Scheldt is the Dutch part of the Scheldt estuary and is the focus area of our study. The Western Scheldt is a mesotidal to macrotidal estuary, is approximately 50 km long by 5 km wide, and is a multiple-channel system with distinct ebb and flood channels. It forms the navigational access to the Port of Antwerp. For that reason the bathymetry of the Western Scheldt has been recorded over more than a century. River inflow and fluvial sediment supply are limited, and salt and fresh water are well mixed (Van der Spek, 1997). River input over a tide is only 0.6% of the tidal prism. The estuarine bed mainly consists of fine sand (Wartel, 1977). Mud is mainly found in intertidal areas. Erosion-resistant layers are present in the estuary in the form of clay and peat layers (Gruijters et al., 2004; Dam, 2013), sometimes located directly at the bed surface, see Figure 2.3. In the considered period (1860–1970) some minor dredging works took place in the navigational channel in the eastern part of the estuary. Since the 1970s major dredging works have deepened the navigational channel considerably. Dredging works from that moment on have significantly influenced the morphodynamics (Dam et al., 2013).

The Western Scheldt developed during the early Middle Ages, when the tidal inlet Honte connected to the Scheldt river. Floodings and military inundations expanded the surface area of the estuary over the next centuries. The estuary's largest surface area is in the seventeenth century with many side branches and connections to the Eastern Scheldt estuary. Over time the side branches silted up and were embanked. The connections to the Eastern Scheldt estuary also silted up and were closed off in 1867 and 1871. Mud most likely was responsible for a large portion of this sedimentation. The land reclamations decreased the intertidal storage area from 295 km^2 in 1650 to 196 km^2 in 1800 to 104 km^2 in the recent Western Scheldt (>1970) (Van der Spek, 1997). The surface area decreased from 410 km^2 in 1860 to km^2 in the recent Western Scheldt. The morphology of the estuary changed significantly from 1860 to 1970 (Figure 2.2). The main channels all migrated, shoals were eroded and created, and numerous secondary channels appeared and disappeared again. Given the morphological changes, it is clear that the estuary is not in equilibrium in 1860. Since

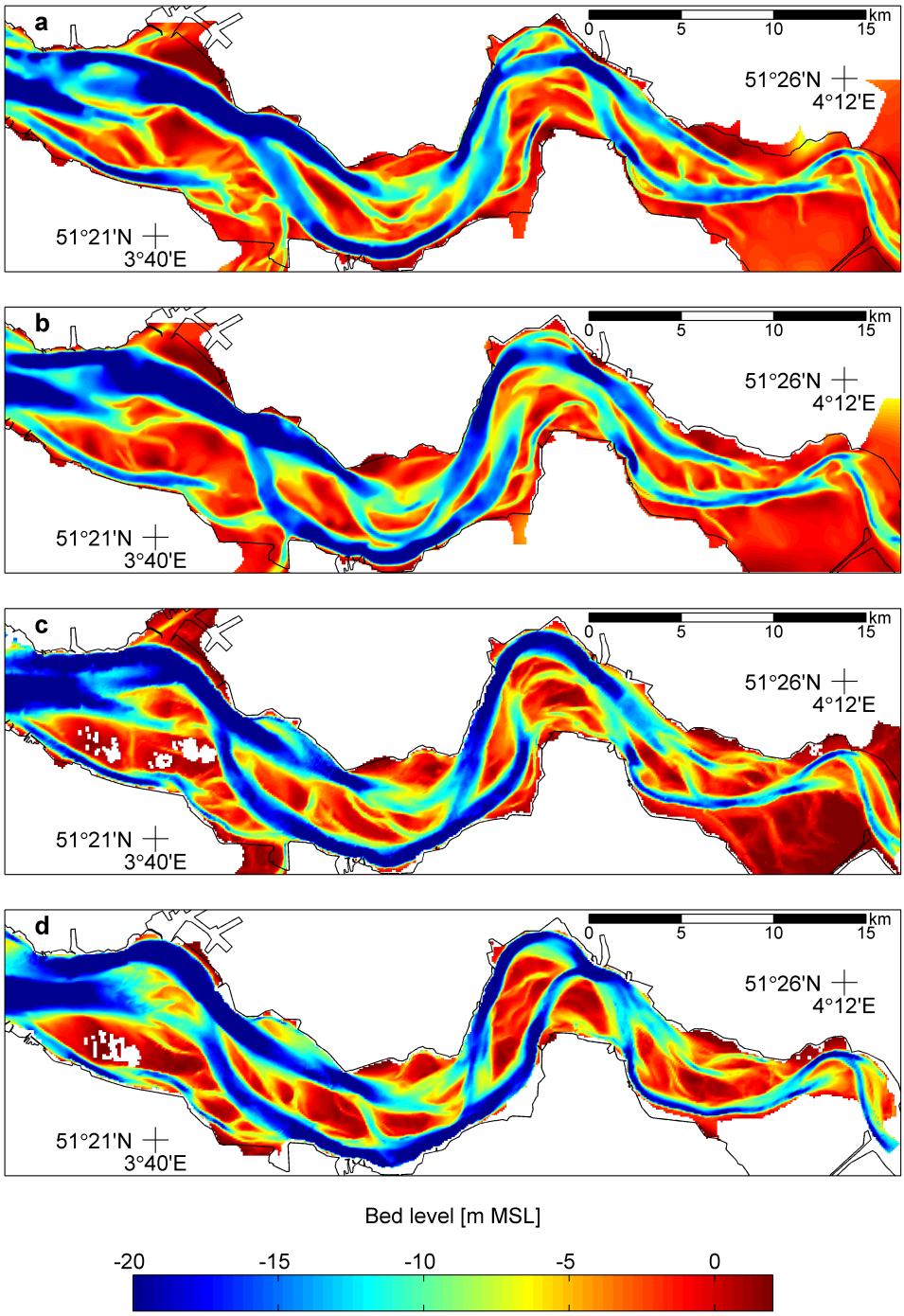

Figure 2.2: Four measured bed levels with respect to Mean Sea Level (MSL) of the Western Scheldt. (a) 1860. (b) 1905. (c) 1931. (d) 1970. Black line indicates the present day plan form.

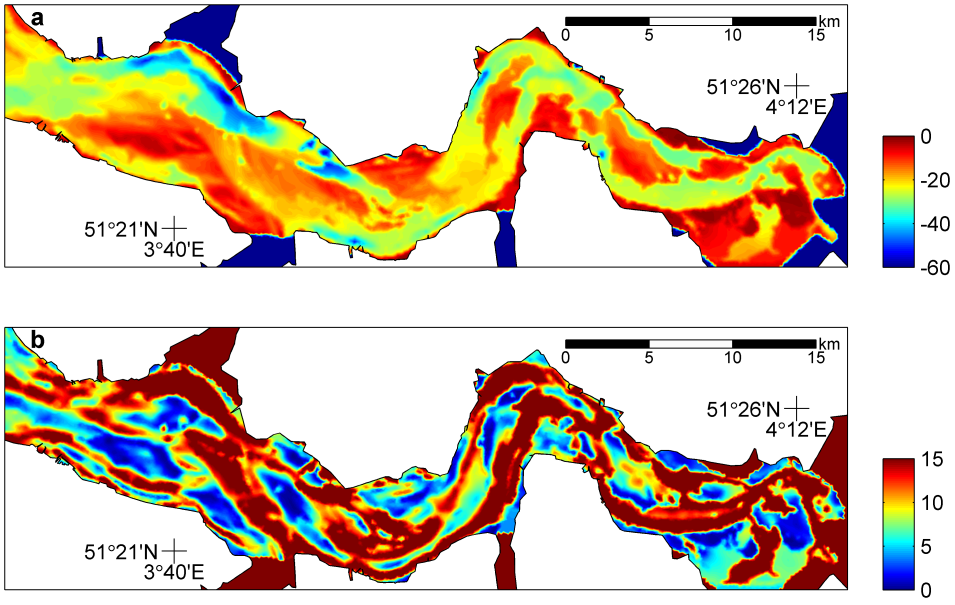

Figure 2.3: Erosion resistant layer. (a) Height of the erosion resistant layer [m MSL]. (b) Sediment layer thickness above erosion resistant layer in 1860 [m], after Dam (2013).

the tidal forcing at the mouth did not change significantly and the sea level rise was limited (15 cm/century), it is unlikely that these external conditions are the cause of the morphodynamic changes. It is more likely that the mentioned changes in the centuries before 1860 resulted in a morphodynamic response of the estuary.

Model assumptions are the following:
(1) outline of 1871 is assumed as starting point of the simulation in 1860;
(2) constant yearly averaged river discharge;
(3) we excluded the period after 1970 from our analysis, because we are interested in natural morphodynamic developments of the estuary;
(4) we only model the sand fraction since we are interested in the main estuarine body that mainly consists of sand; and
(5) sea level rise of 15 cm/century is included in the simulation.

2.4. RESULTS

MODEL results initially do not compare well to the measurements, but after a few decades, the results compare increasingly better to the measurements over time. This is reflected by qualitative visual comparison of erosion and sedimentation patterns for the 1860–1970 run (Figure 2.4) and quantified by an increasing BSS (black line of Figure 2.5a). Appendix B provides erosion-sedimentation figures with measurement-model comparisons for the 1878, 1890, 1905, 1931,1955, and 1960, bathymetries. Figure 2.5a shows

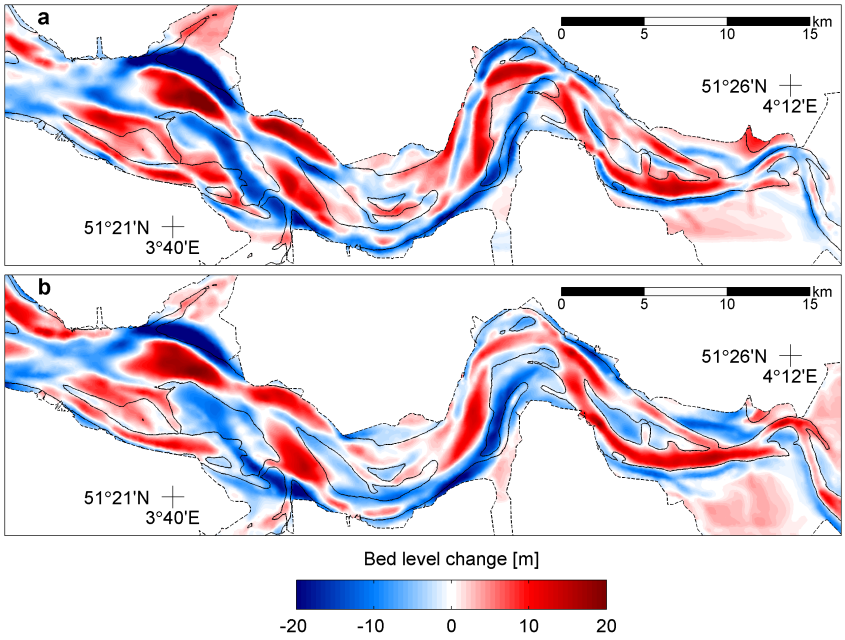

Figure 2.4: Erosion and sedimentation patterns over the 1860-1970 period. (a) Measured. (b) Modeled. Black dashed line indicates the 1860 plan form. Black solid line indicates the -5m contour line of the 1860 bed level. Appendix B includes erosion and sedimentation figures with measurement-model comparisons for 1878, 1890, 1905, 1931, 1955 and 1960.

that the BSS is initially negative but increases to become 0.52 (excellent) after 110 years for the 1860–1970 run.

The model exercise is repeated using the available measured bed levels in the years 1878, 1890, 1905 1931, 1955, and 1960 as initial condition for the bed level in a new computation. These runs also simulate the period until 1970 and BSS values are determined at the available bed level data. Initially, the BSS decreases and has a minimum around 15–20 years after start of the computations (Figure 2.5a). After this period the BSS increases for all simulations, and the model results compare better to the measurement in the longer term. This conclusion is not dependent of the initial condition.

The BSS results can be split into the model error (equation 2.2) and the signal (equation 2.3), see Figure 2.5b. Although the model error indeed increases and is initially even higher than the signal, the signal increases eventually even more leading to a decreasing error to signal ratio over time for all runs with a simulation time greater than 30 years. After 70 years the error remains relatively constant whereas the signal continues to increase, albeit at a decreasingly lower rate.

We performed a sensitivity analysis for the 1860–1970 simulation using different parameter settings, see also supporting information. Generally, the same positive trend of the BSS over time is found in all runs. The results that are presented in Figure 3 are the results of

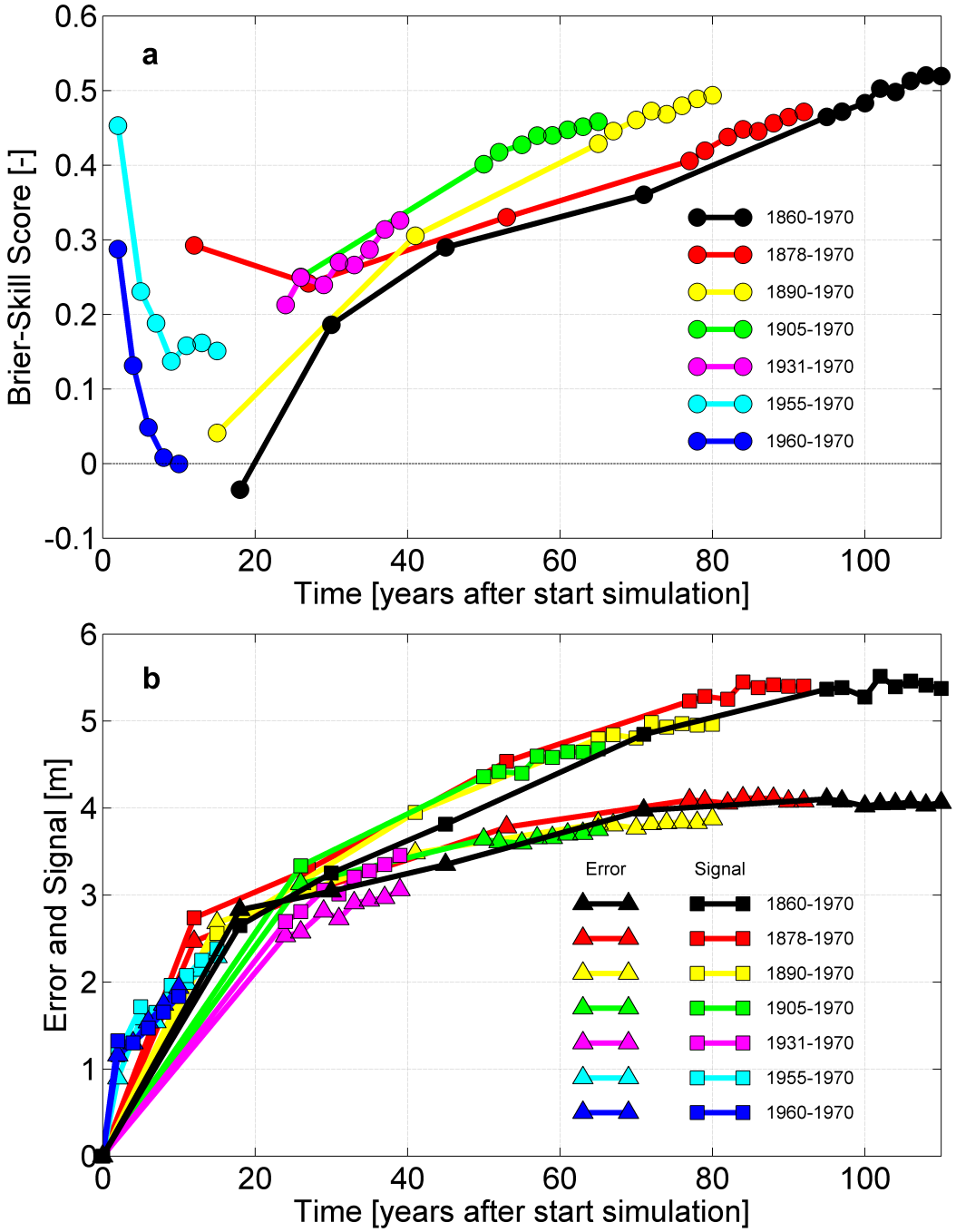

Figure 2.5: Brier-Skill Score and error versus signal for 7 simulations with different start years. (a) BSS. (b) Error and signal. Markers indicate comparisons between model and data, solid lines interpolate between subsequent comparisons. BSS, error and signal are determined over entire Western Scheldt area.

calibration with a maximum BSS of 0.52 for the 1860–1970 simulation. Several simulations with different parameter settings (morphological roughness and constant grain size) show positive BSS values after 110 years with a BSS of minimum 0.3 (good) to maximum 0.52 (excellent). A simulation from 1860 to 1970 without the erosion-resistant layer resulted in a BSS of 0.4. This means that the confinement of the erosion-resistant layer increases the skill of the model, but the effect is not so strong that the model skill is seriously affected.

2.5. TRENDS IN MORPHODYNAMIC ACTIVITY

GIVEN that the model reflects realistic developments, we now closely analyze the morphological behavior of the system. Morphodynamic systems under constant forcing conditions tend to minimize energy dissipation due to bed resistance (Langbein, 1963). This will eventually lead to morphological equilibrium (Cowell and Thom, 1996; Woodroffe, 2002) characterized by lower spatial gradients in shear stress and sediment transport (Rodriquez-Iturbe et al., 1992; Townend and Dun, 2000). A highly schematized process-based morphodynamic model of a tidal basin (similar to the model applied in this study) indeed leads to decreasing energy dissipation levels over long time scales (>decades) (Van der Wegen et al., 2008). The current study provides an excellent opportunity to evaluate the development towards equilibrium for a more realistic case study under constant forcing conditions.

We determine energy dissipation on both measured and modeled bathymetries for the 1860 run. The energy dissipation is determined by running the hydrodynamic model over a spring-neap tidal cycle without morphodynamic updating. Same parameter settings are used for all the simulations. The energy dissipation levels are subsequently averaged over the model domain and over time using the following formula (Van der Wegen et al., 2008):

$$P_e = c_W \rho_W |u|^3 A \tag{2.4}$$

Where: P_e is the energy dissipation in cell e $[W]$; c_W is the friction coefficient $[-]$; ρ_W is the water density $[kg/m^3]$; $|u|$ is the velocity magnitude $[m/s]$ and A is the surface area $[m^2]$.

In this way trends and differences between measured and modeled bathymetries can be made clear. To explore future developments of the system, we also extended the simulation time of the morphodynamic run from 1860 to the year 2110, so that a total of 250 years of morphological development is simulated. Both the measured and modeled bathymetries show similar declining (rates of) energy dissipation levels over time (Figure 2.6a). The total cumulative morphological change from 1860 onwards show for both the measured bed levels and the computed bed levels a pronounced trend to less morphodynamic activity over time and are in the same order of magnitude (Figure 2.6b).

After 250 years the energy dissipation and morphodynamic activity of the model appear

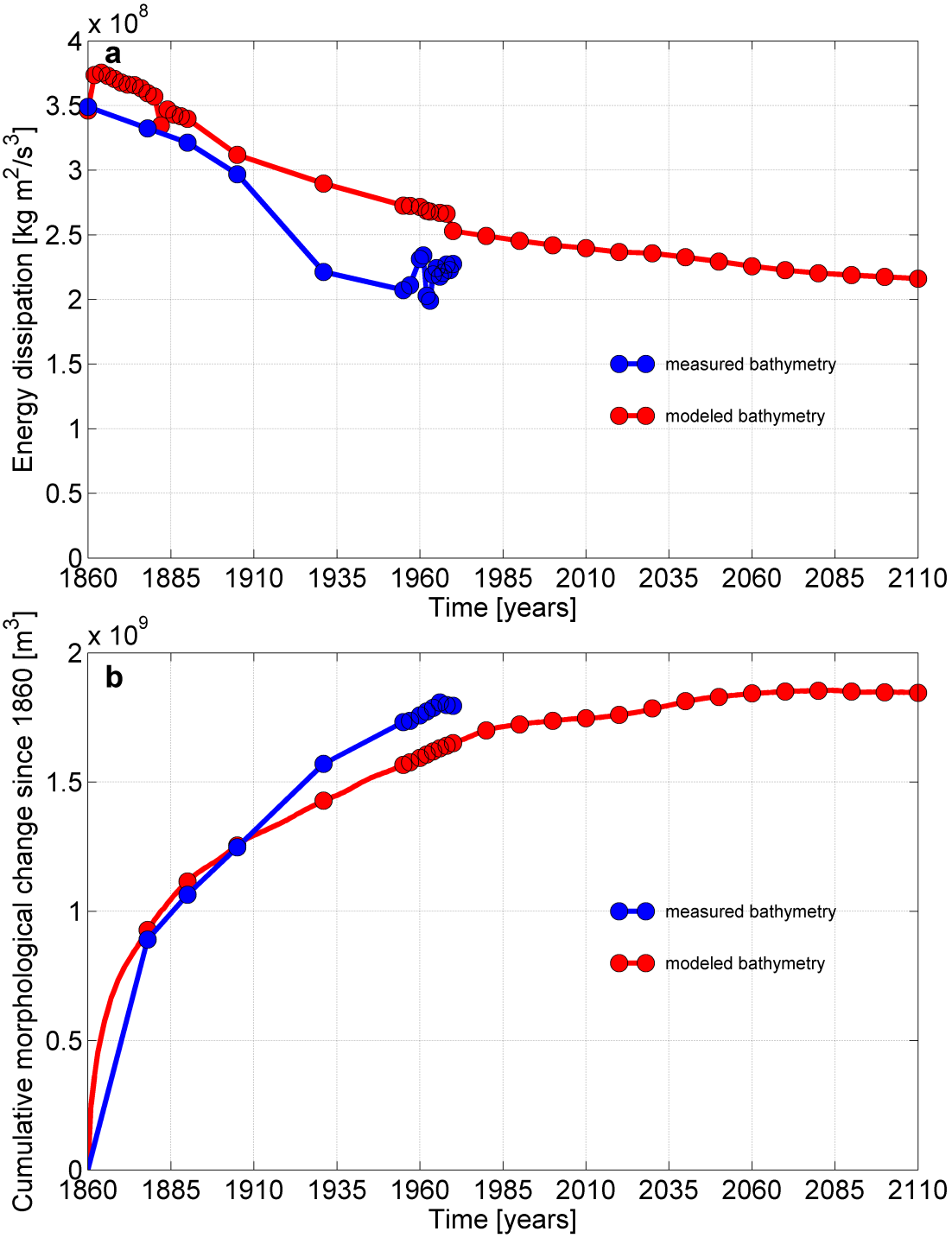

Figure 2.6: Results of energy dissipation and morphological change. (a) Energy dissipation over time. (b) Cumulative morphological change since 1860, defined as erosion volume + deposition volume since 1860. Markers indicate time points when a measured bathymetry is available, after 1970 model results are calculated every 10 years. Lines interpolate between these results.

to have reached a minimum. We attribute the small irregularities of the trend of measured bathymetries to inaccuracies in the (old) bathymetric recordings and subsequent interpolation errors on the computational grid. Land reclamations are included in the simulations causing a reduction of the total energy dissipation. Since these areas do not convey water but rather store it, reducing their surface area also reduces the tidal prism. Consequently, the tidal discharge in the channels decreases involving less energy dissipation. The sudden decreases in energy dissipation level of the modeled bathymetries around 1885 and 1962 can be attributed to this. Sensitivity runs with and without land reclamations however indicate that they are not the cause of the overall declining energy dissipation levels.

2.6. DISCUSSION

THE model skill is initially weak, but increases after decades to become excellent after 110 years. The question why the results become excellent after a century is attributed to the slow, but ultimately governing development of the large scale channel-shoal patterns. Small scale morphological features as secondary channels or the effect of storms may be more dominant on the short term, but are overruled over the long-term by cumulative larger scale developments that have a typical morphological time period of decades to centuries.

A further explanation for the low initial BSS is that the model initially adjusts the bathymetry according to uncertain parameter settings, boundary forcing and process descriptions. Examples are constant and uniform roughness values, the sediment grain size or schematized forcing conditions, like storm surges.

After this period of morphodynamic spin-up the cumulative effect of other subtle but eventually governing processes becomes more pronounced. The probable governing process is the interaction of the tidal forcing with the estuarine geometry (i.e. fixed bank lines and erosion-resistant layers) determining the allocation of channel-shoal patterns (Van der Wegen and Roelvink, 2012).

This suggests that process-based models applied in the confined environment of an estuary (where the morphology is influenced by fixed banks, erosion-resistant layers etc.) and subject to constant tidal and river forcing conditions perform well especially on long (> decades) time scales, which makes the approach potentially suitable for centennial time scale forecasts related to for example sea level rise or other gradual changes in forcing with a similar time scale.

The inclusion of other processes such as mud and sand mud interaction, does not necessarily have to lead to a better BSS. Adding processes could even cause extra weaking of the initial BSS due to the larger uncertainties associated with the process formulations. On the

other hand, longer term BSS could benefit from the extra dynamics. This remains subject of future research.

In contrast to chaotic systems like the atmosphere with a reliable weather forecast time of only several days (Lorenz, 1963), our model results confirm that estuarine morphodynamics strives for minimum energy dissipation (Langbein, 1963), eventually leading to morphodynamic equilibrium (Philips, 1999). Estuarine morphodynamics is thus a self regulating (organizing) system in which negative feedback of the large channels and shoals is dominating the morphological developments.

The results of this paper suggest that this morphodynamic equilibrium is predictable because of self-organization characterized by the tendency for minimum energy dissipation. The degrees of freedom in which the morphology can develop are limited by the plan form, the presence of erosion resistant layers, the well predictable tidal forcing (Haff, 2013) and the limited impact of extreme events like storms on long-term morphology (Van der Wegen and Roelvink, 2012).

The results found in this paper make that the general opinion of morphodynamic models should be revised. Process-based morphodynamic models are generally used for short-term simulations (i.e. maximum a few years), since it is assumed that the model results drift away from reality over time. Low BSS values that are found during this period are interpreted as bad model behavior. The conclusion from this paper is that the low BSS values might well be due to the morphodynamic spin-up time of the model and unresolved scales and that the morphodynamic changes during the initial simulation period are due to model limitations.

In principle the results that are found in this paper are applicable to other confined estuaries and morphodynamic systems. Still it leaves the question open to define "confined" in a strict manner. Obvious important indicators for a systems' confinement are channels aligned with headlands, dikes, rocky outcrops etc. Other important parameters are the autonomous (without lateral boundaries) meander amplitude in relation to the basin width. Further research should attempt to model other estuaries and systems including river and wave forcing and the presence of mud, for example, to explore a wider validity of the results presented in this paper.

2.7. CONCLUSION

We hindcast morphodynamic change of the tide dominated Western Scheldt estuary using a 2D process-based model. Initially the skill is bad, but after 110 years the skill of the model is excellent. The model error increases over time, but the signal increases eventually even more leading to high skill rates. This conclusion does not dependent on the

initial condition. The interaction of the constant tidal forcing with the estuarine geometry (i.e. fixed bank lines and erosion-resistant layers) is determining the allocation of channel-shoal patterns. We find that both the system and the model strive for morphodynamic equilibrium, characterized by the tendency for minimum energy dissipation.

2.8. ACKNOWLEDGEMENTS AND DATA

THIS work was made possible by contributions of Svašek Hydraulics and the Long term vision of the Scheldt project (LTV VT). The project consists of Deltares, IMDC, Arcadis and Svašek Hydraulics and was funded by the Dutch ministry of public works (Rijkswaterstaat) and Flemish department of mobility and public works. We thank Svašek Hydraulics for the use of their software and computational resources. Measured bed level data is available through Rijkswaterstaat (servicedesk-data@rws.nl). Model software is available upon request and against a fee at info @svasek.com. Model input is available at the corresponding author upon request. We declare no conflicts of interest.

3

CONTRASTING BEHAVIOR OF SAND AND MUD IN A LONG-TERM SEDIMENT BUDGET OF THE WESTERN SCHELDT ESTUARY

Understanding trends in estuarine sediment fluxes is of great interest to sustainable estuarine management addressing anthropogenic interferences and climate change. The long-term sediment budget of the Western Scheldt estuary, Netherlands, is investigated by a detailed analysis of a unique and long-term bathymetric data set and data of a three-dimensional subsurface model ('GeoTop'). Different sediment types show contrasting transport behavior. The Western Scheldt narrowed and deepened, while the estuary exported sand (1.5–2.5 million m^3/year) and imported mud (0.5–1.5 million m^3/year) over the 1860 to 1955 period. The eroded sand originated from the channels in the seaward part of the estuary and was dispersed in all directions. A significant amount of mud permanently deposited in the side branches, which were also gradually reclaimed. These results suggest that sediment characteristics potentially play a crucial role in deriving long-term sediment budgets and morphodynamic behavior of estuarine environments. Future morphodynamic sand–mud model studies may reproduce and further explain the underlying transport processes of the current study.

An edited and slightly adapted version of this chapter was published in Sedimentology, copyright Wiley (2022) Dam, G, Van der Wegen M., Taal, M. and A. J. F. van der Spek (2022), Contrasting behaviour of sand and mud in a long-term sediment budget of the Western Scheldt estuary, Sedimentology. https://doi.org/10.1111/sed.12992

3.1. INTRODUCTION

THE management of estuarine sediment fluxes is of great interest in relation to sustainable estuarine management. This includes for example dredging and disposal strategies to maintain port access (e.g. Bale et al. (2007)), sand mining permits, salt marsh management maintaining ecological values (De Vriend et al., 2011; Shellenbarger et al., 2013) and sea-level rise (Friedrichs et al., 1990).

Sediment budgets are a useful tool to establish the dominant influences on sediment transport trends and timescales of change in an estuary. A sediment budget quantifies the amount of sediment entering or leaving a predefined area of a coast or estuary over a selected period, typically years to decades (Rosati, 2005). This long time period is due to the fact that morphodynamic changes are slow and may become significant only after decades to centuries (Townend and Whitehead, 2003). During a tidal cycle, large quantities of sediment are transported in and out of the estuary compared to the net sediment transport. Shellenbarger et al. (2013) states that the net residual transport is usually less than 10% of the total flux in the flood or ebb direction and is difficult to measure. Sediment can originate from both marine and fluvial sources (Schubel and Carter, 1984; Dalrymple et al., 1992) and from the subsurface of the estuary itself. Sediment budgets covering years have been established for several estuaries around the world (e.g. Van der Wal et al., 2002; Thomas et al., 2002; Townend et al., 2007; Townend and Whitehead, 2003; Eyre et al., 1998; Barnard et al., 2013).

Sediment budgets are traditionally based on observational bathymetric data (Rosati, 2005). The data necessary for establishing these sediment budgets requires a long period of detailed and costly data acquisition of both sediment inflow, outflow and accumulation in the domain of interest. Bathymetry-based sediment budgets are derived from measured storage and erosion of sediments within a certain period (Rosati, 2005). Modelling of sediment transport and associated morphodynamics is an alternative method to establish a sediment budget (e.g. Falconer and Owens, 1990; Ganju et al., 2009a; Diaz et al., 2020). Modelling requires detailed and validated models that include all relevant processes and dynamics. The models may include significant uncertainty levels related to model input parameter values and process descriptions (Diaz et al., 2020), related to for example sediment class properties or hydraulic forcing like tides and waves.

Many estuaries encompass multiple sediment classes ranging from coarse gravel or sand to fine, cohesive mud. Because there is not enough field data to discriminate between sediment classes, sediment budget studies often consider only a single sediment fraction. The focus of this study is on sand and mud, because these classes are both abundantly present in the area of interest. Sediment transport measurements and modelling exercises show considerable differences in the behavior of sand and mud fluxes (Green et al., 2000), even

resulting in opposite residual transport directions (Bass et al., 2007; Diaz et al., 2020). Differences in transport behavior between the classes are related to sediment properties (for example, size and erodibility) and their specific response to forcing conditions (tidal currents, and estuarine density currents and waves). Sand is defined by non-cohesive particles with a grain size between 63 μm and 2000 μm. Under stationary conditions, equilibrium sand concentrations will develop in a water column, when deposition and erosion balance over alluvial beds (Van Ledden et al., 2004a). Cohesive sediments, here termed 'mud', are defined by a grain size <63 μm. Cohesive sediments have electrochemical forces that bind them together which depend on physical, geochemical and biological parameters like mineral composition, organic content, biological processes, consolidation, pH, salinity and metal concentrations (Mitchener and Torfs, 1996; Grabowski et al., 2011). In contrast to sandy environments, mud sediment concentration in the water column is often limited by mud availability in the bed and higher erosion resistance of lower lying consolidated mud (Van Ledden et al., 2004a).

The sediment type determines the mode of sediment transport in response to hydraulic forcing. Bed load is a function of local tidal velocities and occurs for coarser sand fractions that immediately react to changing flow conditions. In contrast, the transport of suspended sediment (of sand or mud) lags behind the flow. This phase difference between the sediment concentration and flow causes tide residual sediment transport. Since lag effects depend on the fall velocity of the sediment particle in water, the effect gets larger for finer sediment. Lag effects can be identified by the threshold-lag, the erosion-lag, the scour-lag and the settling lag (Dyer, 1995; Van Straaten and Kuenen, 1957; Groen, 1967). The horizontal sediment fluxes due to phase differences between the velocity, concentration and water depth, which arise mainly because of threshold and erosion lags in sediment response to the tidal current asymmetry, are known as tidal pumping (Dyer, 1995). Luo et al. (2013) show that heterogenic bed sediment conditions also have considerable influence on residual sediment flux direction. In addition to tidal currents, estuarine density currents (gravitational circulation) cause a landward tidal residual flow near the bed and a seaward flow near the water surface with a pronounced effect on the sediment transport and morphology (Olabarrieta et al., 2018). Density effects can create an estuarine circulation resulting in an Estuarine Turbidity Maximum, ETM (Dyer, 1995).

In practice, the differences between sand and mud properties and transport processes imply a horizontal sand–mud segregation. Mud generally settles in quiet areas with low hydrodynamic forcing, such as harbor basins and sheltered intertidal areas with sufficient accommodation space (Van Maren et al., 2016), while sand is dominant in areas with strong forcing conditions, such as tidal channels or wind–wave exposed intertidal shoals (Van Ledden, 2003). In addition, morphodynamic changes over time and anthropogenic influences can result in different sediment transport paths. Lesourd et al. (2016) show that the building of embankments along the Seine estuary (loss of accommodation space) has increased

mud deposition in the mouth of the estuary over time. Similar to the approach applied in this study, Alonso et al. (2021) present a sediment budget study of the Wadden Sea by discriminating between sediment classes. Their conclusion is that the infilling of the Wadden Sea in response to a dam closure caused redistribution of sand and mud, which responded differently spatially and temporally.

The aim of this work is to derive separate sediment budgets for sand and mud fractions over the 1860 to 1955 period in the Western Scheldt estuary. This work differs from other sediment budget studies in the sense that it explicitly differentiates between sand and mud, it includes an analysis of subsurface sediment composition [in contrast to Alonso et al. (2021), who focuses on the top layer only] and it is based on a unique long-term bathymetric data set of more than 100 years. This dataset emerged probably due to the importance of access to the port of Antwerp. The analysis is based on a combination of bathymetric surveys and the subsurface model GeoTop that describes the sediment composition of the Western Scheldt subsurface, based on interpolation of a dense network of borehole data (Stafleu et al., 2011).

The focus is on the period between 1860 and 1955 because high quality bathymetric data for the entire domain is available from 1860 onward. Data from 1955 onward has not been used in this study since the estuarine morphodynamics and sediment budget have been influenced significantly by interventions such as sand mining, maintenance dredging and deepening of the navigational channel.

3.2. STUDY AREA: THE SCHELDT ESTUARY

3.2.1. GENERAL

THE Scheldt estuary (51°25'N, 4°E) is one of the major estuaries of North-West Europe. The coastal plain estuary is approximately 160 km long and is located both in Dutch and Belgian territory. The seaward part with a length of about 60 km is called the Western Scheldt (Figure 3.1) and has a width of almost 5 km near the mouth (Vlissingen) and 1 km near the Dutch-Belgian border.

The estuary is very young compared to other estuaries that were formed during the sea-level rise in the Holocene (Russell, 1967; Van der Spek, 1997). The Western Scheldt was limited in size and had only a small connection with the river Scheldt until around 1400 AD. The main discharge of the river Scheldt was, until then, through the Eastern Scheldt estuary, located north of the Western Scheldt. Shifts in the watershed between the Eastern and Western Scheldt due to storm surges and (man-made) inundations finally tipped the balance in favor of the Western Scheldt in the 16th century (Vos, 2015). In the years after,

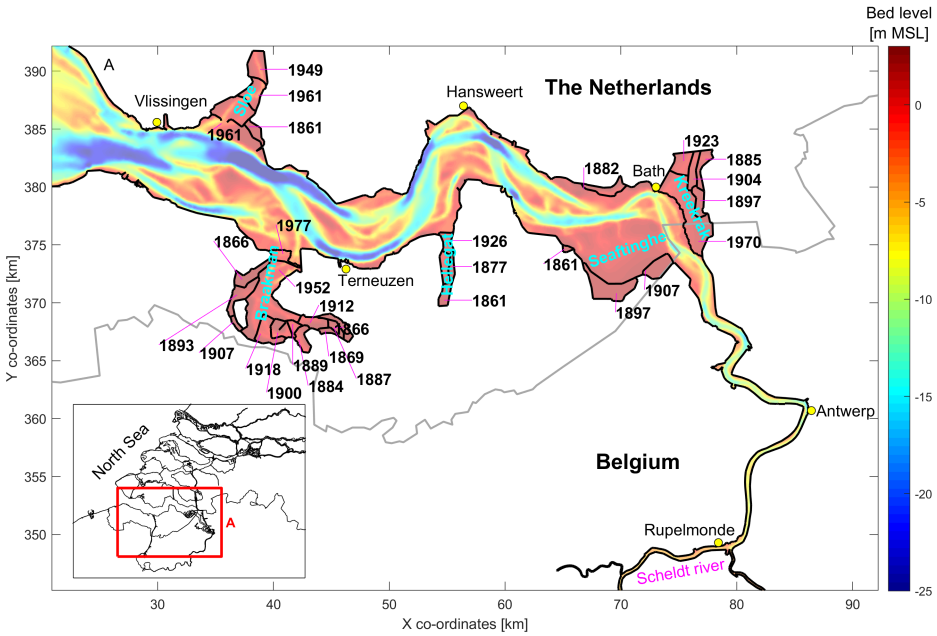

Figure 3.1: Layout of the Western Scheldt around 1860. Depth in MSL. Numbers indicate the year of reclamation. Coordinates in km with reference to Paris.

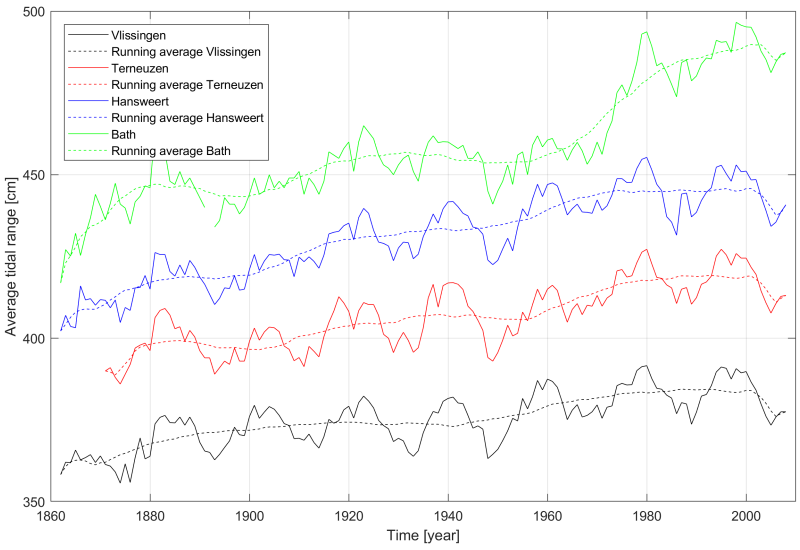

Figure 3.2: Measured yearly average tidal range (difference between high water and low water) for 4 stations in the Western Scheldt, including a running average to compensate for the 18.6 year nodal cycle. Location of the stations are shown in Figure 3.1

the channels eroded (Coen, 1998; Van der Spek, 1997; Vos, 2015) and the estuary expanded. During the 80-year war between the Netherlands and Spain (1568-1648) land around the estuary was deliberately flooded to hold invading armies. In addition, storm surges caused inundations, which resulted in the largest extension of the Scheldt estuary. In the following centuries, the inundated land silted up and was progressively reclaimed (Van der Spek, 1997). The reclamation consisted of constructing dykes. The land reclamations from 1860 onwards together with the present-day layout are shown in Figure 3.1. The connections with the Eastern Scheldt were closed off by damming in 1867 (Kreekrak) and 1871 (Sloe) (Dam et al., 2016).

The Western Scheldt is characterized by a multiple channel system (Figure 3.1). Ebb and flood channels show evasive behavior and are separated by intertidal shoals (Van Veen et al., 2005). The ebb channel has a meandering character, while the flood channel is straighter (Figure 3.1). The ebb flow reaches it maximum velocity near mean sea level (MSL), while the flood flow reaches its peak one hour before high water (Van Den Berg et al., 1996). As a consequence, the ebb flow is more concentrated in the channels, resulting in deeper ebb channels. The ebb channel is therefore generally designated as the navigational channel in the Western Scheldt. The channels are generally sandy (Wartel, 1977) while the intertidal flats are muddier (Braat et al., 2017). Shoals closer to sea become sandier because they are more prone to wave action. The seabed includes peat layers and layers deposited in the Pleistocene and Tertiary periods which are hard to erode (Gruijters et al., 2004; Dam, 2013).

The tidal range amplifies in landward direction as a result of convergence, shoaling and partial reflections of the tidal wave (Jeuken, 2000). Furthermore, the tidal range (Figure 3.2) and the tidal celerity in the estuary have increased significantly over the centuries (Van der Spek, 1997). The increase in tidal range/celerity is stronger towards the head of the estuary (Figure 3.2). Nowadays the tidal range is 3.8 m near the mouth and over 5 m near Antwerp, almost 80 km from the mouth of the estuary. Upstream of Antwerp the tidal range decreases.

The river discharge is on average 100 m^3/s, being only 0.6% of the tidal prism at the mouth. The estuary is therefore well-mixed (Baeyens et al., 1998). Still, density driven flows may play a significant role in transport of fine sediments. The estuary has three estuarine turbidity maxima (ETM). The first marine-dominated ETM is located in the mouth of the estuary, the second river-dominated ETM is located in the upper river and the third, most important, ETM with sediment concentrations up to several hundreds of mg/l is located in the middle estuary (Chen et al., 2005).

The river discharge is on average 100 m^3/s, being only 0.6% of the tidal prism at the mouth. The estuary is therefore well-mixed (Baeyens et al., 1998). Still, density driven flows may play a significant role in transport of fine sediments. The estuary has three estuarine

turbidity maxima (ETM). The first marine-dominated ETM is located in the mouth of the estuary, the second river-dominated ETM is located in the upper river and the third most important ETM with sediment concentrations up to several hundreds of mg/l is located in the middle estuary (Chen et al., 2005).

Figure 3.3 shows the observed bathymetries from 1860 to 2018. Compared to river flow and wave action, the tidal motion dominates the long-term large-scale morphological changes in the Scheldt estuary (Wang et al., 2002; Dam et al., 2016; Coen, 1998) and the migration of the large channels. The erosion/sedimentation pattern of 1860-1955 is shown in Figure 3.4. The channel 'Pas van Terneuzen' moved westwards ('A' in Figure 3.4), while the Honte moved to the north ('B'). At the location of the old channels intertidal bars developed. Furthermore, a new flood channel 'Overloop van Hansweert' was created ('C'). The opposite channel "Middelgat" migrated to the outer bank ('D'). Between the two channels a new intertidal shoal developed. In the eastern part of the estuary, the main ebb channel 'Zuidergat' moved to the outer bank ('E').

3.2.2. VOLUME CHANGE STUDIES

Van Veen (1944) found erosion in the western part of the Western Scheldt for the 1860 to 1931 period based on bathymetric datasets, and also found that in the outer delta (seaward of Vlissingen) over the 1823–1931 period a total of 480 million m^3 was eroded. Van Veen (1944) suggests that the erosion in the outer delta and the western part of the Western Scheldt are in line with one another. One interpretation of this could be that the outer delta and the western part of the estuary should be considered as one (eroding) system. Haring (1948) investigated the volume changes of the Western Scheldt for the period 1878 to 1931 and later for the period 1931 to 1952 (Haring, 1955), and also found that the western part of the estuary eroded, while the side branches and the eastern part of the estuary showed sediment accumulation. Coen (1998), Van der Spek (1997) and Vos (2015) also pointed to the large erosional behavior of the channels during this period. For a more recent period Wang et al. (2002) found a loss of 20 million m^3 in the western part of the estuary for the period 1955 to 1996, which seems to be consistent with the earlier period. Large sand extractions did not occur in this area before 1996, so the erosion during this period is considered to be natural behavior of the system. Unfortunately, no physical explanation regarding the erosion in the western part of the estuary is given in these studies.

3.2.3. MUD STUDIES

BASED on empirical data and numerical modeling, Van Alphen (1990) calculated a net residual input of marine mud of 0.6 million ton/year into the estuary between 1969 and 1986. Manni (1986) calculated an import of marine mud of 0.5 million ton/year at

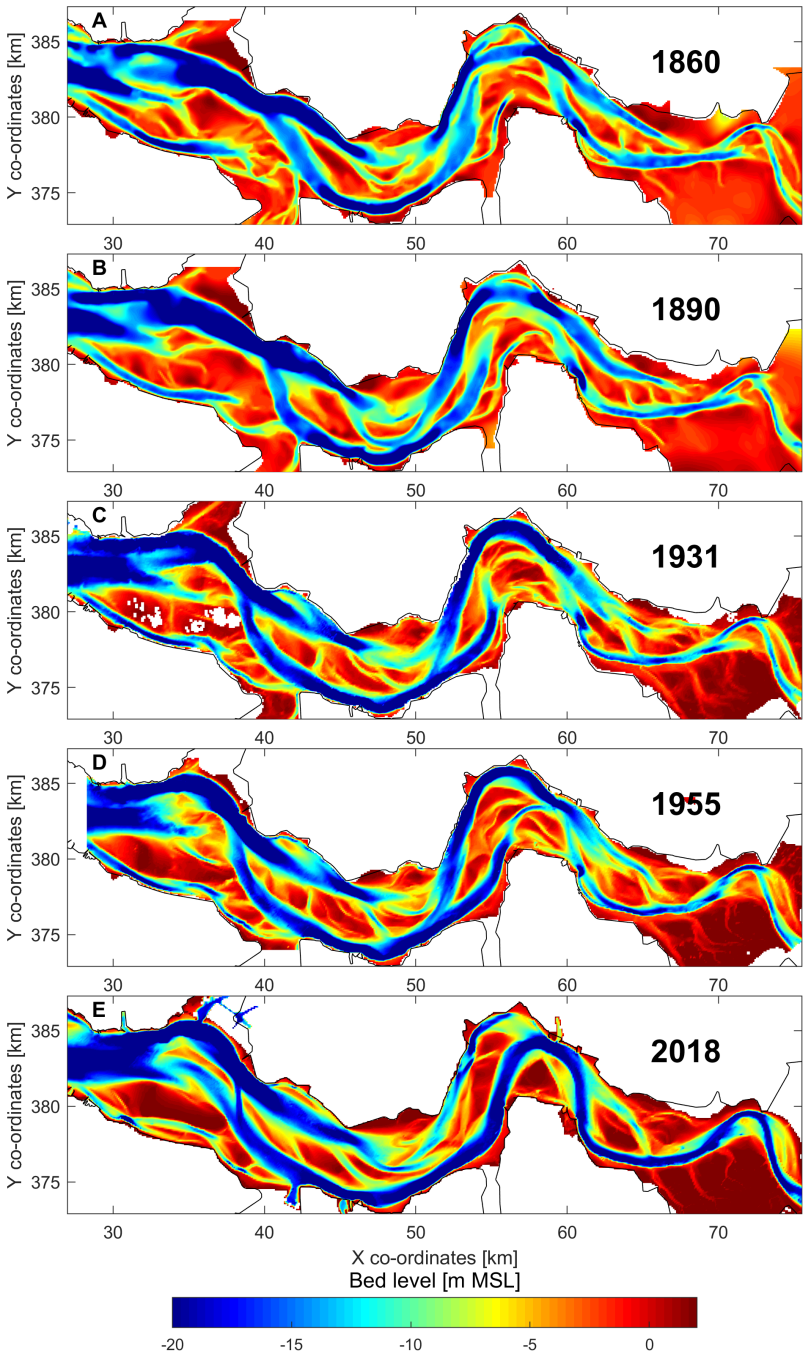

Figure 3.3: Bathymetric observations of the Western Scheldt. (A) 1860 (B) 1890 (C) 1931 (D) 1955 (E) 2018. Coordinates in km with reference to Paris.

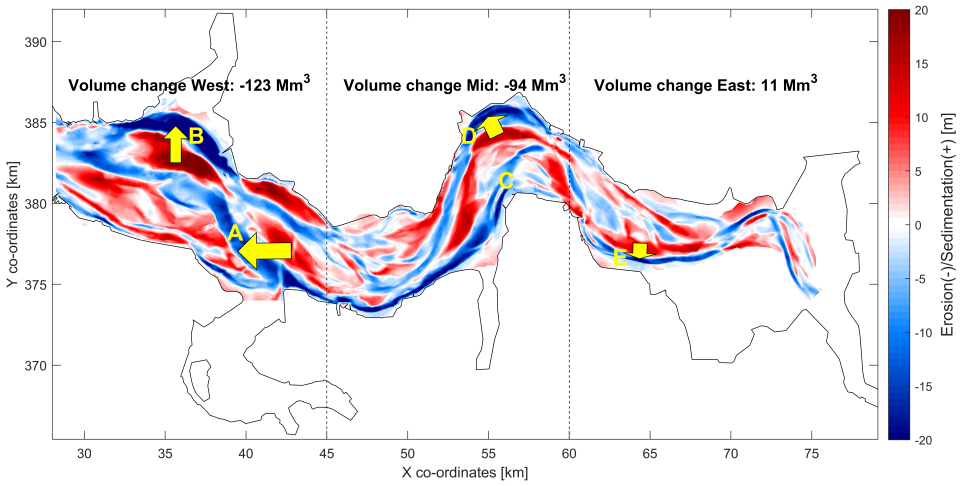

Figure 3.4: Measured erosion/sedimentation pattern 1860-1955; Vertical lines at X-km 45 and X-km 60 indicate the border between the western, middle and eastern section. Numbers indicate the volume change per section during this period. Migration and development of main channels are indicated by A-E. Coordinates in km with reference to Paris.

the mouth over the 1955-1980 period, and estimates that 0.4 million ton/year has permanently deposited in the Western Scheldt. Furthermore, Manni (1986) mentions that especially secondary channels have experienced considerable mud deposition. Van Maldegem et al. (2003) reported an import of marine mud of 0.2 million ton/year at the mouth and 0.1 million ton/yr at the Dutch/Belgium border (Figure 3.1) for the period 1975 to 1985. The natural transport of fluvial mud in seaward direction was estimated at 0.3 million ton/year at Rupelmonde (Figure 3.1), 0.4 million ton/yr at the Dutch/Belgium border and 0.2 million ton/year at the transition between the eastern and western part of the estuary (See Figure 3.1). Verlaan et al. (1998) estimated that the fluvial mud input of the Scheldt lies around 0.37 million ton/year for the years 1973 to 1986. After construction of water treatment plants, the fluvial input reduced to 0.075-0.280 million ton/year for the years 1992-1997. Trapping efficiency of the fluvial mud is the Scheldt estuary is estimated to be around 80% (Van Maldegem et al., 2003) for recent periods. Very little fluvial mud reaches the sea at present.

Several field studies have explored the origin of mud in the Scheldt estuary. Based on the trace mineral manganese, Terwindt (1967) showed that the origin of the mud in the Western Scheldt is marine dominated in the western part, whilst the eastern part has a mixed origin of marine and fluvial mud, and the river section in Belgium has a fluvial background. Verlaan (2000) used heavy metals in bed samples to determine the origin of mud, and concluded that the upper-estuary consists of 10% marine mud, around the Dutch/Belgium border (Figure 3.1) a sharp transition occurred from 10 to 75% marine origin. Further seaward, this number further increases to 95%. Chen et al. (2005) used the natural carbon isotope δ13C as a tool for identifying the origin of suspended mud. The fluvial origin of the suspended mud is 70 to 90% at Rupelmonde (Figure 3.1) and around 55 to 65% at the

Dutch/Belgium border. All of these studies confirm the relative importance of the marine mud import in the Dutch part of the estuary and fluvial mud in the tidal river section in Belgium. Dyer (1995) indicates that in most estuaries the marine import of mud is dominant until the Estuarine Turbitity Maximum (ETM) while Guilcher (1967) stresses that every estuary is different and can be fluvially dominated, marine dominated or a combination of the two.

3.3. METHOD

3.3.1. THE THREE-DIMENSIONAL SUBSURFACE MODEL 'GEOTOP'

GEOTOP is a 3D-model of the subsurface of the Netherlands up until -50 m depth with a resolution of 100 x 100 x 0.5 m (Staffleu et al., 2011). Each gridcell (voxel) contains properties such as the lithographic or geological unit (layer) to which the voxel belongs, the lithoclass (sand, gravel, clay or peat) that is representative for that voxel and a number of properties containing uncertainties of the different geological properties. Besides the voxel model and the layer model, GeoTop also contains the borehole descriptions used to make the model.

The 3D subsurface model GeoTop of the province of Zeeland is used (TNO, 2017), where the Western Scheldt is located. This subsurface model is based on a dataset of 23,000 boreholes describing sediment properties that were collected over the past decades.

The procedure to fill the grid cells (voxels) of the model is as follows. Firstly, the borehole descriptions are schematized into uniform sediment characteristics, using litho-stratigraphical, lithofacies and lithological criteria. Then, 2D bounding surfaces are constructed for the top and base of the litho-stratigraphical units. These surfaces are used to place each voxel into the correct litho-stratigraphical unit. Next, the lithological units in the borehole descriptions are used to make a 3D stochastic interpolation of lithofacies, lithology (clay, sand and peat) and grain-size classes. A measure of uncertainty is also available for each voxel. Generally, the uncertainty is low where a high number of boreholes is available. The bathymetry of the Western Scheldt that is used to build the model is from 1999.

The litho class definitions of Figure 3.5 are used to make a division in clay, clayey sand and sand. The sand class is divided in fine sand (63-150 μm), medium coarse sand (150-300 μm) and coarse sand (300 μm-2 mm). Peat is present at certain locations, sometimes directly at the surface. The peat layers are usually compacted and erosion-resistant layers.

Figure 3.6 shows the lithography in a cross-section and longitudinal section in the Western Scheldt based on the GeoTop data. The 1860 and 1955 bathymetry are plotted in these sections.

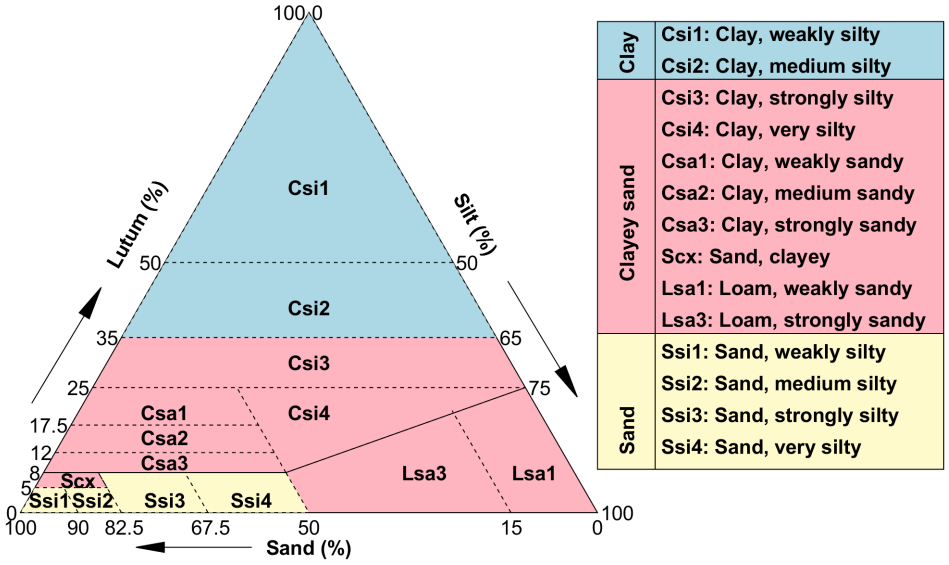

Figure 3.5: Division in litho classes Clay (blue), Clayey sand (pink) and Sand (yellow) after (Vernes and Doorn, 2005)

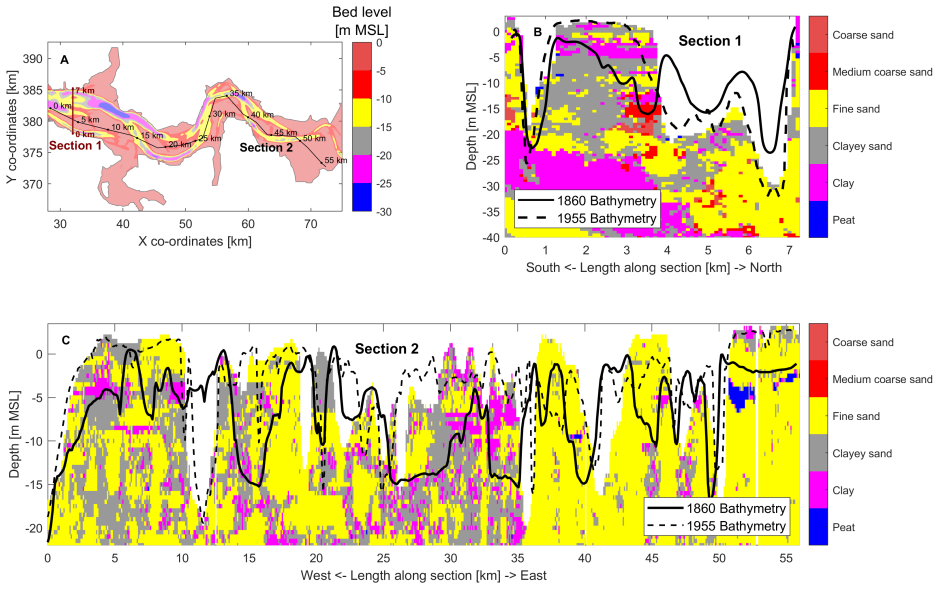

Figure 3.6: A) Overview of section 1 and section 2. B) Cross-section at X=32 km showing most probable litho class. C) Longitudinal cross-section showing most probable litho class. Black solid and dashed lines show the measured depths of 1860 and 1955.

3.3.2. FROM BATHYMETRIC DATA AND GEOTOP DATA TO SEPARATE SAND/MUD BUDGETS

THE following steps describe how to derive sand and mud budgets from the bathymetric data (Rijkswaterstaat, 2013) and the GeoTop data (TNO, 2017). Firstly, subsequent bathymetric data (Rijkswaterstaat, 2013) that cover the entire Western Scheldt over the 1860 to 1955 period are subtracted from one another, which results in volume changes over time. Volume changes are determined for the east, middle and western part of the estuary plus the side branches. Then, separate sand and mud volume changes are extracted from the GeoTop data for the areas that showed deposition during the 1860 to 1955 period and that are (for the most part) present in the GeoTop data of 1999. These depositional areas are mainly the bar systems in the main estuary (red areas of Figure 3.4) and the side branches. However, for the eroded areas (blue areas of Figure 3.4), no lithological information is available. Therefore, two scenarios are defined to investigate the sensitivity. The first scenario assumes that the mud that settled in the main estuary originated from erosion within the estuary. The second scenario assumes that all mud originates from outside the estuary and can have both a fluvial and marine origin. Assumptions are defined on the fluvial sand and mud flux on the river boundary. Finally, a control on the measured marine mud import (see section 'Mud studies') is carried out. The steps defined are elaborated in the next section leading to an estimate of the net sediment transport flux for both sand and mud between the western, middle and eastern part of the estuary.

3.4. RESULTS

3.4.1. VOLUME CHANGES OF THE MAIN BED AND THE SIDE BRANCHES

BY subtracting sequential bathymetric data (Rijkswaterstaat, 2013) from the 1800 bathymetry the cumulative volume change between 1800 and 2015 in the main estuary body is calculated (data presented in Figure 3.4 is defined as 'main estuary body'). The volume change shows a continuous loss of sediment with a total loss of around 400 million m^3 over 2 centuries (Figure 3.7).

Figure 3.4 shows that the western section eroded by some 123 million m^3 between 1860 and 1955. In addition, the middle section also showed erosion. The eastern part is relatively stable with an increase of 11 million m^3. In total 206 million m^3 of sediment eroded from the main estuary body during the 1860-1955 period. The western and middle section are thus the main contributors to the sediment loss of the estuary in this period.

Changes in the reference level of the bathymetries due to sea-level rise are not accounted for. Sea-level rise over this period was about 15 cm per century. This would theoretically

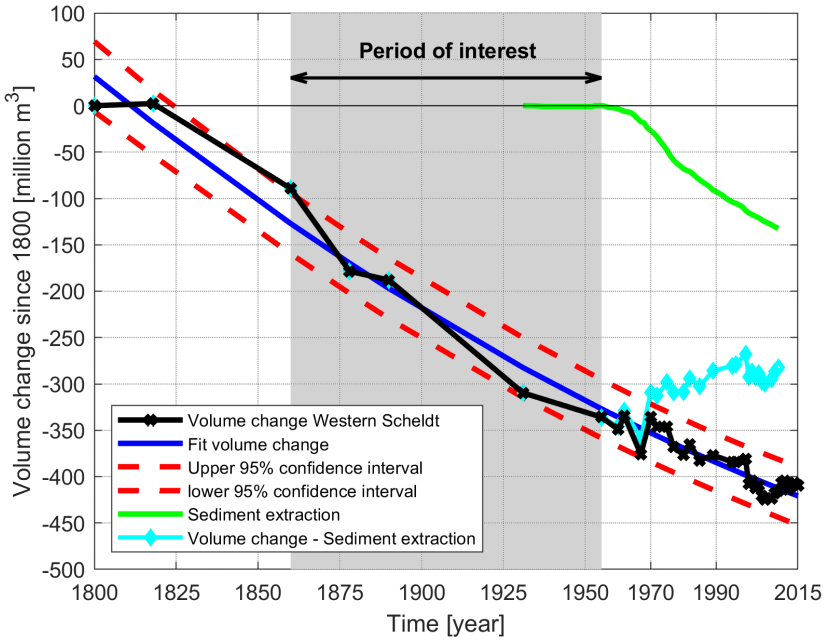

Figure 3.7: Cumulative volume change since 1800

give an import of around 30 million m^3 over 100 year (15 cm times the surface area of the Western Scheldt), assuming that the reference level changed with the sea-level rise. This amount is much smaller than the observed trend. Therefore, the conclusion is that this effect is small, and comparable with the accuracy range of the bathymetrical data. It has therefore been disregarded in this analysis.

The side branches of the Western Scheldt (Sloe, Braakman, Hellegat, Kreekrak, Saeftinghe, see Figure 3.1) have functioned as efficient sediment traps (Haring, 1948, 1955). They were largely reclaimed after the bed level had accreted to supratidal levels (Van der Spek, 1997). The sedimentation in the side branches is determined by digitizing old topographic maps and combining them with bathymetric data where available. For the final bed level of the reclaimed areas recent LiDAR (light detection and ranging) bathymetry data is used. After reclamation, the area is closed off from the sea and its sediment supply. A recent LiDAR data is therefore the best estimate for the final height after closure, although the land might have compacted and been reworked by humans afterwards. Note that there is height information of the unreclaimed Saeftinghe branch of 1955; hence, no LiDAR data was used here. In total a sediment volume of 111 million m^3 is calculated for all the side branches during the 1860 to 1955 period, based on the available bathymetric information (Figure 3.8). The Saeftinghe side branch (Figure 1) is the only branch that is still connected to the estuary to this day with large extents of saltmarshes. In this area, a sedimentation of 42 million m^3 occurred between 1860 and 1955 (Figure 3.8a). This gives an average net sedimentation of around 400.000 m^3/year. After 1955 the salt marsh grew higher and an additional 18 million m^3 was deposited in the period 1955 to 2015. Presently, this salt marsh is only flooded

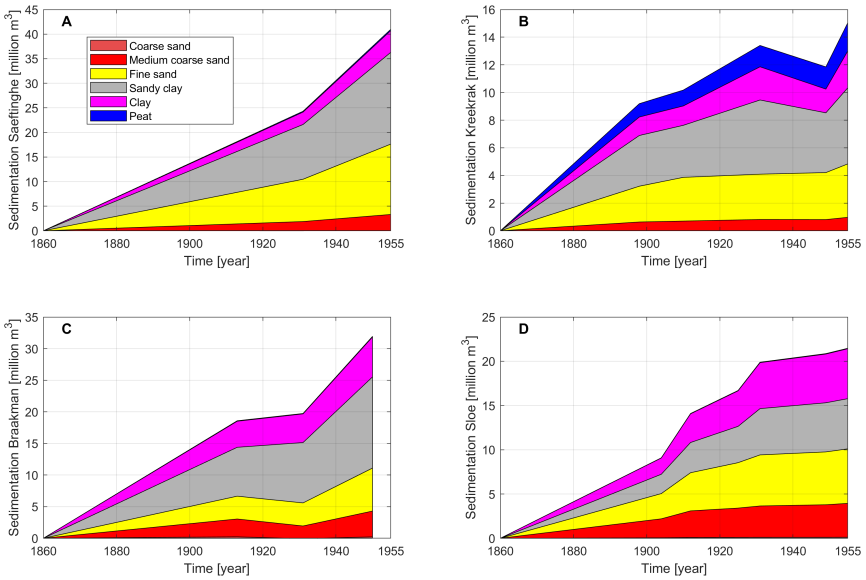

Figure 3.8: Cumulative sediment deposit for the 4 main side branches; A) Saeftinghe B) Kreekrak C) Braakman D) Sloe

during spring and storm tides. The sedimentation of the other side branches ranges from 14 to 32 million m^3 over the 1860-1955 period (Figure 3.8b-d). The Hellegat side branch was not shown in figure 8 since only 2 million m^3 was deposited here over the 1860 to 1955 period.

3.4.2. COMBINING BATHYMETRY AND GEOTOP DATA

IT is now possible to determine the composition of the deposited sediment over the 1860 to 1955 period if the GeoTop subsurface data (TNO, 2017) is combined with the bathymetric data. During the 1860 to 1955 period large bar systems were built (figure 3.4), which are still present. In addition, the side branches showed a large sedimentation. This gives the possibility to look back and see how much and which type of sediment was deposited.

For the main part of the estuary the sediment deposition during this period is coarse at large depths and becomes finer towards the top (Figure 3.9a). Coarse sediments accumulate in deep areas with high current velocities and during the buildup of sediment currents decline, with increasingly finer sediments being deposited. Around MSL there is a sharp transition to clay and clayey sand. However, the amount of sediments above MSL does not contribute significantly to the total amount of deposited material (Figure 3.9b). The total sediment volume that was deposited in this period amounts to 650 million m^3 (Figure 3.9b). These are the red-colored areas of Figure 3.4. Around 91 million m^3 of the deposit is clay (14% of total) and 208 million m^3 is clayey sand (32%). Fine sand amounts to 255 million m^3 (32%) and medium coarse sand around 89 million m^3 (14%). Peat and coarse sand

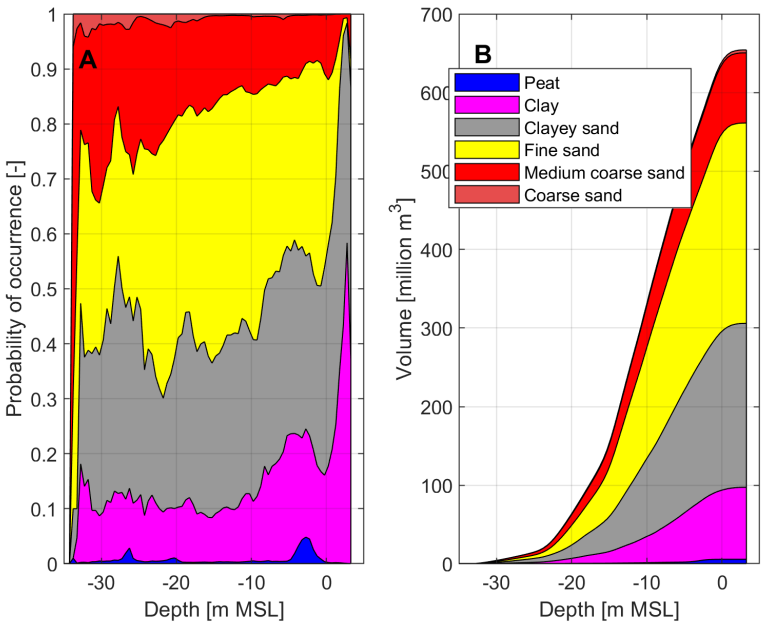

Figure 3.9: Left figure: Probability of occurrence for a litho class over the depth; Right figure: Cumulative build-up of sediment type. Both figures are based on the sediment deposition in the Western Scheldt of the 1860-1955 period (without side branches).

are (almost) absent. The cumulative clay deposit ranges several meters (Figure 3.10) in the deposits of the bar systems. Especially the western part of the estuary shows large clay deposits (48.7 million m^3). The sedimentation in the side branches can also be determined from the GeoTop data (Figure 3.8). The sand fraction (coarse and medium coarse sand) is less than 50% of the total sedimentation. Based on the GeoTop data, large amounts of mud have settled in these areas.

3.4.3. RESULTING SEDIMENT BUDGET

To further construct the sediment budget of the Western Scheldt, certain assumptions need to be defined. First, following (Dam and Cleveringa, 2013), a landward transport for the sand fraction of 300.000 m^3/year is assumed at the Dutch-Belgium border (cross-section 'D' in Figure 3.11). For the mud fraction a seaward transport of 150.000 m^3/year is assumed here (Van Maldegem et al., 2003).

Two scenarios are defined to investigate the sensitivity of mud origin from within or outside the basin: The first scenario assumes that mud settled within the main estuary (91 million m^3 of clay, see Figure 3.10) originates from within the same estuary. That is, the erosion by migrating (large) sandy channels always releases a small fraction of mud (here around 2-5%). The large volume eroded (Figure 3.7) could therefore generate enough mud to account for the observed mud deposition in the main estuary body. For the side

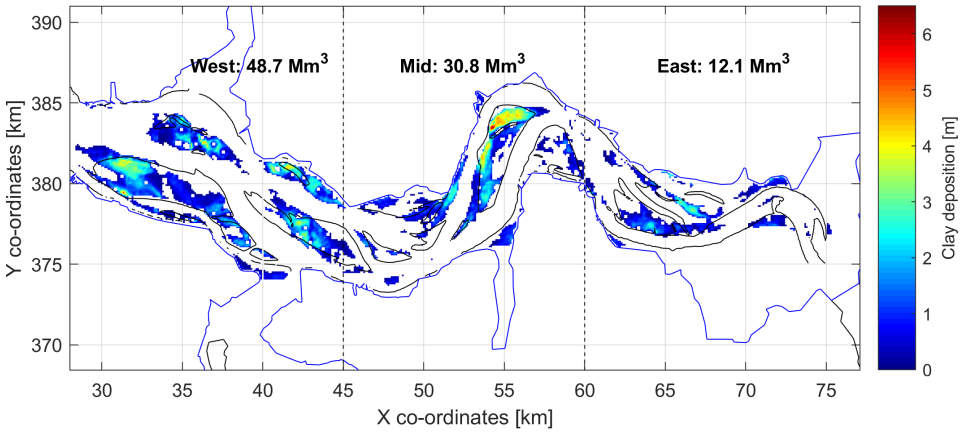

Figure 3.10: Cumulative deposition of clay of the 1860 to 1955 period in the main estuary body based on GeoTop data. Coordinates in km with reference to Paris.

branches, however, it is assumed that the mud originates from the sea or the river. The second scenario assumes that all mud that settled within the main estuary (Figure 3.10) and side branches 3.8 originates from outside the estuary, i.e. either from the river or from the sea.

A subsequent assumption is that both the clay and clayey sand fraction of the GeoTop data in the side branches are defined as mud. Field studies indicate that the mud in the eastern part is mainly from marine origin (Terwindt, 1967; Van Alphen, 1990; Manni, 1986; Van Maldegem et al., 2003). In order for the mud flux to be landward in cross-section 'C' (Figure 3.11), the volumetric amount of the mud fraction in Scenario 1 should consist of the clay and clayey sand fraction in the side branches. By assuming that the mud fraction consists of the clay fraction alone the resulting flux in cross-section C (Scenario 1) is seaward, which is incorrect. Previous studies assumed that half of the sedimentation in the Saeftinghe branch was mud (Dam and Cleveringa, 2013). If the mud fraction in the side branches is 50%, both clay and clayey sand should be considered as mud.

The sand and mud balance can now be generated for both scenarios, see Figure 3.11. Both scenarios give a sand export (135 and 226 million m^3) and a mud import (54 and 146 million m^3) at the mouth of the estuary. This gives a yearly averaged sand export between 1.5–2.5 million m^3/year, while averaged mud import lies between 0.5-1.5 million m^3/year.

The main difference between the scenarios lies in the internally generated mud fraction due to the erosion in the estuary. If this amount is zero (Scenario 2), the marine mud import is higher and in order to close the budget the resulting sand export is also higher.

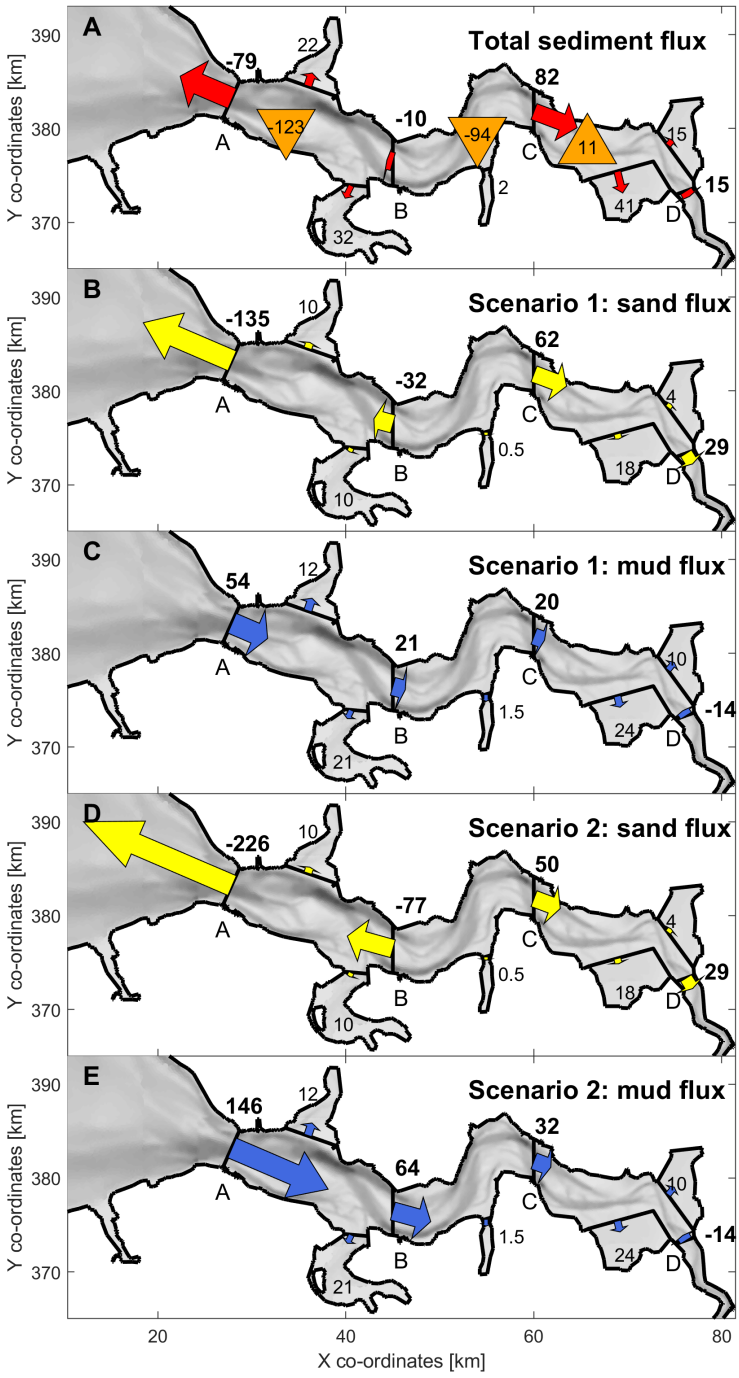

Figure 3.11: Sand and mud budget of the 1860-1955 period. A) Total sediment budget B) Sand budget Scenario 1. C) Mud budget Scenario 1. D) Sand budget Scenario 2 E) Mud budget Scenario 2. Numbers indicate the net sediment flux where negative is seaward. Numbers in triangles indicate the volume change of that section, where negative is erosion. All numbers are in million m^3 cumulative over the 1860-1955 period.

3.5. DISCUSSION

3.5.1. GENERAL UNDERSTANDING OF MORPHODYNAMIC DEVELOPMENT AND RESULTING SAND FLUX

On a geological time scale, and considering that the estuary expansion has started only in the Middle Ages, the Western Scheldt is a relatively young estuary (Vos, 2015). Over the centuries, the tidal channels have become larger (Coen, 1998; Van der Spek, 1997; Vos, 2015). Van Veen (1944) and Haring (1948, 1955) found similar erosion in the western part of the estuary in this period, a trend that is confirmed by this sediment budget study. Although recent bathymetries are more reliable than the historic bathymetries, the large-scale trend in volumetric erosion before 1955 seems logical and trustworthy.

This sediment budget study finds a sand exporting trend at the mouth (Section 'A' of Figure 3.11) and a sand importing trend further landwards in the estuary (Section 'C' of Figure 3.11). This phenomenon of a sediment exporting seaward part and a landward importing part of the estuary has been described earlier by Schuttelaars and de Swart (1999) and Van der Wegen and Roelvink (2008), and is consistent with the concept of a stability shear stress of Friedrichs (1995). Here an equilibrium is reached when the spatially varying shear stress is uniform, resulting in a deep seaward part and a gradual shallower landward part. Based on his volume calculations, Van Veen (1944) also mentions this 'sand flow' that transports sand from mid-basin in landward direction. In the eastern part there is limited storage and the sand import at cross-section C is largely balanced by transport towards the side branches in the eastern section and the upper river section (note that this is assumed).

Van der Wegen et al. (2008) showed that estuarine morphodynamics can be divided into two timescales: a short timescale in which the channel-bar pattern develops; and a second longer timescale in which the longitudinal cross-section develops. The sediment fluxes found in the current study suggests that the longitudinal cross-section was (still) developing over the 1860 to 1955 period. This is in accordance with the results of Dam et al. (2016) that show that the Western Scheldt is striving towards equilibrium, with decreasing morphodynamic activity and energy dissipation (Figure 2.6). This might also be related to the volumetric change (Figure 3.7), which seems to decrease slightly over time. Still this decreasing trend is not very pronounced and within the accuracy range of this sediment budget study.

Van der Wegen et al. (2008) show that an estuarine longitudinal cross-section under constant forcing can take several thousands of years to reach a morphological stable state. In the Western Scheldt, with large areas of erosion resistant layers and anthropogenic interferences, the period required to reach an equilibrium state might be even longer.

The sand export towards the sea found in this study contradicts the common theory and thoughts that the Western Scheldt is sand importing due to tidal asymmetry. Figure 3.7 shows that the sediment exporting trend shifts towards a sediment importing trend after 1955. The total negative volume trend of the estuary (black line in Figure 3.7) is similar before or after the sand extractions and dredging activities, although the total extracted volume is large (total ca 130 million m^3 from 1955 to now). The extracted volume thus should have been replaced with sediment from outside the estuary in order to close the sediment budget (cyan line of Figure 3.7). This makes the estuary a net sediment-importing estuary after around 1970. The sediment importing trend is confirmed by the studies of Nederbragt and Liek (2004) and Haecon (2006), and may be related to the large sand extractions and dredging activities after 1955. These human interventions might change the natural morphological development of the estuary in such a way that it provokes a sediment import. The sediment import after 1955 may consist of sand or mud. For a more recent period (1990 to 2000) (Dam and Cleveringa, 2013) also found a mud import and a sand export. The mud import exceeded the sand export, making the estuary a net sediment importing estuary. A probable explanation is that more mud settles in the main branch, since the side branches either are closed off or are full.

3.5.2. MUD FLUX

BOTH of these scenarios indicate that there is a marine mud import into the estuary. The mud budget studies confirm this conclusion (Terwindt, 1967; Van Alphen, 1990; Manni, 1986; Van Maldegem et al., 2003). In the eastern part of the Western Scheldt both fluvial mud (note that this is assumed) and marine mud show a net import. Verlaan (2000) and Chen et al. (2005) show that in this area around 75% of the mud settlement is from marine origin. Both scenarios indicate that the marine mud contribution is larger than the fluvial mud, although the marine/fluvial ratio of Scenario 2 lies closer to the 75% ratio (32 vs 14 million m^3 = 70% marine mud). It is important to note that the net sediment transport directions are generally not sensitive to the applied assumptions. A sediment budget for the 1994 to 2010 period of the Western Scheldt shows similar trends in sediment transport direction for sand and mud (Dam and Cleveringa, 2013). Here also a mud import and a sand export are found, while further landward the sand flux changes from sand export to sand import. Future sand-mud modelling can reveal more information about which scenario is most likely.

Estuarine turbidity maximuma (ETMs) are areas of persisting high mud concentrations that may evolve due to convergence of residual mud flows or a local bed source. Based on this study, the role of ETMs on the sediment budget in the estuary is difficult to assess. To the authors' knowledge there are no studies available that relate ETMs to morphodynamic

behavior, due to the complex nature of high suspensions, consolidation and morphodynamics. This will thus be left for future research.

3.5.3. APPLICABILITY FOR OTHER ESTUARIES

USUALLY sediment core data is used to investigate sedimentation on geological scales. In this paper the core data (interpolated to a subsurface model) is combined with historical bathymetric data to see which type of sediment was deposited over a 100-year period. This new method has proven to be useful for important insights in sediment transport directions for both sand and mud.

Lessons learned from this study for other estuaries are that a sediment budget should be constructed carefully with consideration of all the relevant sediment classes. Net sediment transport directions can be different for sand and mud, since the sediment transporting processes are different. However, the procedure used is only possible for estuaries with an extensive subsurface data set. In addition, the analysis should preferably be carried out over longer timescales so that trends become more obvious, requiring bathymetric data over multiple decades. With increasing anthropogenic influences and the potential threat of sea-level rise on estuaries, it becomes more and more important to have a good understanding of the relevant sediment fluxes in estuaries for sustainable sediment management. Identification of the relevant sediment classes is essential for morphodynamic forecast modelling studies, for example sea-level rise scenarios.

Future research includes a sand–mud model to hindcast this period in order to provide more insight into the dominant sediment transport processes underlying the observations of this study. This includes the erosion of the channels in the western part of the estuary and the siltation of the side branches. The effect of these morphodynamic changes over this period on the changing tidal properties (Figure 3.2) will be investigated as well.

3.6. CONCLUSIONS

BATHYMETRIC surveys are combined with a subsurface sediment composition model to derive a sediment-type specific sediment budget for the Western Scheldt over the 1860 to 1955 period. The analysis shows that the Western Scheldt changed from a relative shallow but wide estuary into a narrow and deep estuary. Side branches silted up and were reclaimed, while the sandy channels in the seaward part of the estuary deepened. The data analysis shows that the eroded sand has been transported in all directions; to the inner part of the estuary, to the side branches and towards the sea. The basin shows seaward sand transport in the seaward section and landward transport in the more landward sections. In contrast, a large import of marine mud took place during this period and filled the side

branches and bar systems in the main estuarine body.

Two scenarios investigated the assumption of mud origin from within or outside the basin. This showed quantitative rather than qualitative changes in the sediment budget. Averaged sand transport volumes throughout the basin appeared to be always larger (1.5 to 3 times) than transported mud volumes. For example, averaged sand export at the most seaward section lies between 1.5–2.5 million m^3/year, while averaged mud import lies between 0.5-1.5 million m^3/year.

Future modelling studies may reveal the underlying and deviating sand and mud transport mechanisms as well as the relationship between the larger channels and side branch siltation on the changed tidal properties observed during this period.

3.7. ACKNOWLEDGEMENTS

WE wish to thank two anonymous reviewers and the (associate) editors for their supportive and constructive comments. We thank Jan Staffleu from TNO for his support with GeoTop. We thank Rijkswaterstaat for providing the bathymetrical data. Furthermore, we thank Svašek Hydraulics and Deltares for their financial support. The authors declare no conflict of interest.

3.8. DATA AVAILABILITY

THE subsurface data that support the findings of this study are openly available in DinoLoket at www.dinoloket.nl. The bathymetrical data is available upon request at helpdesk-data@rws.nl.

4

CONTRASTING BEHAVIOR OF SAND AND MUD IN A CENTENIAL TIMESCALE MORPHODYNAMIC MODEL OF THE WESTERN SCHELDT

Many estuaries worldwide developed when sea level rise during the Holocene drowned river valleys. Part of these estuaries may be considered ephemeral systems gradually filling in with sediments. The infill time scale amounts to millennia depending on local conditions like tidal forcing, sediment supply and basin size. We investigate the sediment budget, sediment transport patterns and morphodynamic behaviour of the Western Scheldt estuary over 250 years using a 2D, process-based, morphodynamic model. A hindcast over the 1860-1955 period shows that the model is capable of reproducing observed increase in tidal range, mud import, sand export as well as erosion and sedimentation patterns. The side branches fill in with sand and mud before being closed by historic land reclamation works. These have had a decelerating effect on the morphodynamic trend. Adding a 150-year forecast model results shows that the high historic trapping efficiency of fluvial mud becomes less over time leading to higher prevailing mud concentrations in the water column. The net mud transport direction at the mouth changes from marine mud import to fluvial mud export. In contrast, the sand transport changes from export to a very limited exchange through the mouth section. Our study shows that sediment composition and grading have a profound effect on estuary infilling processes and morphodynamic adaptation time scales. This should be considered in

An edited and slightly adapted version of this chapter was submitted in Marine Geology.
Dam, G, Van der Wegen M., (2024), Contrasting behavior of sand and mud in a centenial timescale morphodynamic model of the Western Scheldt

studies exploring estuarine morphodynamic development and climate change impact with scenarios of sea level rise and changing sediment supply.

4.1. INTRODUCTION

ESTUARIES are located between the river and the sea and are subject to both tidal and river influences. Many estuaries were formed during the Holocene when sea level rise drowned former river valleys (Wolanski et al., 2009). General theory suggests that estuaries are ephemeral features that can exist thousands of years but will eventually fill in completely and turn into a delta, as a sediment exporting system (Dalrymple et al., 1992). Sediment transport in estuaries is controlled by a mixture of waves, tides and/or river forcing while sediment can originate from both fluvial and marine sources. Sediment in estuaries usually consists of different types, such as sand and mud, of which the transport processes and morphodynamic behaviour differ and may even result in opposite net transport directions (Dam et al., 2022). Channels often consist of coarser sediment fractions while more wave-sheltered environments and shallow shoals will be more mud-covered.

4.1.1. HYDRODYNAMIC FORCING

RIVER runoff is one of the dominant mechanisms in transporting fine river-supplied sediment seaward (Garel et al., 2009; Guo et al., 2014). Trapping efficiency is defined as the ratio between sediment depositing in the estuary and the fluvial sediment input (Dyer, 1995) where river floods decrease trapping efficiency by flushing sediments out to sea (Syvitski et al., 2005; Wolanski et al., 2016). The trapping efficiency of fluvial fine sediment is generally better known in micro-and meso-tidal estuaries (Dyer, 2000; FitzGerald and Knight, 2005), since macro-tidal estuaries are subject to tidal pumping importing marine mud as well (Chappell, 1993; Chappell and Woodroffe, 1994; Woodroffe, 2002; Wolanski et al., 2016). Tidal pumping is the result of a combination of density driven flows, tidal asymmetry and lag effects between the sediment concentration and the tidal velocities.

Tidal asymmetry is an important controlling factor for estuarine sediment infilling and redistribution. Under conditions of a purely reflective tidal wave, the time lag between maximum water levels and velocities is about 90 degrees leading to equal flood and ebb velocities and sediment transports. However, many estuaries show a much smaller time lag. The maximum flood discharge then shifts towards relative high-water levels which reduces the velocity and sediment transport. The tidal wave coming from the ocean is distorted by the shallow environments in the estuary. The ebb period becomes longer and the flood period shorter due to friction effects, changes in tidal propagation at different water levels and the presence of intertidal flats (e.g. Speer and Aubrey, 1985; Dronkers, 1986; Friedrichs and Aubrey, 1988; Wang et al., 2002). A shorter flood period results in higher flood velocities, hydrodynamic flood dominance and landward sediment transport. Intertidal areas shift the maximum ebb velocity to a later stage when lower water levels are present. This enhances ebb transport and export of sediment. Shallower systems with low lying inter-

tidal areas tend to be flood-dominant, while deeper basins with high intertidal areas tend to be ebb-dominant (Wang et al., 2002). (Brown and Davies, 2010) show that flood (or ebb) asymmetry, in terms of the peak tidal current strength, does not necessarily imply flood (or ebb) dominance the net sediment transport direction. Furthermore, a Stokes' drift return flow may enhance ebb flow in longer tidal basins (e.g. Van der Wegen et al., 2008), while river flow may significantly alter tidal intrusion and tidal asymmetry (e.g. Guo et al., 2014; Hoitink, 2003).

4.1.2. SAND AND MUD

MUD and sand transports react differently to estuarine flow patterns and can be quite distinct in their behaviour (Green et al., 2000; Bass et al., 2007; Diaz et al., 2020). Sand (here defined as non-cohesive with a d_{50} between 63 μm and 2000 μm) transport magnitude relates directly to the local velocity, e.g. by a power function of 3 to 5. An equilibrium sand concentration over depth develops relatively fast depending on local velocities and turbulence. In contrast, mud concentration is often supply limited so that prevailing mud concentrations remain much less than the mud transport capacity. Equilibrium between mud erosion and deposition only occurs at high mud concentrations (Van Ledden et al., 2004a). Mud particles can stay longer in suspension than sand particles because of their lower fall velocity. Sediment suspension lags the flow change. The lags effect gets larger for finer sediment. This generates a horizontal sand-mud segregation in most estuaries where, generally, more mud can be found in wave-sheltered areas, such as inter tidal areas or harbour basins. Estuarine salt-fresh water density currents like gravitational circulation cause a tide residual flow landward near the bed and seaward near the water surface. This also enhances sand-mud segregation since sand concentrations are much higher near the bed while mud is typically more uniformly distributed over the water column.

4.1.3. MORPHODYNAMIC MODELING

LONG-TERM morphodynamic process-based models have become useful and robust tools to quantify, hindcast and predict morphological changes in estuarine environments (Roelvink and Reiniers, 2011). The focus of early morphodynamic model applications has largely been on non-cohesive sediments (sand). Hibma et al. (2003a),Hibma et al. (2004a), Marciano et al. (2005), Van der Wegen et al. (2008), Van der Wegen and Roelvink (2008), and Van der Wegen and Roelvink (2012) show that it is possible to reproduce realistic channel-shoal formation in schematized tidal inlets or estuaries starting from an initially flat bed. Later studies show that morphodynamic models are able to reproduce observed bathymetric developments in complex environments over decades to centuries with significant skill (Ganju et al., 2009b; Barnard and Kvitek, 2010; Van der Wegen and Jaffe, 2013; Elmi-

lady et al., 2019). Dam et al. (2016) show that model skill score increases over decades to become "good" after a century. The reason for this is that model shortcomings (e.g. due to schematized forcing conditions, limited process-description or rough assumptions on sediment properties) are eventually overtaken by the well-modelled cumulative effect of the estuarine plan form steering morphodynamic developments (Cayocca, 2001; Dastgheib et al., 2008; Dissanayake et al., 2009; Van der Wegen and Roelvink, 2012). This suggests that process-based, morphodynamic models are useful tools for predicting longer-term dynamics in confined estuarine systems.

4.1.4. AIM AND METHODOLOGY

BASED on an interpolation of sediment core data Dam et al. (2022) reconstructed the sediment budget of the Western Scheldt for the period 1860-1955 and showed that the estuary changed into a narrower and deeper basin while side branches filled in with sand and mud. The main estuary (approximately the present-day layout) lost 206 million m^3 of sediment, while the side branches have been effective sediment traps where 111 million m^3 of sediments permanently deposited. The estuary exported sand due to the erosion of the large seaward channels and imported marine and fluvial mud that ended up in the side branches and on shoal systems. Sand export from the estuary to the sea in the period 1860-1955 is estimated to have been about 135-226 Mm^3 (1.4-2.4 Mm^3/yr), while mud import is estimated at 54-146 Mm^3 (0.6-1.5 Mm^3/yr).

This study aims to reproduce and further substantiate the findings by Dam et al. (2022) as well as to derive a future sediment budget using a 2D, process-based high resolution, sand-mud model including a closer analysis of the distinct behaviour of sand and mud. Since models should first be validated against observations an important part of this paper deals with the validation on observed bed level changes, the sediment budget based on analysis by Dam et al. (2022) and the hydrodynamic changes in the estuary over the 1860-1955 period. We then explore the impact of historic land reclamations to gain more insight in their hydro- and morphodynamic impact. Finally, we extend the simulation to a total of 250 years, looking at development towards equilibrium and changes in fluvial trapping efficiency. Despite the fact that dredging activities since 1955 have had a major impact on the morphology and sediment budget of the Western Scheldt (Dam et al., 2013), we choose to focus on the natural trends of the estuary and explore morphodynamic equilibrium states to be able to draw conclusions on more general estuarine morphodynamic behaviour.

The content of this paper is as follows: We introduce the Scheldt estuary in section 4.2. The process-based model is described in section 4.3. We perform the validation of the model results to observations in section 4.4. Scenario runs with land reclamations are described in section 4.5. Discussion follows in section 4.6 and conclusions in section 4.7.

4.2. THE SCHELDT ESTUARY

THE Scheldt estuary is located both in Dutch and Belgian territory and is one of the major estuaries of North-West Europe. The estuary is approximately 160 km long. The seaward marine section with a length of about 60 km is called the Western Scheldt (Figure 4.1 and 4.2). The Western Scheldt has a multiple channel system, with tidal channels and intertidal areas, such as sandy shoals, mudflats and salt marshes. The channels provide access to the ports of Antwerp, Vlissingen and Terneuzen/Gent, while the intertidal areas are important ecological areas. The present-day Western Scheldt has a funnel shaped geometry and has a width of almost 5 km near the mouth (Vlissingen) and 1 km near the Dutch-Belgian border (Figure 4.2). The tidal range increases from 3.8m in the mouth of the estuary to 5.2m near Antwerp as a result of convergence, shoaling and partial reflection of the tidal wave.

Figure 4.1: Detail of the historical map of the Scheldt, Jacob van Deventer, 1560 (Public domain)

The estuary is geologically very young compared to other estuaries that were formed during the sea-level rise in the Holocene (Russell, 1967; Van der Spek, 1997). The Western Scheldt formed around 1000 years ago when, during storm surges in the early Middle Ages, a new channel formed between an existing small embayment and the river Scheldt. Figure 4.1 shows the estuary around the year 1560, where several side branches still had connections to the main estuary. Amongst them were two connections to the Eastern Scheldt (to the north of the Western Scheldt). The year 1560 (Figure 4.1) coincides with approximately the maximum surface area of the estuary. In following centuries, the side branches silted up and were reclaimed bit by bit when the land became high enough (Van der Spek, 1997). The approximate outline in 1860 and the present-day outline (Figure 4.2) shows that the estuary surface area was slowly reduced over time to the present-day area of approximately 370 km^2. The last reclamations took place in the 1970's.

In the estuary both the sand and mud fraction are present. Sand is dominant in the sandy channels and shoals, while mud becomes more dominant in more sheltered areas, such as harbour basins and inter-tidal areas (mudflats and salt marshes). The mud concentration in the water shows variations over the tidal cycle, spring–neap cycle, and seasonal variations depending on the river discharge (Fettweis et al., 1998; Van Kessel et al., 2011). The estuary has three estuarine turbidity maxima (ETM). The first is located in the mouth delta near Zeebrugge. Here the concentrations can get up to a few hundred mg/l (Chen et al., 2005). The second lies near Antwerp and the third is located near Rupelmonde in the tidal river. The SPM concentration in the Western Scheldt is lowest between Vlissingen and Hansweert and increases both towards the Dutch– Belgian border and towards the North Sea (Van Kessel et al., 2011). Riverine mud input of the Scheldt is estimated to be around 370 kT/yr. Trapping efficiency of the riverine mud is around 80% (Van Maldegem et al., 2003), which means that at present the fluvial mud almost does not reach the sea.

4.3. FINEL2D SAND-MUD MODEL

FOLLOWING Van Ledden (2003), Van Ledden et al. (2004a), Van Ledden et al. (2004b), Waeles et al. (2007), Luan et al. (2017), Braat et al. (2017) and Mengual et al. (2021), we apply a sand-mud model in which both sand and mud and their interaction contribute to morphological changes. The FINEL2d model is equipped with a bed module in which the sand and mud content is administrated in the seabed (Dam and Bliek, 2013) The principal

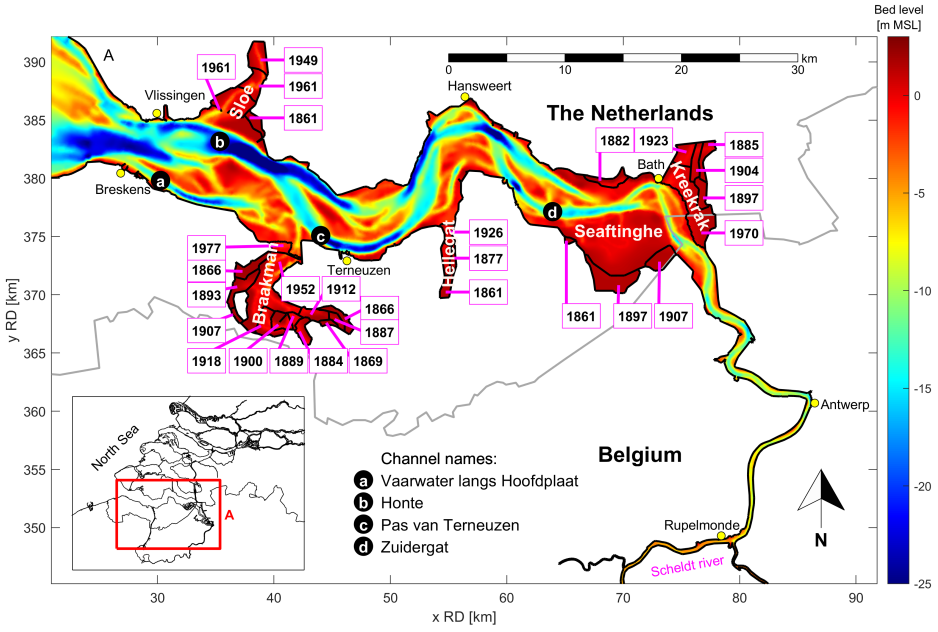

Figure 4.2: Layout and bed level of the Western Scheldt around 1860. Numbers indicate the year of reclamation. Coordinates in km with reference to Paris. After Dam et al. (2022)

equations are described in Appendix A and the sand-mud model in Appendix C.

4.3.1. COMPUTATIONAL GRID AND BOUNDARY CONDITIONS

THE model FINEL2d uses an unstructured triangular mesh. Arbitrary coastlines and complex geometries can be resolved accurately.

The seaward boundaries of the computational mesh of the Western Scheldt are situated approximately 40 km away from the coastline and coincide with the boundaries of existing models covering the North Sea. The latter can be used to obtain the corresponding boundary conditions. A major part of the Scheldt-estuary in Belgium is also included in the schematization (Figure 4.3a). In the area of interest, the Western Scheldt, the average grid size is approximately 1.1 ha (see Figure 4.3b). Near the seaward boundaries the grid size is approximately 2.5 km^2. The total number of elements (triangles) of the mesh is 59,937.

On the river side constant (yearly averaged values) river discharges are assumed. The average discharge of the Scheldt River and tributaries is around 100 m^3/s. The discharge fluctuates between 50 m^3/s during summer and 180 m^3/s during winter periods. The river influence is small, since the freshwater discharge over a tidal period is only 0.6% of the tidal prism (Van der Spek, 1997). On the seaward side of the grid 60 astronomical tidal boundary conditions are given. The historical sea level rise is approximately 15 cm/century and is included in the simulation. The sea level rise in the 110-year period is approximately 15 cm and is included in the simulation. Only the influence of the tidal action on the morphology is considered. Wave action is ignored for simplicity reasons, although intertidal areas can be influenced by wave action. The computational domain follows the exact outline of the estuary in 1860. Since then, land reclamations have decreased the surface area of the estuary from 410 km^2 to 323 km^2. The land reclamations are taken into account in the computation. The borders of the land reclamations coincide with the computational mesh. At the year of closure, a weir is implemented in the model, so that this section is closed off from the tidal influence and morphodynamic activity in the closed-off section stops.

4.3.2. MODEL SETTINGS

WE follow initially the model settings of Dam et al. (2016). A morphological acceleration factor of 24.75 is applied (Roelvink, 2006). This factor is used to multiply the computed bed level changes. A constant bottom roughness of 1 cm is used in the model in both space and time. Erosion resistant layers are included in the simulation and are based on core sample data throughout the estuary (Gruijters et al., 2004; Dam et al., 2016). We use one sand fraction, although a spatially varying grain size is used to calculate the equilibrium sand concentration. Field data shows that the grain size varies spatially and

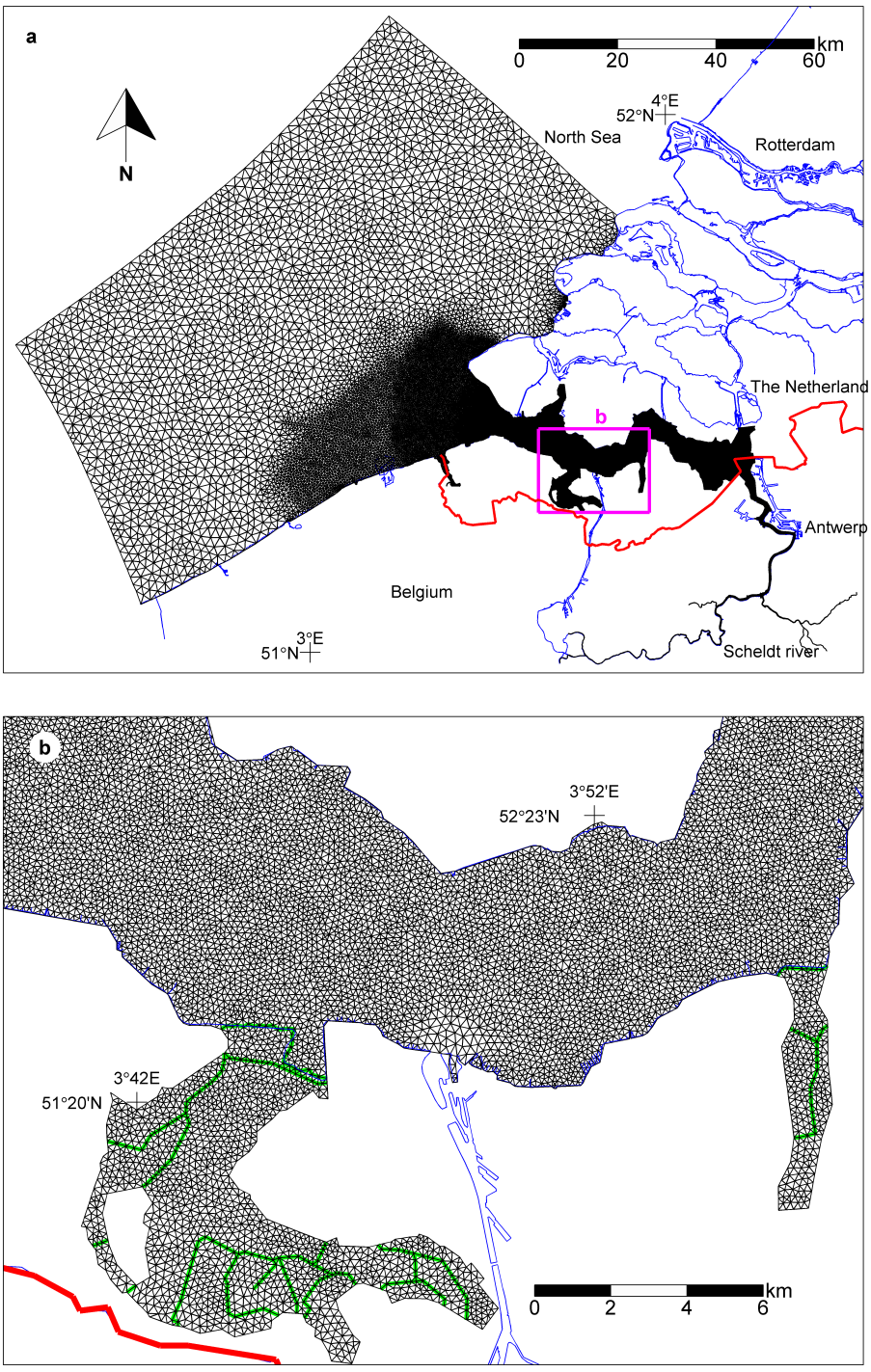

Figure 4.3: Computational grid (black lines). (a) Complete computational grid (b) Detail of the grid inside the estuary. Blue line indicates the land boundary; red line indicates the border between Netherlands and Belgium. Green line indicates the land reclamations in figure 2b. After Dam et al. (2016)

generally is coarser in the western part than in the eastern part (McClaren, 1994). Therefore, we apply an average grain size (d_{50}) of 300 μm in the western part, linearly decreasing in landward direction to 150 μm to the eastern part of the estuary. The d_{50} is an input for the Engelund-Hansen sediment transport formula (Engelund and Hansen, 1967). A fall velocity of 1.5 cm/s is used for sand. One mud fraction is used following the formulations of Krone (1962) for deposition and Partheniadis (1965) for erosion of mud. We apply a constant concentration at both the river (100 mg/l) and the sea (100 mg/l). Here we ignore seasonal fluctuations of the mud concentration (Van Kessel et al., 2011), since we are interested in long-term behavior of the system. A land reclamation is modelled by placing a weir at the location of the levee and in the year of construction (Dam et al., 2016). The bed module is used with 5 layers and applied with a thickness of 25cm. Each time step in the simulation the mud content in each cell is updated.

4.4. CALIBRATION RESULTS

4.4.1. EROSION/SEDIMENTATION PATTERN

SIMILAR to the sand model by Dam et al. (2016), the sand-mud model skilfully reproduces the large-scale erosion-sedimentation pattern from 1860-1955 (Figure 4.4). This suggests that the large-scale changes are mainly due to the sand fraction. Mud is found mainly in the side branches and on shoals (Figure 4.5).

4.4.2. SEDIMENT FLUXES AND VOLUME CHANGES

THE model shows (Figure 4.6a) that there is a strong sand export (seaward flux) and a mud import (landward flux) through the mouth section (Vlissingen-Breskens transect). The modelled export amount of sand is 155 million m³ after 95 years in 1955 (Scenario 1 in Figure 6a). The modelled import amount of mud is 50 million m³ after 95 years (Scenario 1 in Figure 6a). These values are in line with the value ranges suggested in the sediment budget study by Dam et al. (2022), indicated in Figure 4.6a by the vertical yellow and grey arrows. The modelled mud import is in the lower range (ca. 50 million m³) of the sediment budget study, which may be attributed to our 2D approach that disregards the gravitational circulation driven marine mud import. Figure 4.6b shows the sediment flux at the estuary head. There is a constant linear inflow (seaward flux) of mud due to the applied constant river discharge and mud concentration in the model. Total volume development in the estuary (Scenario 1 of Figure 4.6c) is showing an eroding trend in the model of around 80 million m³ over the calibration period of 95 years. In the sediment budget of Dam et al. (2022) the total eroding volume change was calculated at 95 million m³.

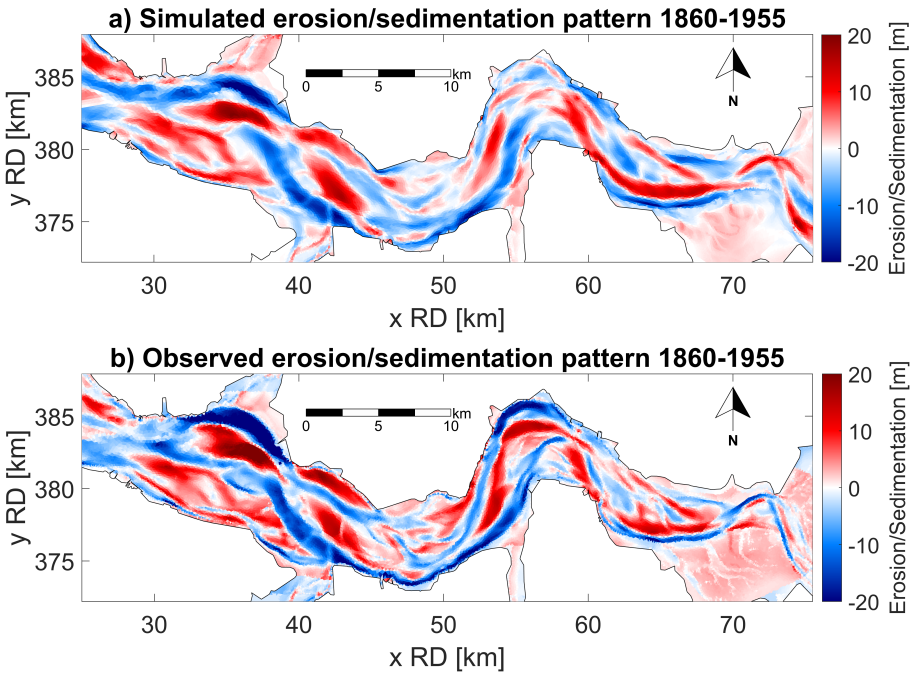

Figure 4.4: Erosion-sedimentation 1860-1955; a) simulated (Scenario 1); b) observed

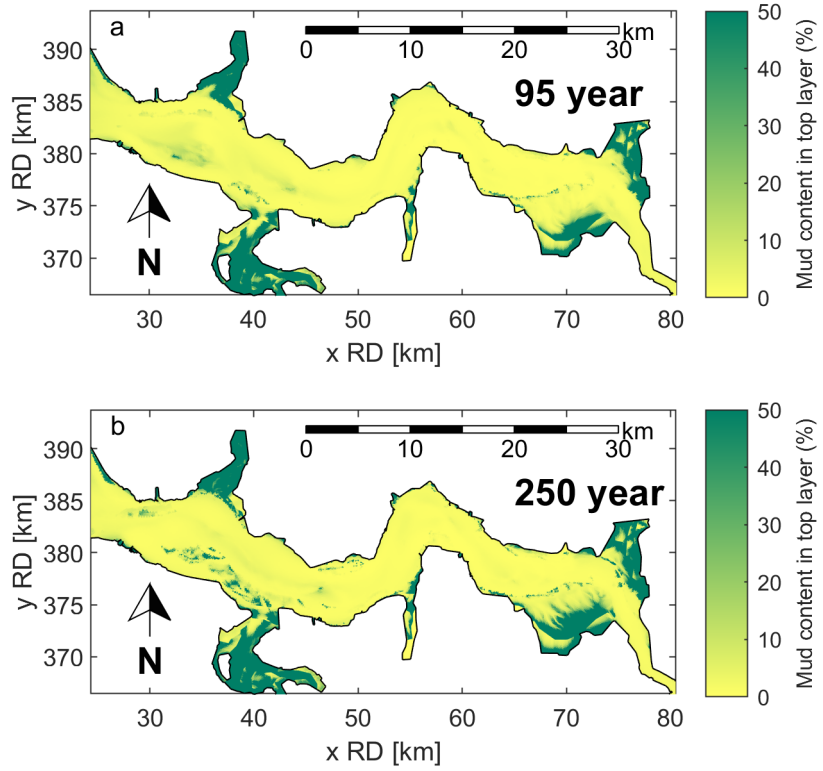

Figure 4.5: Mud content in top layer (%) a) after 95 years b) after 250 years (Scenario 1)

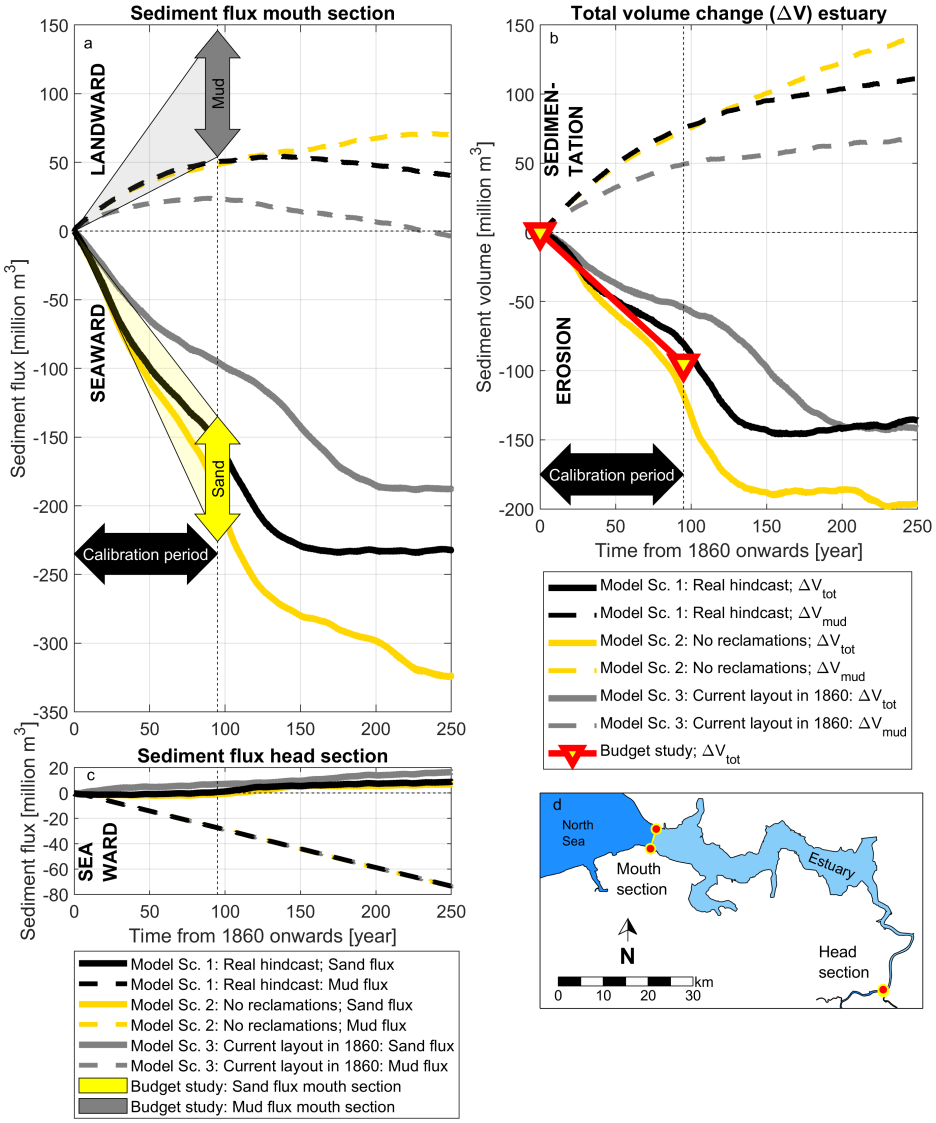

Figure 4.6: (a) Simulated sand and mud fluxes at the mouth section (Vlissingen-Breskens transect). Positive values imply landward sediment transport. Arrows indicate the range of sand export (yellow) and mud import (grey) over the 1860-1955 period as found by a sediment budget study by Dam et al. (2022). (b) Simulated sand and mud fluxes at the head of the estuary (Near Rupelmonde). Positive values imply landward sediment transport. (c) Total volume change of the estuary from 1860 onwards between the mouth and head section. Positive values imply sedimentation. Volume change as found by Dam et al. (2022) indicated with triangle. Three model scenarios: Scenario 1: Real hindcast, Scenario 2: No reclamations, Scenario 3: Present day layout applied in 1860.

We take a closer look to the sand export through the mouth section (Figure 4.7). Here we analyze one springtide cycle in 1860 in which the amount of water that enters and leaves the estuary is about equal (1363 versus 1368 Mm^3; Figure 4.7d). The horizontal tide is flood-dominant, where the flood phase is shorter than the ebb phase (367 minutes versus 375 minutes; Figure 4.7e), resulting in higher maximum flood velocities (0.85 m/s versus 0.72 m/s). The maximum sedimenttransport is also larger during flood (flood: 3.2 m^3/s versus ebb: 2.3 m^3/s; Figure 4.7f), but the total amount of sediment transported is larger during ebb than during flood (18600 m^3 versus 17500 m^3; Figure 4.7f). This 1100 m^3 difference over one tide is about 5% of the total ebb or flood transport. So, we see relative short and strong flood velocities, versus long and weak ebb velocities. The estuary is hydrodynamically flood-dominant with short flood duration and large flood velocities, yet the model shows ebb-dominant sediment transport. Van der Wegen et al. (2008) and Dastgheib (2012) find similar ebb-dominating transport in a flood dominant estuary and relate this to the Stokes' drift return flow that enhances ebb-velocities and ebb sediment transport. We obtain the same result when doing a manual sediment transport calculation using the model velocities over the cross-section and the Engelund-Hansen sediment transport formula.

The reason why the estuary is ebb-dominant is because the maximum ebb velocities occur at a relative low water level, where the flow is more confined in the channels leading to higher velocities. In contrast, maximum flood velocities occur at higher water levels and larger cross-sectional areas (approximately one hour before high water, see also Van Den Berg et al. (1996). This leads to a lower maximum flood velocity than would occur at a lower water level. The longer ebb phase (ebb is 41 minutes longer than flood) combined with the enhanced ebb velocities lead to more ebb transport despite the higher maximum flood velocities. In the mouth section (Figure 4.7b), a distinct separation between a northern ebb channel and a southern flood channel occurs. The northern, shallower ebb channel provides stronger ebb transport than the deeper flood channel.

4.4.3. HYDRODYNAMICS

THERE is measured water level data of 4 main stations in the Western Scheldt available starting from 1860-1870. The water level data shows an increase in tidal range from 1860 onwards. For each 10 years of the morphodynamic results we determine the tidal range. The model results (Scenario 1 of Figure 4.8) show that increase in tidal range is largely reproduced over a 100-year period. Increase in tidal range is thought to be related to the infilling and reclamation of the side branches and the natural deepening of the main channels (Dam et al., 2022).

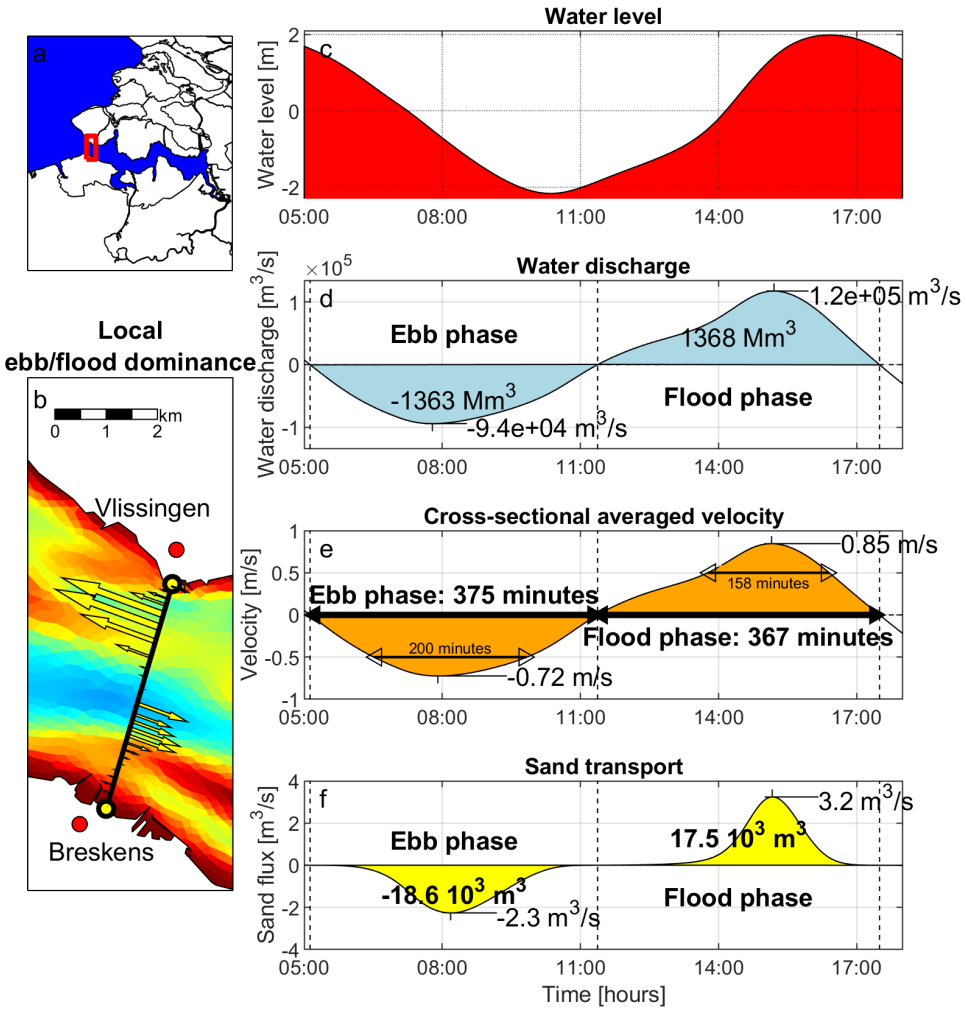

Figure 4.7: Detail of hydrodynamics and sand transport over a spring tidal cycle at the estuary mouth section using the 1860 bathymetry: a) overview b) local ebb/flood dominance of sediment transport c) water level d) water discharge e) Cross-sectional averaged velocity f) sand transport

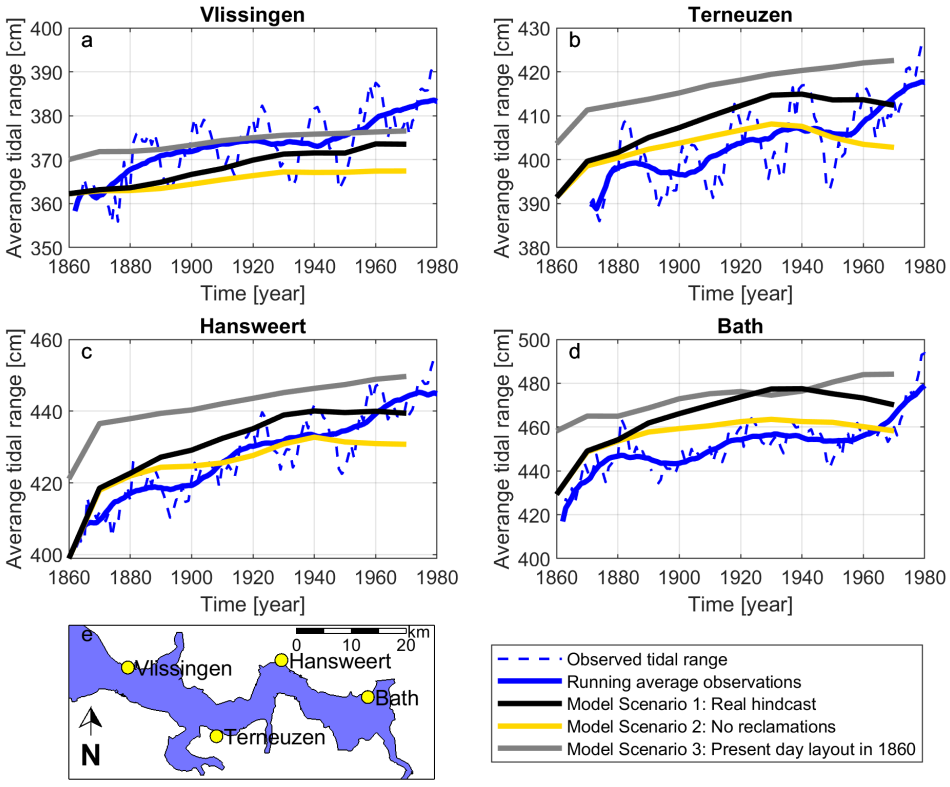

Figure 4.8: Observed tidal range and modelled tidal range for main water level stations in the Western Scheldt a) Vlissingen b) Terneuzen c) Hansweert d) Bath. Scenario 1 (Historical reclamations), Scenario 2 (no reclamations), Scenario 3 (Extreme reclamation; present-day layout applied in 1860).

4.5. SCENARIO RUNS

4.5.1. INTRODUCTION

To gain more insight into the behavior of the system and to look at the effect of land reclamations we define three scenarios that simulate 250 years of morphological change, starting from the year 1860.

- Scenario 1: Scenario with historical reclamations. Hindcast from 1860 until 1955 with the land reclamations as occurred (=calibration run of previous section). After that, continuation of the present-day layout into the future. From 1955 onwards, this scenario is continued without dredging and deepening of the navigational channel, therefore it might not reflect a realistic state of the estuary anymore. The reason for this is that we want to look at autonomous ('natural') estuarine behaviour.
- Scenario 2: As Scenario 1, but without the land reclamations.
- Scenario 3: Extreme land reclamation scenario by using the present-day layout at the start year 1860.

The first and most obvious effect of land reclamations is that tidal prism (i.e. the amount of water that enters and leave the estuary within a tidal cycle) is reduced by closing off surface area. Secondly, tidal wave attenuation is also reduced (e.g. Stark et al., 2017), leading to an increasing tidal range (e.g. Zhang et al., 2022) and increasing tidal prism. Thirdly, accommodation space (i.e. space for sediment to settle) is reduced, leading to different sediment transport patterns and higher sediment concentrations (Van Maren et al., 2016). Fourthly, the large-scale morphodynamic system is potentially affected by land reclamations, since tidal prism relates to an equilibrium tidal channel depth (e.g. O'Brien, 1931, 1969; Bressolier-Bousquet, 1991). Finally, the restricted planform of the estuary with reclamations, probably influences the location of channels (Dam et al., 2016; Nnafie et al., 2018). Since the morphological effect of land reclamations affects the macro scale of the estuary, the adaptation timescale is potentially decades to centuries (De Vriend, 1991).

4.5.2. RESULTS OF THE SCENARIO RUNS

We find that the tidal prism is one of the controlling factors in explaining the differences between the scenario runs. Land reclamations reduce the tidal prism due to closed off areas, but on the other hand the tidal range and thus tidal prism increases due to less tidal wave attenuation (Figure 4.8). The tidal prism can become either higher or lower depending on which process is dominant. The results from the model simulations show

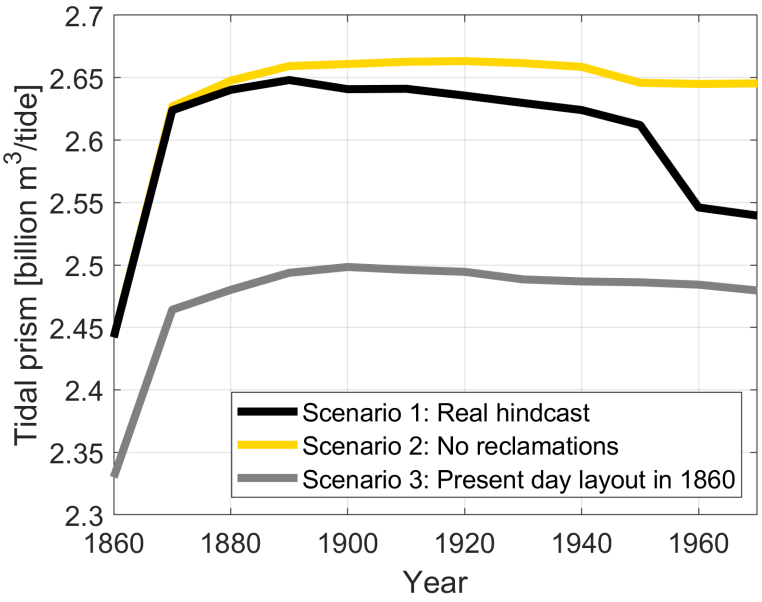

Figure 4.9: Tidal prism over the 1860-1970 period. Scenario 1: hindcast from 1860-1955 with reclamations as occurred: Scenario 2: No reclamations; Scenario 3: Present day layout in 1860.

that tidal prism reduces due to the land reclamations (compare scen.1 and scen.2 in Figure 4.9), which means that closing of the areas is more dominant for the tidal prism reduction than the tidal range increase. Figure 4.9 shows an initial increase in tidal prism in the first decade of the simulation. We relate this partly to morphodynamic spin-up of the model and partly due to the reproduced increase in tidal range between 1860 and 1870 (Figure 4.8), probably as a result of the construction of the Kreekrak dam between 1861-1867 (Figure 4.2, north-east).

In Scenario 2 (no reclamations), which has the largest tidal prism (Figure 4.9) of the scenario runs, there are relatively high tidal velocities and larger morphological activity. This results in larger sand export and the highest mud import of the three scenario runs (Figure 4.6). The presence of accommodation space in the side branches leads to this significant mud import. In contrast, in Scenario 3 with extreme land reclamations, the tidal prism is reduced (Figure 4.9) resulting in decreased sand export and mud import (Figure 4.6a).
When comparing Scenario 2 to Scenario 1, a larger tidal prism leads to increasing tidal velocities and enhanced morphodynamic activity. Higher velocities impact the timescale of the morphological changes in the ebb and flood channels. Notably, in Scenario 2, the Pas van Terneuzen and Honte channels exhibit faster expansion compared to Scenario 1 after 95 years (Figure 4.10). Conversely, in Scenario 3, with extreme land reclamation, the tidal prism is reduced. Consequently, the expansion of the Pas van Terneuzen and Honte channel becomes less pronounced.

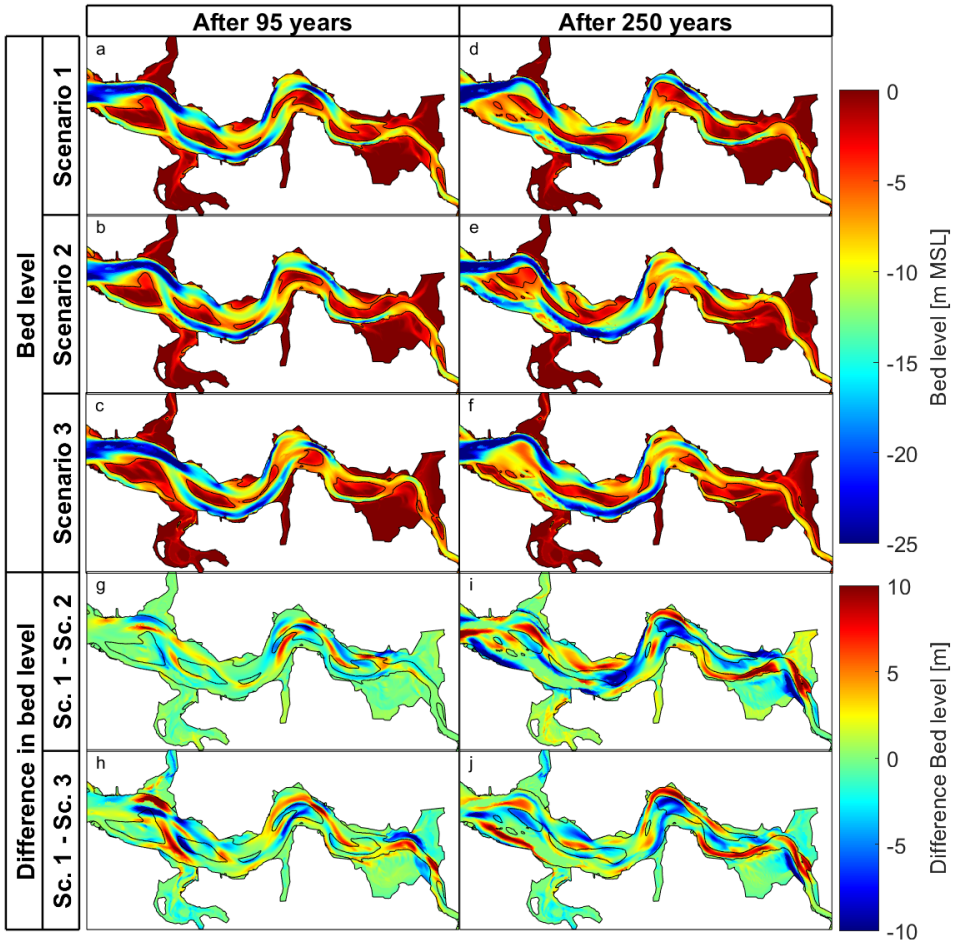

Figure 4.10: a-f) Computed bed levels after 95 years (1955) and 250 years simulation for Scenario 1 (Historical reclamations), Scenario 2 (No reclamations) and Scenario 3 (Extreme reclamations: Present day layout in 1860). Black line indicates the -5m MSL contour line. Figure g-j: difference in bed level compared to Scenario 1. Black line indicates the -5m MSL contour line for Scenario 1.

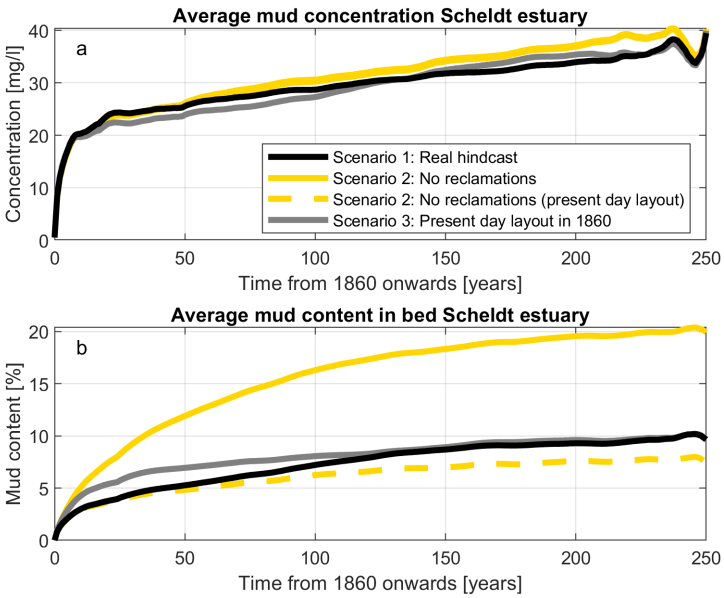

Figure 4.11: a) Average mud concentration in Scheldt estuary over time b) Average mud content in bed in Scheldt estuary over time

4.5.3. MUD CONCENTRATION

OVER long time scales the accommodation space for the mud in the side branches becomes exhausted and residence times for mud in the water column increase, leading to increasing mud concentrations (Figure 4.11a). Furthermore, with the filling of the accommodation space for mud, the initial dominant marine mud becomes less over time, until at a certain moment the marine mud import becomes a fluvial mud export. Fluvial mud is then flushed out to the sea since there is very little or no accommodation space for mud to deposit (Figure 4.6a). The mud content in the bed increases over time for all scenarios at a decaying rate (Figure 4.11b). The decay rate is fastest in Scenario 3 due to less available accommodation space than in the other scenarios. An average mud content of approximately 10% is obtained. Scenario 1 exhibits the same behaviour as Scenario 3, but at a slower pace, due to settlement of mud in the side branches. Scenario 2 shows an average mud content of 20% after 250 years. This is double of Scenario 1 and 3 and can be explained by the continuous settlement of mud in the side branches that remain open. When looking at the area of the present-day layout only, i.e. without the side branches, the mud content in the bed is less than Scenario 1 and 3. This is due to the higher tidal prism (Figure 4.9) and tidal velocities, which keep the mud more in suspension.

4.6. DISCUSSION

4.6.1. MUD DYNAMICS

ESTUARIES can be supplied with mud from both the river and the sea. From the sea, tidal asymmetry, tidal pumping and gravitational circulation will transport mud into the estuary. At a certain landward distance from the mouth, the intrusion of marine mud is hampered by fluvial processes. The balance between marine and fluvial supply is affected by processes of different timescale such seasonally varying river discharge.

The model hindcast shows that initially there is sufficient accommodation space for marine mud to be stored in the side branches and mud flats. Over time the side branches become higher and transform into salt marshes while other areas are reclaimed when they fill in with sediment. The mud storage in these areas becomes less over time since accommodation space becomes less. Over time no significant new accommodation space for mud is created, most likely since the flow velocities in the remaining part of the estuary are too high for the mud to permanently settle. Thus, over time, the marine mud entering the estuary remains in suspension, leads to higher mud concentrations, and is more easily flushed back into the sea. For the fluvial mud the estuary is no longer a sink when the accommodation space is exhausted. Trapping efficiency for mud becomes decreases over time to approach zero over long-time scales. Sea level rise will create more accommodation space and promotes trapping of marine and fluvial mud in the estuary again.

Model results suggest that a transition from marine mud import to fluvial export has not occurred yet in the Scheldt. There are still sufficient mud sinks available, although with less accommodation space as before. In other estuaries similar changes in import/export can occur. Land reclamations in the Seine for example have decreased the accommodation space for mud over time. This has led to increased (fluvial) mud export and mud deposition at the mouth of the estuary (Lesourd et al., 2016).

Due to increasing mud concentrations hyper turbid conditions have occurred in other estuaries (Jalón-Rojas et al., 2017; Dijkstra et al., 2019a) most likely caused by anthropogenic effects (Winterwerp and Wang, 2013; Winterwerp et al., 2013). In a feedback loop, the higher mud concentrations damp turbulence, decrease roughness, enhance flow, mud import, suspension, and mud concentration. Dijkstra et al. (2019b) however, suggest that it is not likely that this would occur in the Western Scheldt, due to lower long-term average sediment concentrations in most of the estuary.

Sensitivity runs using different mud concentrations on the boundary or settings show the same behavior from mud import to mud export over long time scales. However, timescales can be affected due to different settings. Only when no mud supply from the river is applied a continuous mud import from the sea can be observed.

The model approach is a 2D depth averaged model. So, in this model no gravitational circulation is included. We believe that a 3D approach where this gravitational circulation is included would perhaps change timescales. A 3D approach would probably bring more marine mud into the estuary and the change from mud import to mud export is expected to happen more quickly.

The mud transport module does not include more complex processes such as flocculation. We believe that this is again a process that would affect timescales but would not affect our main conclusion.

4.6.2. SAND DYNAMICS

THE model results show a clear sand export out of the estuary from 1860-1955. This sand export is comparable to the sand export found in a sediment budget study (Dam et al., 2022). In the period from 1860 to 1955 the estuary moved slowly into a morphological less active state (Dam et al., 2016). We see also that the sand export after 150 years becomes less (Figure 4.6) and approaches zero. The model results indicate that the estuary evolves towards an equilibrium state. Note that dredging is not included in the modelling. In reality, anthropogenic influences, such as dredging and deepening of the navigational channel and sand mining might have altered this picture since a sand import was found in more recent sand budget studies. (Dam et al., 2013) found that dredging/dumping and sand mining increased the tidal celerity and tidal range and had a profound effect on the morphology.

Nature restoration plans are scheduled in the Scheldt estuary by extending the surface area of the estuary. This is done by removing dikes around cultivated areas and let the tides come in again (called 'depoldering'). It is expected that these areas will fill up with sediment, as with the old side branches in the centuries before. As such they will contribute to extra tidal attenuation. Over time the areas fill in with sediment and become higher. Therefore, the tidal attenuation effect will become less over time. As the 'depoldered' areas create new accommodation space, it will attract sediment from nearby and possibly changing the net sediment transport direction in the vicinity. As the tidal prism increases due to 'depoldering', channels in the neighborhood might show an effect in the form of more rapid change or scouring. However, depoldering areas should be considerable in size to affect tidal wave propagation and sediment budgets.

4.6.3. LAND RECLAMATIONS AND MORPHOLOGICAL ADAPTATION

THE morphological adaptation time of these large-scale land reclamations is long. Based on the scenario run we find an adaptation time scale of centuries. Th reclamations had a decelerating effect on the morphological trend by reducing the tidal prism and slightly

lowering the tidal velocities. The reclamations slowed down the erosion and sedimentation trends. Due to reclamations and a reduced tidal prism the export magnitude of sand became less (Figure 4.6). Furthermore, the import of mud became less due to less accommodation space. Despite the decreasing tidal prism (Figure 4.9), the simulation shows that land reclamations have increased the tidal range by about 10 cm over the 1860-1955 period. Reclaiming of land in the Western Scheldt was mostly done after the secondary basins had already filled in and had lost most of its tidal attenuation effect. Closing off an area with dikes (the actual reclamation) was merely strengthening an ongoing trend.

However, the final state of the estuary after 250 years simulation is not the same. The most noticeable effect is that the sediment amount differs (Figure 4.6) by around 140 million m^3 for sand between the three scenarios and around 90 million m^3 for mud after 250 years. Thus, the reclamations have had an impact on the (final) morphological equilibrium state of the estuary. This is in line with the findings of Randarian et al. (2022) who states that antecedent morphology leads to a different morphological state and equilibrium. Even though the initial bathymetry is the same in this case, the response to land reclamations is different, and after the reclamations have stopped (around 1970) the three simulations lead to a different state of the estuary around 150 years further into the future. As such morphodynamic simulations can provide valuable insight into long-term estuarine behavior.

4.7. CONCLUSIONS

IN this paper we successfully hindcast the morpho- and hydrodynamic changes of the Scheldt estuary with a sand-mud model. The model is capable of reproducing the erosion-sedimentation pattern, the observed sand and mud fluxes at the mouth of the estuary and the observed tidal range changes over the 1860-1955 period.

We show that there is sand export and mud import at the mouth of the estuary. The mud import changes into a mud export over long timescales of centuries, since accommodation space for mud in the estuary becomes exhausted and fluvial mud will be flushed to the sea.

Scenario runs with and without land reclamations show that reclamations lead to less tidal prism, lower tidal velocities and decreasing morphodynamic changes and sand export. Land reclamations increased the tidal range by approximately 10 cm over a 100-year timescale. The land reclamations did not significantly alter the general erosion-sedimentation patterns, but the timescale of change and the sediment volume in the basin.

4.8. DATA STATEMENT

Historical bathymetric and tidal data that is used to validate the model has been described in (Dam et al., 2016, 2022).

4.9. DECLARATION OF COMPETING INTEREST

The authors declare no conflict of interest. The funders had no role in the design of the study; in the collection, analysis, or interpretation of data; in the writing of the manuscript, or in the decision to publish the results.

4.10. ACKNOWLEDGEMENTS

We thank Svašek Hydraulics and Deltares (in particular Marcel Taal) for their support and financial contributions.

5

LONG-TERM MODELING OF THE IMPACT OF DREDGING STRATEGIES IN MORPHO- AND HYDRODYNAMIC DEVELOPMENTS IN THE WESTERN SCHELDT

The natural morphological developments of the Western Scheldt and the impact of human activities on these developments are investigated using a process-based morphological model called FINEL2d. The historical period of 1965-2002 is simulated in a T0 scenario including all the human activities that have taken place in that period. Besides this T0 scenario two extreme scenarios are modeled for the same period. The T1 scenario is carried out without any human activities from 1965 onwards. In the T2 scenario regular dredging of the navigational channel takes place, but the dredged material is not distributed back into the Western Scheldt like in the T0 scenario. In this way insight is obtained into how human activities have influenced and will influence the tide in and the morphology of the Western Scheldt.

By modeling these different sediment strategies it is concluded that the applied strategy has had a large impact on the morphology of the estuary and tide during this period. The channels have deepened and the tidal flats have increased in the 1965-2002 in the model, because of which the hypsometry of the Western Scheldt has probably has become steeper over the last decades. The results also show significant effects on the propagation of the tide in the estuary. Due to the actual human activities over the past decades the tidal range in the estuary

An edited and slightly adapted version of this chapter was publiched in the conference proceedings of WODCOM (2013)

Dam, G, S. Poortman, A.J. Bliek, and Y. Plancke (2013), Long-term modeling of the impact of dredging strategies in morpho- and hydrodynamic developments in the Western Scheldt.

has increased by about 0.4m in Antwerp and accelerated the propagation of the tide with approximately 20 minutes. This corresponds to the observed phase shift in Antwerp over the past decades.

The extreme scenario in which all dredged material was removed from the estuary shows that the process of increasing tide levels in the estuary may continue in case that the human activities are intensified.

5.1. INTRODUCTION

THE Western Scheldt is a highly morphological active estuary. The tide and the morphology are inter related, i.e. any change in tide causes a change in morphology and vice versa. Managing the estuary requires deepened knowledge and sophisticated decision making tools to be able to safeguard all the functions of the estuary with regard to nature, safety and access to the Port of Antwerp. The morphological timescales of large scale impacts, such as land reclamation, deepening of the navigational channel, sand mining and sea level rise are in the order of years to decades. For this reason investigating these impacts requires long-term morphological models. Until now long-term morphological predictions were mainly carried out by using (semi-)empirical models, like ESTMORF (e.g. Wang et al., 1999) and ASMITA (e.g. Kragtwijk et al., 2004). Process-based morphological models were not yet able to reproduce the morphological development very well over decades, partly because of the large amount of computational time involved, although its use on decadal scale begins to be more common practise (e.g. Van der Wegen et al., 2011; Van der Wegen and Jaffe, 2013). Focus of long-term research using process-based models was mainly on highly schematised estuaries like Hibma et al. (2003b) and Van der Wegen and Roelvink (2012). In Dam et al. (2007) a long-term morphological model of the Western Scheldt was presented that was successfully used in a hindcast of the period 1965-2002. In this paper a revision of the model of Dam et al. (2007) is used to investigate the effect of human activities in this historical hindcast, focussing on the second half of the 20th century. The main research question in this paper is to establish the impact of human activities in the second half of the 20th century on the morphology and the tide in the Western Scheldt. Three scenarios are defined:

- T0: Real hindcast of the 1965-2002 period including dredging/disposal and sand mining;
- T1: Scenario 1965-2002 without any human interference;
- T2: Scenario 1965-2002 in which all dredged sediment of the navigational channel is

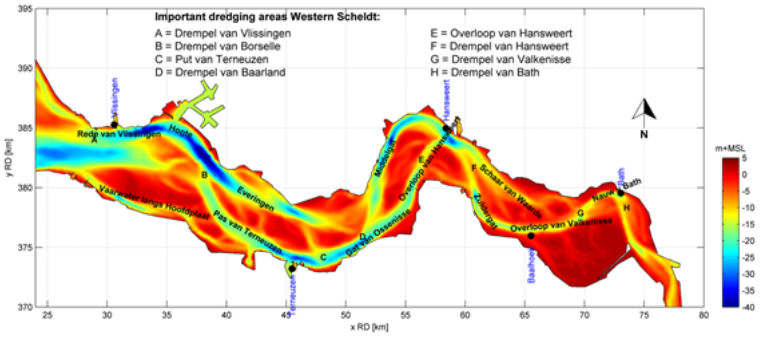

Figure 5.1: The Western Scheldt estuary

taken out of the Western Scheldt.

The scenarios T1 and T2 are fictive, and show the range of effects from the case no human interference had taken place at all over the period 1965-2002 (T1) to an interference in which huge volumes of sediment are removed from the estuary (T2), with the factual T0 scenario in between. The applied morphological model is a finite element based model called FINEL2d using an unstructured grid with triangular elements that covers the complete Western Scheldt estuary (Dam et al., 2007). Besides a hydrodynamic and morphodynamic module, a dredging module is used to model the three scenarios. The content of this paper is as follows. In section 2 the Western Scheldt estuary is introduced and section 3 describes the applied FINEL2d model. Section 4 presents the morphological and hydrodynamic results and section 5 finally summarizes the conclusions.

5.2. WESTERN SCHELDT

THE Scheldt estuary is one of the major estuaries of North-West Europe. The estuary is approximately 160 km long and is located both in Dutch and Belgian territory. The down-estuarine part (last 60 km) is called the Western Scheldt (Figure 5.1) and is characterised by a width of almost 5 km near the mouth and 1 km near the Dutch-Belgian border. The mean tidal range increases from 3.8m at the mouth to over 5.0m near Temse, almost 100 km from the mouth of the estuary. The morphological changes in the Scheldt estuary are dominated by the tidal motion. The river discharge is of minor importance since the fresh water discharge, on average 120 m^3/s, is only 0.6% of the tidal prism at the mouth (Van der Spek, 1997). The estuary is well-mixed, meaning a horizontal rather than a vertical salinity gradient.

The Western Scheldt incorporates large areas of tidal flats and salt marshes. Nature is therefore an important function and stringent EU and national legislation is applicable

to safeguard its natural values. Equally important are the functions of the estuary in the safety against flooding and the access to the Port of Antwerp. The Western Scheldt is a multiple channel system. Ebb and flood channels show an evasive character separated by inter tidal shoals (Van Veen, 1950). The ebb channel has a meandering character, while the flood channel is straighter. The ebb flow reaches it maximum velocity near mean sea level (MSL), while the flood flow reaches its peak one hour before high water (Van Den Berg et al., 1996). As a consequence the ebb flow is more concentrated in the channels, resulting in deeper ebb channels. The ebb channel is therefore generally designated as the navigational channel in the Western Scheldt. The Western Scheldt consists mainly of fine non-cohesive sediments; only at inter tidal areas mud can be found.

The tidal flats and surrounding ebb and flood channels form morphological macro cells (Winterwerp et al., 2001). At the locations where the cells coincide sills develop, which reduce the navigational depth of the fairway to the port of Antwerp and therefore require maintenance dredging (Meerschout et al., 2004). The sills are indicated in Figure 5.1 by the capital letters. Several million m^3 are dredged annually to maintain the guaranteed depth of the navigational channel to the Port of Antwerp. This material is redistributed in the estuary. In addition on average 2 million m^3 of sand is mined annually from the Western Scheldt.

In the 1970's and 1990's a deepening and widening of the navigational channel has been carried out to allow vessels with greater draught to enter the port of Antwerp. In 2010, a third deepening has been completed. Most of the dredging had to be done at the sills. The annual dredging volumes (maintenance plus deepening) range from 5 million m^3 in 1968 to 14 million m^3 during the second deepening. After the second deepening the volumes seem to stabilise around 7 to 8 million m^3 per year. The dredged material is deposited back into the estuary in designated areas, usually in the secondary branches. During the last enlargement of the navigation channel a new disposal strategy was used (Plancke et al., 2010). Within this strategy dredged sediments are also being used to reshape the edges of certain intertidal flats and create ecological valuable habitats. This new strategy should be seen as a first step in a morphological management approach for estuaries, in which an holistic approach is adopted, taking into account the different ecosystem functions.

In the past centuries large land reclamations have narrowed the estuary, resulting in increasing tidal levels. The tidal amplitude and celerity also increased during the 1965-2002 period for which this research is carried out, but this is believed to be due to the dredging works (Taal et al., 2013). The tide is important for all functions related to the Scheldt estuary: safety, accessibility and nature. Safety against flooding is directly affected by a change in the tidal propagation. Accessibility is dependent on the bed level of the navigational channel in relation to the lowest astronomical tide (LAT). The tide further determines accessibility because of tidal windows and tidal (cross-current) flow. The time that an inter

tidal area is dry is important for its ecological value; a change in the tide has thus an effect on the ecology. Furthermore an increase in tidal velocities generally reduces the ecological richness of the bed (e.g. Raffaelli and Hawkins, 1996).

The tide and morphology are inter related. In Wang et al. (2002) this is described by saying that (1) changes in morphology lead to (2) changes in tidal levels, which lead to (3) differences in ebb and flood velocities that (4) causes residual transport of sediment, with a feedback into (1).

5.3. THE MORPHOLOGICAL MODEL

5.3.1. GENERAL

THE process-based model that is applied in this study is called FINEL2d. The model is a 2DH process-based model based on the finite element method. The depth-integrated shallow water equations are the governing equations of the flow module. For details about FINEL2d reference is made to Dam et al. (2007) and Appendix A. Other examples of the application of the FINEL2d model are Dam et al. (2005, 2009); Dam and Bliek (2013) and Dam et al. (2016). FINEL2d uses an unstructured triangular grid. The advantage of such a mesh in comparison to for example a finite difference grid is the flexible mesh generation. In FINEL2d no nesting techniques are required in regions of specific interest, where a higher degree of resolution is needed, while arbitrary coastlines and complex geometries can be resolved very well, see Figure 5.2.

5.3.2. MODEL GRID AND BOUNDARY CONDITIONS

THE seaward boundaries of the computational mesh of the Western Scheldt are chosen approximately 40 km away from the coastline and coincide with the boundaries of existing models. The latter have been used to obtain the corresponding boundary conditions. The major part of the Scheldt estuary in Belgium is also included in the schematisation. In Figure 2 the whole mesh is shown. In the area of interest, the Western Scheldt, the average grid size is approximately 1.1 ha (see lower panels of Figure 5.2). Near the seaward boundaries the grid size is approximately 2.5 km^2. The total number of elements (triangles) of the mesh is 52,840.

On the seaward boundary of the model domain tidal boundary conditions are imposed, whereas on the river side constant (yearly averaged values) discharges are imposed. Since the estuary is tide dominated (Van der Spek, 1997) only the influence of the tidal action on the morphology is taken into account. It is assumed that the major morphological changes in the estuary are tidally driven. For simplicity reasons wave action is ignored, although

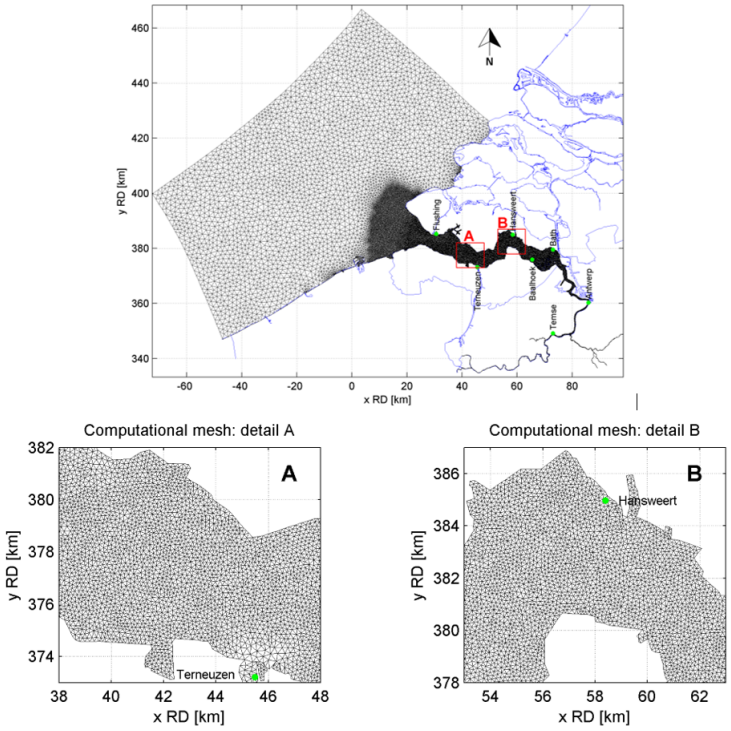

Figure 5.2: Computational mesh of the FINEL2d model; full grid (top) and details (bottom)

inter tidal areas are influenced by waves.

5.3.3. MODELING OF DREDGING/DISTRIBUTION AND SAND MINING

SINCE the major part of the Western Scheldt is dominated by the sand fraction, in the model only non-cohesive sediment is taken into account. Dredging can have an important impact on the morphodynamics in the Western Scheldt. Therefore this needs to be taken into account when performing a hindcast of the morphological developments of the last decades. In reality a navigational depth is guaranteed between the navigational buoys of the fairway. If the depth becomes too shallow a dredger deepens the area to the required depth. In FINEL2d a dredging module was developed based on the same principle. For each grid cell in the fairway a required depth is defined. If the depth in the grid cell is insufficient, sand is removed from the element and distributed according to a certain distribution key over depositing sites. The distribution key is established using historical data of the deposited material. For each historical year an input file is defined, since the buoys, the depositing areas and the maintained depth in the navigational channel may vary over the years. See Consortium Deltares-IMDC-Svasek-Arcadis (2013) for more information about this model input.

Sand mining is simulated in the model by removing the actually mined volume equally

Table 5.1: Model settings

Parameter	Value
Sediment transport formula	Engelund-Hansen
Grain size (d_{50})	Variable (150 μm up to 300 μm)
Fall velocity of sand	0.015 m/s
Morphological acceleration factor (MF)	24.75
Morphological start-up period	1 year
Non-erodable layers	After Dam (2013)
Hydraulics roughness	0.01 m

spread over the specified sand mining area. Since sand mining quantities and locations differ per year an input file for each year is specified. The morphodynamics of the estuary due to the combined effects of natural processes and dredge/depositing activities is continuously calculated, and the riverbed is updated accordingly.

5.3.4. MODEL SETTINGS

THE calibration of the model on the water motion and the sandy morphology for the entire Scheldt estuary is carried out in Dam et al. (2007) with an update in 2013 (Consortium Deltares-IMDC-Svasek-Arcadis, 2013). The hydrodynamic model is calibrated on water levels at the main tidal stations, as indicated in Figure 2. This resulted in a global nikuradse roughness k of 0.01 m. The model is validated on tidal currents in both the channels and inter tidal areas. The hydrodynamic model shows good agreement between observations and model results (Consortium Deltares-IMDC-Svasek-Arcadis, 2013). The morphodynamic model is calibrated on the period 1998-2002 (Consortium Deltares-IMDC-Svasek-Arcadis, 2013).

To speed up the morphological calculation the bed level changes at every time step are multiplied by a morphological acceleration factor (MF) , see Roelvink (2006). In this case a MF of 24.75 is applied in accordance with Dam et al. (2007) meaning that one neap-spring cycle for the water motion represents a morphodynamic year.

The optimal settings for the morphodynamic model found in the calibration are given in Table /refmodelsettings. These settings are used in the model computations discussed in this paper.

A validation of the years 1965 to 2002 is described in Dam et al. (2007), which was updated in (Consortium Deltares-IMDC-Svasek-Arcadis, 2013). This validation period is equal to scenario T0, which includes all the human activities as they have occurred. Starting point is the bathymetry of 1964, see Figure 5.3, and a start-up period of 1 year. This means that

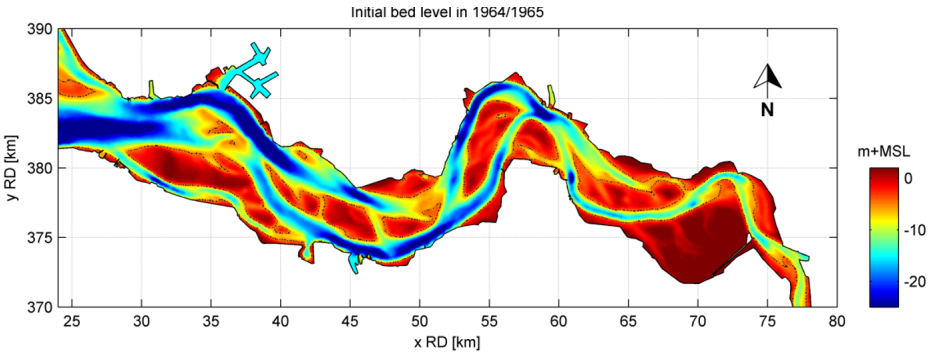

Figure 5.3: Initial bed level of the Western Scheldt (1964/1965). The MSL-5m contour is indicated by the dashed black line. The depths are given in NAP (dutch Ordnance Level), which is approximately MSL

the model requires a start-up time to enable for the initialisation of the sand transport and the adaption of the initial bottom, which was interpolated from GIS data. It was found that a spin-up time of 1 year is sufficient to account for these factors.

5.4. VALIDATION OF THE MODEL ON THE PERIOD 1965-2002

SCENARIO T0 represents the real hindcast period of 1965-2002. The simulated erosion /sedimentation pattern of these years is displayed in Figure 5.4, together with the observed erosion /sedimentation pattern. For some areas good agreement is found for the large scale variations (Middelgat-Overloop van Hansweert, Zuid-Everingen), but in other areas and for the smaller scales important differences can be seen (e.g. Schaar van Waarde, Schaar van Spijkerplaat). The morphological changes are in the order of metres to 10 metres over 38 years.

Since the model is equipped with a dredging module the calculated dredging locations of the model can be compared to the actual dredging locations. In Figure 5.5 this is shown for the eastern part of the Western Scheldt, where the model results are plotted (in colour) together with the actual dredging areas of the sills. The model is capable of reproducing the locations of the large dredging sites; from west to east: Overloop van Hansweert, Drempel van Hansweert, Drempel van Valkenisse, and Drempel van Bath (see Figure 5.1 for their locations).

Figure 5.6 shows the calculated and actual total dredging volume over the 1965-2002 period. The calculated dredging volumes are generally comparable to the actual dredging volumes. Please note the increase of dredging volumes in the 1970's and 1990's, which represent the two deepenings of the navigational channels. A Brier-Skill Score (BSS) is a measure how good the model performs (Sutherland et al., 2004). A BSS value of 0.14 is obtained from the 1965-2002 period. This means that the model has performing skill. From the BSS

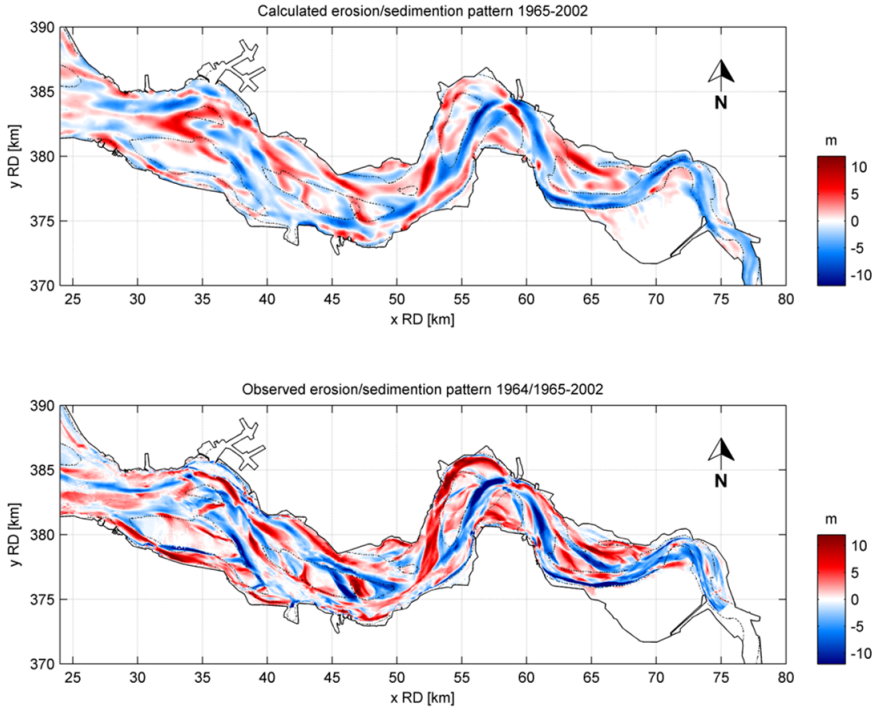

Figure 5.4: Simulated erosion/sedimentation pattern between 1964/1965 and 2002 (top panel) and observed erosion /sedimentation pattern (lower pattern). Red indicates sedimentation; blue indicates erosion. The MSL -5m contour fo the bed in 2002 is indicated with a dashed black line

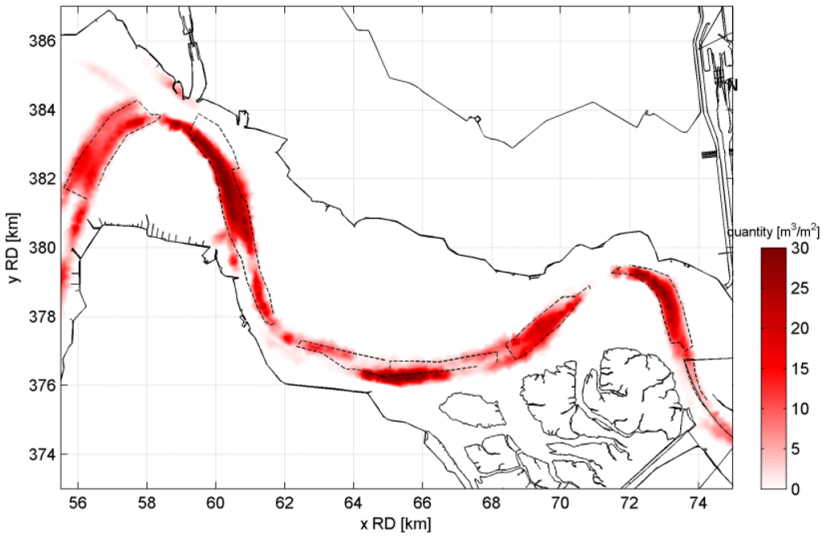

Figure 5.5: Calculated total dredging amount per grid cel for the period 1965-2002 (in color) and the actual dredging areas (dashed black line).

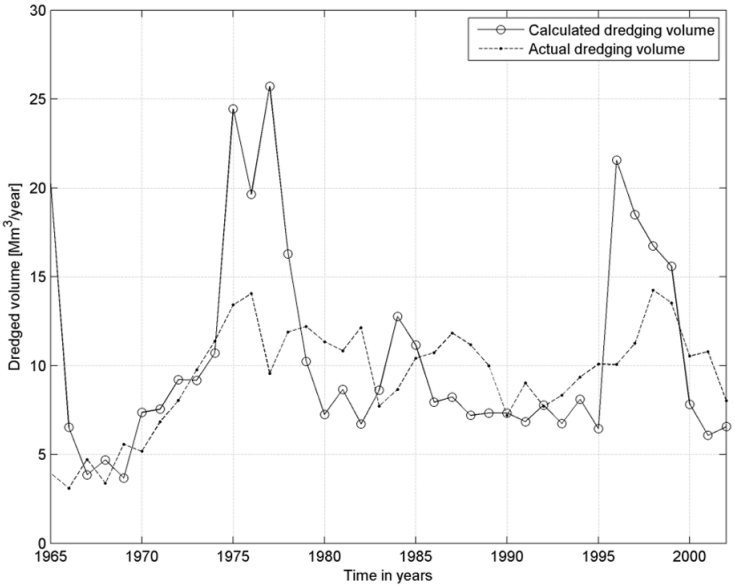

Figure 5.6: Calculated and actual total dredging amount per year for the entire Western Scheldt for 1965-2002

value of 0.14, a reasonable erosion/sedimentation pattern, the correct dredging volumes and spatial distribution of dredging amount, it is concluded that the model is sufficiently accurate to be used to evaluate different scenarios.

5.5. MORPHOLOGICAL SCENARIOS 1965-2002

FOR the 2 fictitious "extreme" scenarios T1 and T2 the same settings given in Table 1 are used. The bathymetry of 1964 is used as a starting point, similar to the T0 scenario (see Figure 5.3. In scenario T1, a simulation is performed without any human interference. This means that in the model computation dredging, distribution of the dredged material and sand mining are not taken into account. In scenario T2 both dredging and sand mining are included, however the dredged material is taken out of the Western Scheldt and not distributed back into the system. In Table 5.2 the three scenarios are summarized. Autonomous behavior (e.g. morphological adaptation due to the historical land reclamations) is included in all three scenarios and so the relative changes between these simulations show the relative effect of these sediment strategies. The question that has to be answered after analyzing the results of the three scenarios is how human activities have influenced the morphology and the tide of the Western Scheldt in the past and what can happen if human activities are intensified in the future.

The bed level of the year 2002, which is at the end of the 38 year model simulation, is for each of the three scenarios shown in Figure 5.7. Especially in the eastern part of the Western Scheldt, distinct differences between the bed levels can be seen. Most prominent

Table 5.2: Scenario definition

Scenario	Dredging	Distribution of dredged material	Sand mining
T0: real hindcast scenario	Yes	Yes	Yes
T1: no human activities	No	No	No
T2: no distribution of dredged material	Yes	No	Yes

is the bed level of the T1 scenario. In this case the sills become shallow (less than 10 m), because they are not maintained by dredging. The secondary channels in the eastern part are more morphodynamic active when no human activities take place. The Eastern part shows distinct evasive ebb and flood characteristics in Scenario T1, as described by Van Veen (1950), while the T0 and T2 scenario are more dominated by the navigational channel, which is kept at its place. In the T0 scenario the secondary branch "Schaar van Waarde" shows severe sedimentation (see Figure 5.1 for the location of this branch). This is due the distribution of the dredged material from the navigational channel. However it should be mentioned that the formation of a new channel in the Schaar van Waarde that took place in reality, is not reproduced in the hindcast. Therefore it seems that the model does not accurately reproduce the morphological behaviour of the disposed sediments in this secondary channel. Since Scenario T1 and T2 do not have this distribution of dredged material the "Schaar van Waarde" is much more pronounced.

The difference in bed level of the three scenarios is given in Figure 5.8. The top panel of Figure 5.8 represents the difference between the bed level of scenario T0 and T1 in 2002 after a morphological time of 38 years. From this figure the large (relative) sedimentation of the navigational channel in scenario T1 can be seen in the eastern part. Also the relative erosion of the secondary channels and intertidal areas is shown. The eastern part of the Western Scheldt is clearly influenced by human activities. The dredged material of the navigational channel in the eastern part is mainly distributed in secondary channels. As a consequence these channels become shallower in comparison to scenario T1 where no human activities take place. The lower panel presents the difference between the bed level of scenario T0 and T2 in 2002. Since dredged material is extracted from the system, mainly relative erosion is visible, both at intertidal areas and in the channels.

The difference in the morphology of the Western Scheldt for the three scenarios is noticeable in the tidal range as well. It should be mentioned that the hydrodynamic boundaries are kept constant at the sea- and landward boundary. This means that effects of sea level rise are not taken into account in the simulations. The sea level rise of the past century was around 10 cm in Flushing. In the considered period of 38 years sea level rise would only concern a few centimetres, which is considered negligible. The tidal range for several water

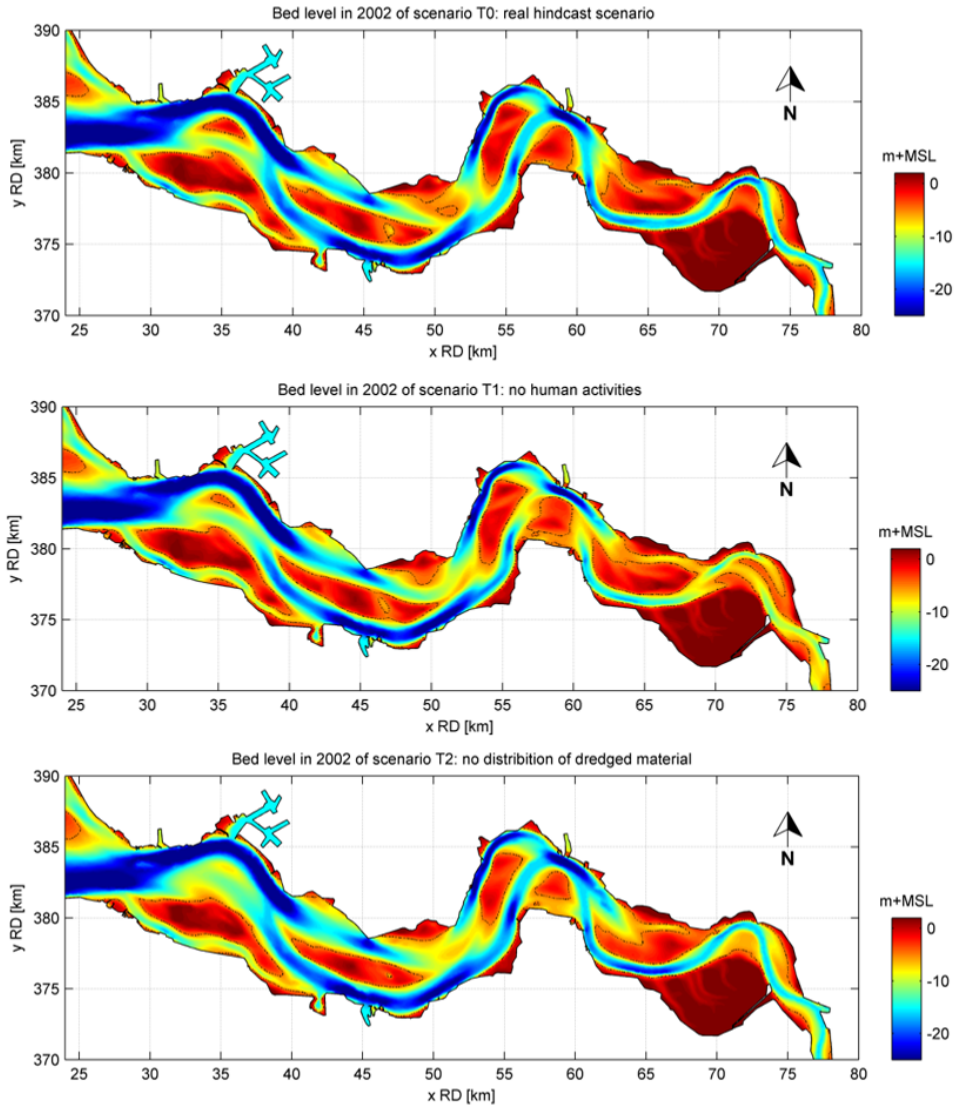

Figure 5.7: The bed level of the Western Scheldt at the end of the FINEL2D model simulations (2002) for scenario T0 (top panel), scenario T1 (middle panel) and scenario T2 (lower panel). The MSL -5 m contour of the bed level in 2002 is for each scenario indicated with a dashed black line.

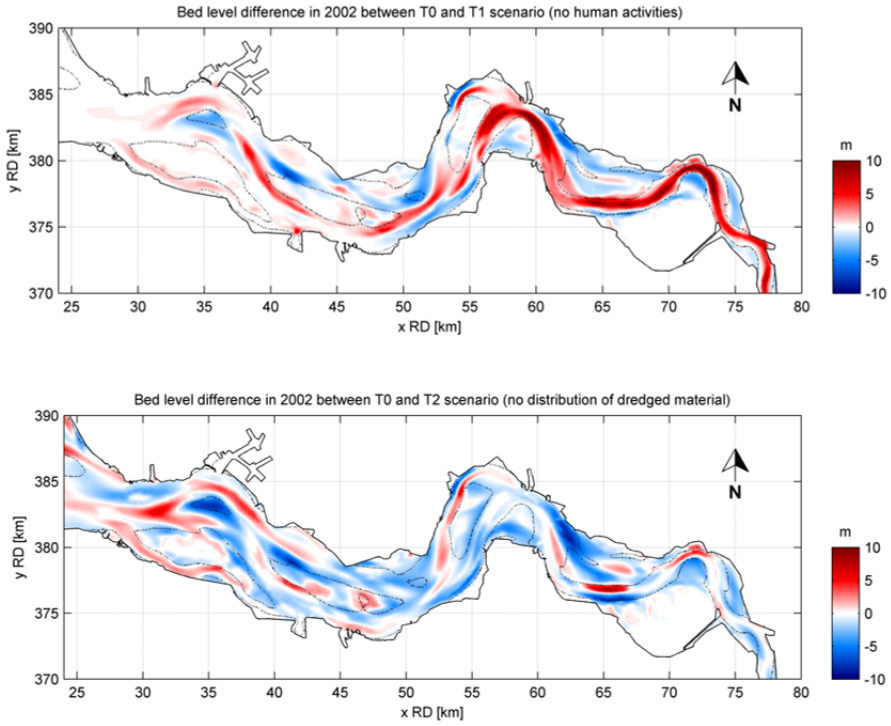

Figure 5.8: Bed level difference in 2002 between scenario T0 and scenario T1 (top panel) and scenario T0 and scenario T2 (lower panel). Red indicates more sedimentation in scenario T1/T2 than in scenario T0; blue indicates more erosion in scenario T1/T2 than in scenario T0. The MSL -5 m contour of the bed level of scenario T0 in 2002 is indicated with a dashed black line.

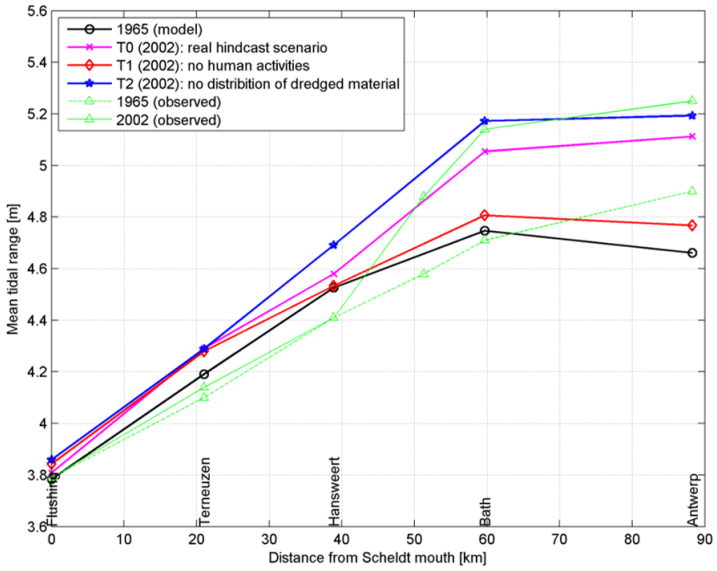

Figure 5.9: Mean tidal range for the three scenarios and observed tidal range in both 1965 and 2002.

level stations along the Western Scheldt is given in Figure 5.9, in which the stations are plotted from west to east. The calculated tidal range of the model in 1965 is shown as well as the observed tidal range of 1965 and 2002. The observed tidal range shows a large increase of the tidal range in the eastern part from 1965 to 2002 (green lines). This is reproduced by the model where in the western part till Hansweert the effect on the tidal range is minimal and in Bath and Antwerp there is a large increase in tidal range (compare the 1965 (model) and T0 (2002) lines). The scenario with the smallest effect on the tidal range is logically scenario T1, which does not include human impacts. Note that this scenario does show a small increase in tidal range in comparison to the 1965 tidal ranges. The actual situation, presented in scenario T0, leads to a higher tidal range than scenario T1. In Antwerp the increase in tidal range from 1965 is calculated at around 40 cm. Scenario T2, in which the dredged material is extracted from the system, results in an even higher tidal range. The increase in tidal range has consequences for ecology, safety against flooding and navigational access, as pointed out in section 2. Note that in reality the maximum tidal range is located 20km upstream from Antwerp, whereas the model shows a maximum somewhere between Bath and Antwerp. This is believed to be a model artefact because the bed upstream from Antwerp is kept constant in the model at the level in the 1960's, while in reality it has deepened. The results should therefore be interpreted carefully.

The average phase difference of the tide compared to Flushing is given in Figure 10 for both the model results as the observed phase differences. Figure 5.10 shows that the calculated phase difference in Antwerp in Scenario T0 increases with approximately 20 minutes compared to the 1965 scenario. This corresponds with the observed tidal celerity increase in Antwerp of 15- 20 minutes of both the high and low waters (Plancke et al., 2012). This is

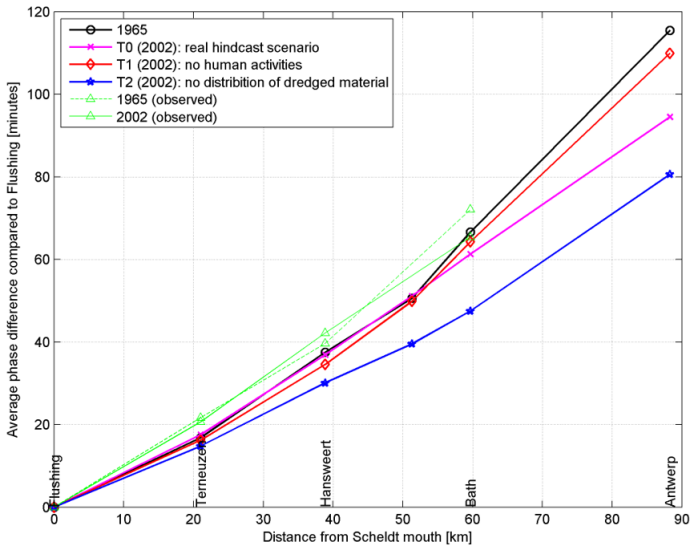

Figure 5.10: Phase difference for the three scenario's in 2002.

Table 5.3: Inter tidal area in 2002 for the 3 scenarios

Scenario	Intertidal area (higher than -2m MSL)	Difference with T0
T0: real hindcast scenario	7560 ha	-
T1: no human activities	7410 ha	-2%
T2: no distribution of dredged material	6840 ha	-10%

not shown in Figure 5.10 as this absolute phase difference compared to Flushing was not available. In the western part the effect on the phase difference is minimal from 1965 to 2002 in both the model as the observed phase difference. In Bath the effect on the phase difference between 1965 and 2002 begins to be clear in both the model as the observations and is further increased towards Antwerp. In the western and middle part of the Western Scheldt, the phase difference in scenario T1 slightly decreases with respect to scenario T0. This corresponds with the observed phase differences over this period. The largest impact can be seen in the eastern part of the Scheldt, from Bath to Antwerp. Scenario T1 shows a small increase in tidal celerity. The largest effect however has Scenario T2; compared to the actual scenario T0, a further 15 minutes increase in tidal celerity can be seen.

This leads to the conclusion that human activities in the Western Scheldt have influenced the tidal range and celerity in the estuary. The extreme scenarios indicate a band width in Figure 5.9 and Figure 5.10 and show what could have happened if other sediment management strategies would have been applied.

In Table 5.3 the inter tidal area in 2002 is given for the three scenarios (although it is

known that the low water varies in the estuary, inter tidal area is for simplicity reasons defined as the area above -2m NAP, which is approximately MSL). The T0 scenario shows the highest amount of inter tidal area. Interestingly the T1 scenario (without human activities) shows a decrease of 2% of inter tidal area. The T2 scenario shows a larger decrease of 10% inter tidal area in comparison to the T0 scenario. This leads to the conclusion that the distribution of dredged material, which is only present in scenario T0, results in more inter tidal area in the model. As a result the hypsometry of the Western Scheldt steepens as a result of a deepened navigational channel and more inter tidal area. Waves, which have been neglected in the model, do have a morphological influence on the inter tidal area, so this conclusion should therefore be interpreted carefully.

5.6. CONCLUSIONS

THE presented FINEL2d morphodynamic model of the Western Scheldt estuary shows that a realistic hindcast of the sea bed development in the estuary can be made over a period of decades (1965-2002). Good agreement is found in overall patterns, although many differences can be seen in detail. By investigating two 'extreme' scenario's (no human activities on the one hand, and removal of all dredged material from the estuary on the other) it is demonstrated that human interference has had a significant influence on the morphology and tide of the estuary during this period.

The model shows that due to the historical human interference of dredging, distribution and sand mining, the channels have deepened and the tidal flats have increased, by which the Western Scheldt probably has become steeper over the 1965-2002 period. The results also show significant effects on the propagation of the tide in the estuary. Due to the actual human activities over the past decades the tidal range in the estuary has increased by about 0.4m in Antwerp and advanced the propagation of the tide with approximately 20 minutes. This corresponds to the advancing of the tide which has been noticed in Antwerp over the past decades. The extreme scenario where all dredged material was taken out of the estuary shows that the process of increasing tide levels in the estuary may continue in case that the human activities are intensified.

The FINEL2d morphodynamic model of the Western Scheldt estuary has proven to be able to calculate the erosion/sedimentation pattern fairly accurate over several decades, while computation time is limited. Computational time for this model is 1.5 hour per morphological year on a 16 core 2.64 GHz machine. This makes the model a useful tool for decision making processes, especially when it is used to compare different scenario's to each other. In this way the calculated sea bed developments and changes in tide are considered relative to the autonomous development, which makes the results more outspoken and more reliable.

5.7. ACKNOWLEDGEMENTS

THIS work has been carried out as part of the LTV V&T project (Long-term vision of the Scheldt estuary, safety and accessibility), which is a consortium of Deltares, IMDC, Arcadis and Svašek Hydraulics, funded by the Dutch ministry of Public Works (Rijkswaterstaat) and the Flemish department of Mobility and Public Works. We thank all the members of the consortium and the client for their input.

6

CONCLUSIONS AND RECOMMENDATIONS

6.1. INTRODUCTION

THE previous chapters describe modeling and data analysis studies and can be read separately. This chapter summarizes the results and is intended as a synthesis of the discussions of the previous chapters. This section answers the research questions as posted in Chapter 1. The detailed conclusions of each chapter are not repeated, but reference is made to the relevant sections in the different chapters.

6.2. ANSWERS TO RESEARCH QUESTIONS

PROCESS-BASED morphodynamic models in previous research were able to produce realistic morphodynamic patterns in schematic settings, such as rectangular basins. An initial thought was that similar like weather forecasting models, process-based models might deviate from reality over long times scales in real case studies. The first question for this research is of these morphodynamic models in real environments where heterogeneity of sediments characteristics, non-constant forcing conditions, and other factors play a role can produce realistic morphodyamic patterns.

Q1: What is the skill of process-based models in long-term morphological hindcasts of estuaries?

Bed level data is available from 1860 onwards in the Western Scheldt estuary and com-

parison is made between a morphodynamic process-based model called FINEL2d and bathymetric data for each year where data is available. Based on a 110-year hindcast of the Western Scheldt estuary (from the year 1860 to 1970) model results show that model skill is initially bad but becomes good over long-time scales (Chapter 2). Self-organization of the morphodynamic system, together with the confinement of the estuarine plan form is thought to be the cause why the model shows good behavior over such long timescales. Both measured and modeled bathymetries reflect a trend of decreasing energy dissipation, less morphodynamic activity and thus a more stable morphology over time. Unlike weather models the degrees of freedom of morphodynamic systems in estuaries are restricted. The estuarine plan form, constant and predictable tidal forcing, self-organization and a developing trend towards morphodynamic equilibrium makes that process-based models may perform well especially on long (>decades) time scales. Since the erosion/sedimentation pattern gives good results over long time scales, the next logical step is to check sediment fluxes in and out of the estuary using this process-based model. For this a data analysis of the bathymetric data and sediment composition was necessary, leading to research question 2:

Q2: What is the long-term behaviour of sand and mud in estuaries?

Bathymetric data of the Western Scheldt from 1860 onwards was combined with a three-dimensional underground model ('GeoTop') in order to create a long-term sediment budget study (Chapter 3). Since data of an underground model was taken into account a differentiation between sand and mud could be made. This research showed that the estuary narrowed and deepened, while the estuary exported sand (1.5-2.5 million m^3/year) and imported mud (0.5-1.5 million m^3/year) over the 1860-1955 period. The eroded sand originated from the eroding channels in the seaward part of the estuary and transported towards the sea, the inner part and in the side branches. The imported marine mud deposited permanently in shoal areas and the side branches, which were gradually reclaimed over time. Being able to differentiate between sand and mud in this sediment budget study it is shown that different sediment types can react differently to the same forcing conditions and even can have opposite net directions. By extending the morphodynamic sand model of Chapter 2 with a sand-mud module, a reproduction of the sand and mud fluxes are carried out for the 1860-1955 period, explaining the underlying transport mechanisms of sand and mud.

The model results show that the observed sand export and mud import of the 1860-1955 period is reproduced by the sand-mud model. Furthermore, the observed erosion/ sedimentation pattern is (still) skillfully reproduced, together with the observed increase in tidal range over this period. The marine mud import in the mouth of the estuary changes

into a mud export when the simulation is extended to 250 years. Accommodation space for mud settlement becomes exhausted over long timescales and fluvial mud will be flushed to the sea. Since mud settlement becomes less over time mud concentrations are increasing according to model results. The observed sand export (Chapter 3) is reproduced by the morphodynamic sand-mud model (Chapter 4). Even tough the tide is hydrodynamically flood dominant, there is a clear sand export due to longer ebb times. Extending the model simulation towards 250 years the sand export eventually approaches zero. These model results indicate that the estuary evolves towards an equilibrium state, as observed in Chapter 2. These model simulations are performed without dredging of the navigational channel that really took off in the 1970's. In reality, the import/export of sediment during more recent periods (after 1970's) are likely to have been affected by anthropogenic influences.

Q3: What are the long-term effects on the estuarine morphology and tides of historic anthropogenic interventions, such as land reclamations, dredging and sandmining

Land reclamations from 1860 onwards have increased the tidal range with about 10 cm over a 100-year period (Chapter 4). Reclamation was mostly done after the secondary basin had already filled inn with sediment. Closing off an area with dikes (the actual reclamation) was merely strengthening of an ongoing trend. However, the final state of the estuary is different over long timescales. Noticeable is that the sediment amount in the total estuary differs due to reclamation. Reclamation leads to less tidal prism (i.e., the amount of water that enters and empties the estuary each tide), slightly less tidal velocities, and deceleration of the morphodynamic trend. The export of sand is noticeably slower due to reclamation. Furthermore, the net import of mud over long time scales is less due to less accommodation space for the mud to settle in the reclaimed side branches. Dredging and dumping has significantly altered the morphodynamics in the Western Scheldt estuary over long time scales (Chapter 5). Scenario runs with and without dredging over the 1965-2002 show that not only the navigational channel has become deeper, but the secondary channel has become shallower. Especially the morphology of the eastern (landward) part of the estuary has been affected greatly. Dredging and dumping has led to increased tidal ranges over time and a faster celerity of the tidal wave into the estuary. Model results are compared to measured tidal range increase and celerity and show good comparisons. An extreme (unrealistic) sand mining scenario show that the tidal wave can increase further if there is less sediment available in the estuary.

6.3. RECOMMENDATIONS

THE unique aspect of the bed level data used in this study lies in the scarcity of available long-term data for estuaries, tidal basins, and coastal seas. While there may be numerous locations with data on shorter timescales, the availability of data spanning over 100 years is quite limited. This makes the data used in this study valuable and significant for understanding long-term morphodynamic processes. However, the study acknowledges the need for further research to evaluate the performance of process-based morphodynamic models in real-world situations over extended periods. Each case study may present different dominant processes that play a crucial role in morphodynamic behavior. These processes can include for example waves, 3D currents, flocculation, varying river discharge, and ecological effects. It is uncertain if morphodynamic models that perform well in one situation retain the same level of performance in the presence of other dominant processes. This highlights the importance of conducting diverse studies to gain a comprehensive understanding of the performance of these models.

The ability to model long time scales is limited by computational power. For this reason, morphodynamic studies usually do not cover more than a few years. It becomes evident from this research that the influence of human activities becomes noticeable over longer time scales, usually spanning several decades. Therefore, studies that evaluate effects of anthropogenic influences on morphodynamics, such as Environmental Impact Assessments (EIA) should extend their assessment periods. It is crucial for these studies to explicitly consider the effects of human impacts on long time scales, even if computational time is lengthy. This shift in approach ensures a thorough understanding of the long-term consequences of anthropogenic influences.

Sea level rise is identified as one of the major threats to coastal societies. The impact of sea level rise on estuarine morphodynamics is expected to be a significant challenge in the coming decades to centuries. Process-based modeling studies provide a valuable tool for assessing the large-scale impact of sea level rise on morphodynamics and exploring potential mitigation measures. These studies help in understanding how estuarine systems may respond and adapt to changes in sea level, allowing for better management and planning to minimize the impacts on coastal environments and communities.

ACKNOWLEDGEMENTS

I extend my deepest gratitude to Mick van der Wegen. Your supervision was crucial in keeping me on track and completing my PhD. Your calm and relaxed approach were instrumental in finishing this thesis. I will truly miss our regular update sessions!

Dano, thank you for your supervision. You and Mick make a fantastic duo.

I also want to express my appreciation to Bram Bliek and the entire team at Svašek Hydraulics for their moral and financial support. My thanks extend to Marcel Taal (Deltares) and everyone from the LT&V project for their interest and financial support.

I am grateful to Ali Dastgeib, Johan Reyns, Leicheng Guo, and Rosh Ranasinghe—for our time together at IHE Delft. I would also like to recognize Ad van der Spek, Robert-Jan Labeur, Nil Eryilmaz, William Helland-Hansen, Jarle Berntsen, and many others who may not be explicitly mentioned here.

My heartfelt thanks go to my COWI colleagues in Norway and Denmark, as well as my former colleagues from Asplan Viak, especially Tom Monstad, for their moral support.

A special shout-out to the Crangon team—I look forward to our next trip together!

I am grateful for the support from my brothers Fokke and Bertus, my nieces Lianne and Marleen, and my parents Hennie and Evert; finally you no longer need to ask how my PhD is going!

Patrick and Katja, Dad is finally ready, which means more time for you both! Lelian, thank you for your support throughout these years.

Gerard Dam
Bergen, February 2025

BIBLIOGRAPHY

Ahnert, F., 1960. Estuarine meanders in the Chesapeake Bay area. Geographical review 50, 390–401.

Alonso, A.C., van Maren, D.S., Elias, E.P.L., Holthuijsen, S.J., Wang, Z., 2021. The contribution of sand and mud to infilling of tidal basins in response to a closure dam. Mar. Geol. 439, 106544.

Baas, J., Davies, A., Malarkey, J., 2013. Bedform development in mixed sand-mud: The contrasting role of cohesive forces in flow and bed. Geomorphology 18, 19–32.

Baeyens, W., Eck, B.V., Lambert, C., Wollast, R., Goeyens, L., 1998. General description of the Scheldt estuary. Hydrobiologia 366, 1–14.

Bakker, W., De Vriend, H., 1995. Resonance and morphological stability of tidal basins. Marine Geology , 5–18.

Bale, A.J., Uncles, R.J., Vilena-Lincoln, A., Widdows, J., 2007. An assesment of the potential impact of dredging activity on the Tamar estuary over the last century: Bathymetric and hydrodynamic changes. Hydrobiologia 588, 83–95. doi:10.1007/s10750-007-0654-1.

Barbier, E.B., Hacker, S.D., Kennedy, C., Koch, E.W., Stier, A.C., Silliman, B.R., 2011. The value of estuarine and coastal ecosystem services 81(2), 169–193. doi:10.1890/10-1510.1.

Barnard, P., Kvitek, R., 2010. Anthropogenic Influence on Recent Bathymetric Change in West-Central San Francisco Bay. San Francisco Estuary and Watershed Science. San Francisco Estuary and Watershed Science 8(3). doi:10.15447/sfews.2010v8iss3art2.

Barnard, P., Schoellhamer, D., Jaffe, B., McKee, L., 2013. Sediment transport in the San Francisco Bay coastal system: an overview. Mar. Geol. 345, 3–17.

Bass, S., Mccave, I., Rees, J., Vincent, C., 2007. Sand and mud flux estimates using acoustic and optical backscatter sensors: Measurements seaward of the Wash, southern North Sea. Geol. Soc. Lond, Spec. Publ. 274, 25–35.

Bertin, X., Chaumillon, E., Sottolichio, A., Pedreros, R., 2005. Tidal inlet response to sediment infilling of the associated bay and possible implications of human activities: The

Marennes-Oléron Bay and the Maumusson Inlet, France. Cont. Shelf Res. 25, 1115–1131. doi:10.1016/j.csr.2004.12.004.

Blott, S.J., Pye, K., van der Wal, D., Neal, A., 2006. Long-term morphological change and its causes in the Mersey Estuary, NW England. Geomorphology 81, 185–206. doi:10.1016/j.geomorph.2006.04.008.

Borsje, B.W., de Vries, M.B., Hulscher, S.J.M.H., de Boer, G.J., 2008. Modeling large-scale cohesive sediment transport affected by small-scale biological activity. Estuarine, Coastal and Shelf Science 78, 468– 480. doi:10.1016/j.ecss.2008.01.009.

Braat, L., Kessel, T.V., Leuven, J., Kleinhans, M., 2017. Effects of mud supply on large-scale estuary morphology and development over centuries to millennia. Earth Surf. Dynam. 5, 617–652.

Bressolier-Bousquet, C., 1991. Geomorphological Effects of Land Reclamation in the Eighteenth Century at the Mouth of the Leyre River, Arcachon Bay, France. Journal of Coastal Research 7, 113–126.

Brown, J., Davies, A., 2010. Flood/ebb tidal asymmetry in a shallow sandy estuary and the impact on net sand transport. Geomorphology 114(3), 431–439.

Cayocca, F., 2001. Long-term morphological modeling of a tidal inlet: the Arcachon Basin, France. Coastal Engineering 42, 115–142. doi:10.1016/s0378-3839(00)00053-3.

Chappell, J., 1993. Holocene sedimentary geologies of the lower Daly River, northern Australia, and lower Sepik-Ramu, Papua New Guinea. Sedimentary Geology 83, 339–358.

Chappell, J., Woodroffe, C., 1994. Macrotidal estuaries. in: Carter, r.w.g., woodroffe, c.d. (eds.), coastal evolution. Cambridge University Press , 187–218.

Chen, M.S., Wartel, S., Eck, B.V., Van Maldegem, D., 2005. Suspended matter in the Scheldt estuary. Hydrobiologia 540, 79–104. doi:10.1007/s10750-004-7122-y.

Coen, I., 1998. Ontstaan en ontwikkeling van de Westerschelde (in dutch). Water 43, 156–162.

Consortium Deltares-IMDC-Svasek-Arcadis, 2013. Actualisatie van het FINEL2d model van de Westerschelde (in Dutch).

Cowell, P.J., Thom, B.J., 1996. Morphodynamics of coastal evolution, in Coastal Evolution, Late Quaternary Shoreline Morphodynamics, edited by r. w. g. carter and c. d. woodroffe. Estuarine shores: Evolution, Environments and Human Alterations .

Cuvilliez, A., Deloffre, J., Lafite, R., Bessineton, C., 2009. Morphological responses of an estuarine intertidal mudflat to constructions since 1978 to 2005: The Seine estuary (France). Geomorphology 104, 165–174. doi:10.1016/j.geomorph.2008.08.010.

Dalrymple, R., Zaitlin, B., Boyd, R., 1992. Estuarine Facies model: conceptual basis and stratigraphic implications. J. Sed. Petrol. 62, 1130–1146.

Dam, G., 2013. Erosion resistant layers Western Scheldt (in dutch).

Dam, G., Bliek, A., 2013. Using a sand-mud model to hindcast the morphology near Waarde, the Netherlands. Maritime Engineering 166, 63–75. doi:10.1680/maen.2011.43.

Dam, G., Bliek, A., Bruens, A., 2005. Band Width analysis morphological predictions Haringvliet Estuary, in: Proceedings of the 4th IAHR Symposium on River, Coastal and Morphodynamics Conference, Urbana, USA, pp. 171–179.

Dam, G., Bliek, A.J., 2011. Hindcasting the morphological impact of 2 dams in the Western Scheldt using a sand-mud model, in: Proceedings of the 7th IAHR Symposium on River, Coastal and Morphodynamics Conference, Beijing, China.

Dam, G., Bliek, A.J., Labeur, R.J., Ides, S.J., Plancke, Y.M.G., 2007. Long-term process-based morphological model of the Western Scheldt estuary, in: Proceedings of the 5th IAHR Symposium on River, Coastal and Morphodynamics Conference, Enschede, The Netherlands, pp. 1077–1084.

Dam, G., Bliek, A.J., Nederbragt, G.J., 2009. High resolution long term morphological model of the northern part of the Holland Coast and Texel Inlet, in: Proceedings of the 6th IAHR Symposium on River, Coastal and Morphodynamics Conference, Santa Fe, Argentina.

Dam, G., Cleveringa, J., 2013. De rol van het slib in de sedimentbalans van de Westerschelde (in dutch available at https://www.vnsc.eu/uploads/2014/02/g-3-de-rol-van-slib-in-de-westerschelde-v1-0.pdf). Consortium Deltares IMDC Svasek, Arcadis, Report G03 .

Dam, G., Poortman, S., Bliek, A., Plancke, Y., 2013. Long-term modeling of dredging strategies on morpho- and hydrodynamic developments in the Western Scheldt, in: WODCON 2013, Brussels, Belgium.

Dam, G., van der Wegen, M., Labeur, R.J., Roelvink, D., 2016. Modeling centuries of estuarine morphodynamics in the Western Scheldt estuary. Geophysical Research Letters 43, 3839–3847. doi:10.1002/2015GL066725.

Dam, G., der Wegen, M.V., Taal, M., van der Spek, A., 2022. Contrasting behavior of sand and mud in a long-term sediment budget of the Western Scheldt estuary. Sedimentology 69(5), 2267–2283. doi:10.1111/sed.12992.

Dastgheib, A., 2012. Long-term process-based morphological modelling of large tidal basins. Ph.D. thesis. UNESCO-IHE and Delft University of Technology.

Dastgheib, A., Roelvink, J.A., Wang, Z.B., 2008. Long-term process-based morphological modeling of the Marsdiep Tidal Basin. Marine Geology 256, 90–100. doi:10.1016/j.margeo.2008.10.003.

De Vriend, H.J., 1991. Mathematical modelling and large-scale coastal behaviour, Part 1: physical processes. Journal of Hydraulic Research 29, 727–740.

De Vriend, H.J., 1996. Mathematical modeling of Meso-tidal barrier island coasts. Part I: Empirical and Semi-Empirical Models, in: Liu, P.L.F. (Ed.), Advances in Coastal and Ocean Engineering, World Scientific, Singapore. pp. 115–149.

De Vriend, H.J., Capobianco, M., Chesher, T., de Swart, H.E., Latteux, B., Stive, M.J.F., 1993. Approaches to long-term modelling of coastal morphology: A review. Coastal Engineering 21, 225–269. doi:10.1016/0378-3839(93)90051-9.

De Vriend, H.J., Wang, Z.B., Ysebaert, T., Herman, P.M.J., Ding, P., 2011. Eco-Morphological Problems in the Yantse Estuary and the Western Scheldt. Wetlands 31, 1033–1042. doi:10.1007/s13157-011-0239-7.

Diaz, M., Grasso, F., Hir, P.L., Sottolichio, A., Caillaud, M., Thouvenin, B., 2020. Modeling Mud and Sand transfers between a Macrotidal Estuary and the Continental shelf: Influence of the Sediment Transport Parameterization. J. Geoph. Res. 125(4).

Dijkstra, Y.M., Schuttelaars, H.M., Schramkowski, G.P., 2019b. Can the Scheldt river estuary become hyperturbid? Ocean Dynamics 69(7), 809–827.

Dijkstra, Y.M., Schuttelaars, H.M., Schramkowski, G.P., Brouwer, R.L., 2019a. Modeling the transition to high sediment concentrations as a response to channel deepening in the Ems River Estuary. Journal of Geophysical Research: Oceans 124(3), 1578–1594.

Dissanayake, D.M.P.K., Roelvink, J.A., van der Wegen, M., 2009. Modelled channel patterns in a schematized tidal inlet. Coastal Engineering 56, 1069–1083. doi:10.1016/j.coastaleng.2009.08.008.

Dronkers, J., 1986. Tidal assymetry and estuarine morphology. Netherlands Journal of Sea Research 20, 117–131.

Dyer, K., 1995. Sediment transport processes in estuaries, in: Perillo, G. (Ed.), Geomorphology and Sedimentology of Estuaries, Elsevier, Amsterdam, The Netherlands. pp. 423–449.

Dyer, K., 2000. Estuaries, a Physical Introduction. second ed. John Wiley & Sons .

Elmilady, H., van der Wegen, M., Roelvink, D., Jaffe, B.E., 2019. Intertidal area disappears under sealevel rise: 250 years of morphodynamic modeling in San Pablo Bay, California. Journal of Geophysical Research: Earth Surface 124, 38–59. doi:10.1029/2018JF004857.

Engelund, F., Hansen, E., 1967. A Monograph on Sediment Transport in Alluvial Streams. Teknisk Forlag , 1–63. Copenhagen, Denmark.

Escoffier, 1940. Stability of Tidal Inlets. Shore Beach 8, 114–115.

Eyre, B., Hossain, S., McKee, L., 1998. A suspended sediment budget for the modified subtropical Brisbane river estuary. Estuar. Coast. Shelf. Sci. 47, 513–522.

Falconer, R., Owens, P., 1990. Numerical modelling of suspended sediment fluxes in estuarine waters. Estuar. Coast. Shelf. Sci. 31, 754–762.

Fettweis, M., Sas, M., Monballiu, J., 1998. Seasonal, Neap-spring, and Tidal variation of cohesive sediment concentration in the Scheldt Estuary, Belgium. Estuarine, Coastal and Shelf Science 47, 21–36.

FitzGerald, D., Knight, J., 2005. High Resolution Morphodynamics and Sedimentary Evolution of Estuaries. Springer, Dordrecht .

Friedrichs, C., 1995. Stability shear stress and equilibrium cross-sectional geometry of sheltered tidal channels. J. Coastal Res. 11, 1062–1074.

Friedrichs, C., Aubrey, D., 1988. Non-linear tidal distortion in shallow well-mixed estuaries: a synthesis. Estuarine, Coastal and Shelf Science 27(5), 521–545.

Friedrichs, C., Aubrey, D., Speer, P., 1990. Impacts of Relative Sea-level Rise on Evolution of Shallow Estuaries, springer, new york, ny. In: Residual Currents and Long-term Transport. Coastal and Estuarine Studies, (Ed. Cheng, R.T.) 38.

Galappatti, R., 1983. A depth integrated model for suspended transport, Communications on Hydraulics, Vol. 83-7. Technical Report. Delft University of Technology.

Ganju, N.K., Schoellhamer, D.H., Jaffe, B.E., 2009a. Hindcasting of decadal-timescale estuarine bathymetric change with a tidal-timescale model. J. Geophys. Res. 114, F04019. doi:10.1029/2008JF001191.

Ganju, N.K., Schoellhamer, D.H., Jaffe, B.E., 2009b. Hindcasting of decadal-timescale estuarine bathymetric change with a tidal-timescale model. Journal of Geophysical Research 114. doi:10.1029/2008jf001191.

Garel, E., Pinto, L., Santos, A., Ferreira, O., 2009. Tidal and river discharge forcing upon water and sediment circulation at a rock-bound estuary. Estuarine Coastal Shelf Sci. 84, 269–281.

George, D.A., Gelfenbaum, G., Stevens, A.W., 2012. Modeling the Hydrodynamic and Morphologic Response of an Estuary Restoration. Estuaries and Coasts 35, 1510–1529. doi:10.1007/s12237-012-9541-8.

Gill, J., Norris, K., Potts, P.M., Gunnarsson, T.G., Atkinson, P.W., Sutherland, W.J., 2001. The buffer effect of large-scale population regulation in migratory birds. Nature 412, 436–438.

Glaister, P., 1993. Flux difference splitting for open-channel flows. International Journal for Numerical Methods in Fluids 16, 629–654.

Grabowski, R.C., Droppo, I.G., Wharton, G., 2011. Erodibility of cohesive sediment: The importance of sediment properties. Earth-Science Reviews 105, 101 – 120. doi:10.1016/j.earscirev.2011.01.008.

Green, M., Bell, G., Dolphin, T., Swales, A., 2000. Silt and sand transport in a deep tidal channel of a large estuary (Manukau Harbour, New Zealand). Mar. Geol. 163, 217–240.

Groen, P., 1967. On the residual transport of suspended matter by an alternating tidal current. Netherlands Journal of Sea Research 3-4, 564–574.

Gruijters, S.H.L.L., Schokker, J., Veldkamp, J.G., 2004. Mapping erosion resistant layers in the Scheldt estuary (in dutch).

Guilcher, A., 1967. Origin of sediments in estuaries. In: Estuaries (Ed. Lauff, G.H.), American Association for the Advancement of Science Publication 83, 149–157.

Guo, L., der Wegen, M.V., Roelvink, J., He, Q., 2014. The role of river discharge and tidal asymmetry on 1d estuarine morphodynamics. J. Geophys. Res. Earth Surf. 119, 2315–2334. doi:10.1002/2014JF003110.

Haecon, 2006. Actualisatie van de zandbalans van de Zee- en Westerschelde (in Dutch).

Haff, P., 1996. Limitations on predictive modeling in geomorphology, in: Rhoads, B., Thorn, C. (Eds.), The scientific nature of geomorphology, Wiley: New York. pp. 337–358.

Haff, P.K., 2013. Prediction in geology versus prediction in engineering. Geol. Soc. Am. Spec. Pap. 502. doi:10.1130/2013.2502(06).

Haring, J., 1948. Inhouds- en diepteveranderingen Westerschelde over de periode 1878-1931 (in Dutch available at http://publicaties.minienm.nl/documenten/inhouds-en-diepteveranderingen-in-de-wester-schelde-over-de-peri) .

Haring, J., 1955. Inhouds- en diepteveranderingen Westerschelde over de periode 1931-1952 (in Dutch) .

Hervouet, J.M., 2000. Telemac modelling system: An overview. Hydrol. Processes 14, 2209–2210.

Hibma, A., de Vriend, H.J., Stive, M.J.F., 2003a. Numerical modelling of shoal pattern formation in well-mixed elongated estuaries. Estuarine, Coastal and Shelf Science 57. doi:10.1016/s0272-7714(03)00004-0.

Hibma, A., Schuttelaars, H., de Vriend, H.J., 2004. Initial formation and long-term evolution of channel-shoal patterns. Cont. Shelf Res. 24, 1637–1650. doi:10.1016/j.csr.2004.05.003.

Hibma, A., Schuttelaars, H.M., de Vriend, H.J., 2004a. Initial formation and long-term evolution of channel shoal patterns. Continental Shelf Research 24, 1637–1650. doi:10.1016/j.csr.2004.05.003.

Hibma, A., Vriend, H.J.D., Stive, M.J.F., 2003b. Numerical modelling of shoal pattern formation in well-mixed elongated estuaries. Estuarine Coastal Shelf Sci. 57(5-6), 981–999. doi:10.1016/s0272-7714(03)00004-0.

Hoitink, A., 2003. Flow asymmetry associated with astronomical tides: Implications for the residual transport of sediment. Journal of Geophysical Research 108(C10).

Hughes, T.J.R., 1987. The finite element method : linear static and dynamic finite element analysis. Prentice-Hall, Englewood Cliffs, N.J.

Jagers, H.R.A., 2003. Modelling Planform Changes of Braided Rivers. Ph.D. thesis. University of Twente.

Jalón-Rojas, I., Schmidt, S., Sottolichio, A., 2017. Comparison of environmental forcings affecting suspended sediments variability in two macrotidal, highly-turbid estuaries. Estuarine, Coastal and Shelf Science 198, 529–541.

Jeuken, M., 2000. On the morphological behaviour of tidal channels in the Western Scheldt estuary. Ph.D. thesis. Utrecht University.

Kalkwijk, J.P.T., Booij, R., 1986. Adaptation of secondary flow in nearly-horizontal flow. Journal of Hydraulic Research 24, 19–37. doi:10.1080/00221688609499330.

Karunarathna, H., Reeve, D., Spivack, M., 2008. Long-term morphodynamic evolution of estuaries: An inverse problem. Estuarine, Coastal and Shelf Science 77, 385–395. doi:10.1016/j.ecss.2007.09.029.

Kragtwijk, N., Zitman, T.J., Stive, M.J.F., Wang, Z.B., 2004. Morphological response of tidal basins to human interventions. Coast. Eng. 51, 207–221. doi:10.1016/j.coastaleng.2003.12.008.

Krone, R.B., 1962. Flume studies of the transport of sediment in estuarial shoaling process, Final report Hydraulic Engineering Laboratory and Sanitary Engineering Research Laboratory. Technical Report.

Langbein, W.B., 1963. The hydraulic geometry of a shallow estuary. Bulletin of Internat, Assoc. Sci. Hydrol. 8, 84–94.

Lanzoni, S., Seminara, G., 2002. Long-term evolution and morphodynamic equilibrium of tidal channels. J. Geophys. Res. 107(C1). doi:10.1029/2000JC000468.

Le Hir, P., Cayocca, F., Waeles, B., 2011. Dynamics of sand and mud mixtures: A multiprocess-based modelling strategy. Continental Shelf Research 31, S135–S149. doi:10.1016/j.csr.2010.12.009.

LeConte, L., 1905. Discussion on river and harbour outlets. notes on the improvement of river and harbour outlets in the united states,paper nr 1009, by D.A. Watts. Trans. Am. Soc. Civ. Eng. 55, 306–308.

Lesourd, S., Lesueur, P., Fisson, C., Dauvin, J., 2016. Sediment evolution in the mouth of the Seine estuary (France): A long-term monitoring during the last 150 years. C R Geosci. 348, 442–450.

Lesser, G., Roelvink, J., van Kester, J., Stelling, G., 2004a. Development and validation of a three-dimensional morphological model. Coastal Engineering 51, 883 – 915. doi:10.1016/j.coastaleng.2004.07.014.

Lesser, G.R., Roelvink, J.A., Kester, J.A.T.M.V., Stelling, G.S., 2004b. Development and validation of a three-dimensional morphological model. Coast. Eng. 51, 883–915. doi:10.1016/j.coastaleng.2004.07.014.

Lorenz, E.N., 1963. Deterministic Nonperiodic Flow. Journal of the Atmosperic Sciences 20, 130–141.

Luan, H., Ding, P., Wang, Z., Ge, J., 2017. Process-based morphodynamic modeling of the Yangtze estuary at a decadal timescale: Controls on estuarine evolution and future trends. Geomorphology 290, 347–364. doi:10.1016/j.geomorph.2017.04.016.

Luo, J., Li, M., Sun, Z., Connor, B., 2013. Numericall modelling of hydrodynamics and sand transport in the tide dominated coastal-to estuarine region. Marine geology 342, 14–27.

Maanen, B.V., Coco, G., Bryan, K.R., 2013. Modelling the effects of tidal range and initial bathymetry on the morphological evolution of tidal embayments. Geomorphology 191, 23–34. doi:10.1016/j.geomorph.2013.02.023.

Manni, R., 1986. Slibtransport en slibbalans in de Westerschelde (in Dutch available at http://resolver.tudelft.nl/uuid:db93bdd6-453e-47dc-b907-7ee2b7101eab) .

Marciano, R., Wang, Z.B., Hibma, A., de Vriend, H.J., Defina, A., 2005. Modeling of channel patterns in short tidal basins. Journal of Geophysiscal Research 110. doi:10.1029/2003jf000092.

McClaren, P., 1994. Sediment Transport in the Western Scheldt between Baarland and Rupelmonde.

Meerschout, Y., Parker, W., Peters, J., Plancke, Y., 2004. A dredging and disposal strategy for managing the Western Scheldt's morphology and ecology, in: Dredging in a sensitive environment; Proceedings of the World Dredging Congress XVII, Hamburg, Germany.

Mengual, B., Hir, P.L., Rivier, A., Cailaud, M., Grasso, F., 2021. Numerical modeling of bed-load and suspended load contributions to morphological evolution of the Seine estuary (France). International Journal of Sediment Reseach 36, 723–735.

Mitchener, H., Torfs, H., 1996. Erosion of mud/sand mixtures. Coastal Engineering 29, 1–25. doi:10.1016/s0378-3839(96)00002-6.

Murphy, A.H., Epstein, E.S., 1989. Skill scores and correlation coefficients in model verification. Monthly Weather Review 117, 572–581.

Murray, A.B., 2003. Contrasting the goals, strategies, and predictions associated with simplified numerical models and detailed simulations, in Prediction in Geomorphology. Geophys. Monogr. 135, 151–165.

Nederbragt, G.J., Liek, G.J., 2004. Beschrijving zandbalans Westerschelde en monding (in Dutch). Technical Report.

Nnafie, A., Oyen, T.V., Maerschalck, B.D., van der Vegt, M., der Wegen, M.V., 2018. Estuarine channel evolution in response to closure of secondary basins: An observational and morphodynamic modeling study of the Western Scheldt Estuary. Journal of Geophysical Research-Earth Surface 123(1), 167–186. doi:10.1002/2017jf004364.

O'Brien, M., 1931. Estuary and tidal prisms related to entrance areas. Civil Engineering 1, 738–739.

O'Brien, M., 1969. Equilibrium flow areas of inlets on sandy coasts. Journal of the Waterways and Harbours Division, ASCE 95, 43–51.

Olabarrieta, M., Geyer, W., Coco, G., Friedrichs, C., Cao, Z., 2018. Effects of density driven flows on the long-term morphodynamic evolution of funnel-shaped estuaries. J. Geoph. Res. 123, 2901–2924.

Paarlberg, A.J., Knaapen, M.A.F., de Vriesa, M.B., Hulscher, S.J.M.H., Wang, Z.B., 2005. Biological influences on morphology and bed composition of an intertidal flat. Estuarine, Coastal and Shelf Science 64, 577–590. doi:10.1016/j.ecss.2005.04.008.

Partheniadis, E., 1965. Erosion and deposition of cohesive soils. ASCE, Journal of the Hydraulic Division 91, 105–139.

Pethick, J.S., 1994. Estuaries and wetlands: function and form. Thompson Telford, London.

Philips, J.D., 1992. The end of equilibrium? Geomorphology 5, 195–201.

Philips, J.D., 1999. Divergence, convergence and self-organization in landscapes. Ann. Assoc. Am. Geogr. 89(3), 466–488.

Pillsbury, G., 1956. Tidal Hydraulics. Corps of Engineers, Vicksburg, USA.

Plancke, Y., Ides, S., Roose, F., Peters, J., 2010. A new disposal strategy for the Western Scheldt, conciliating port accesibility and nature preservation, in: 32nd PIANC Congress, Liverpool, UK, pp. 1–11.

Plancke, Y., Maximova, T., Ides, S., Peeters, P., Taverniers, E., Mostaert, F., 2012. Werkgroep OM - Projectgroep Veiligheid: Sub project 1: Data analysis and hypothesis - Lower Sea Scheldt.

Pritchard, D., 1967. What is an estuary: physical viewpoint, in: Lauf, G.H. (Ed.), Estuaries, AAAS Publ. 83. pp. 3–5.

Raffaelli, D., Hawkins, S., 1996. Intertidal ecology. Kluwer Academic Publishers, Dordrecht, The Netherlands.

Randarian, A., Bryan, K., Wegen, M.V.D., 2022. On the influence of antecedent morphology on development of equilibrium bathymetry in estuaries past and future. Journal of Geophysical Research: Earth Surface e2022JF006621.

Reynolds, O., 1887. On certain laws relating to the regime of rivers and estuaries and on the possibility of experiments on a small scale .

Rijkswaterstaat, 2013. Bathymetrical data of the Western Scheldt, data available upon request at helpdesk-data@rws.nl .

Rodriquez-Iturbe, I., Rinaldo, A., Rigon, R., Bras, R.L., Marani, A., Vasquez, E.L., 1992. Energy dissipation, runoff production, and the threedimensional structure of river basins. Water Resour. Res. 28(4), 1095–1103. doi:10.1029/91WR03034.

Roelvink, J.A., 2006. Coastal morphodynamic evolution techniques. Coastal Engineering 53, 277–287. doi:10.1016/j.coastaleng.2005.10.015.

Roelvink, J.A., Reiniers, A.J.H.M., 2011. A guide to modelling coastal morphology. Advances in Coastal and Ocean Engineering, World Scientific, Singapore.

Rosati, J., 2005. Concepts in Sediment Budgets. J. Coastal Res. 21, 307–332.

Russell, R., 1967. Origins of estuaries. In: Estuaries (Ed. Lauff, G.H.), American Association for the Advancement of Science Publication 83, 93–99.

Schramkowski, G.P., Schuttelaars, H.M., de Swart, H.E., 2003. Non-linear channel – shoal dynamics in long tidal embayments. Ocean Dynamics 54, 399–407. doi:10.1007/s10236-003-0063-6.

Schubel, J., Carter, H., 1984. The estuary as a filter for fine-grained suspended sediment. Ed: Kennedy, V. S., The Estuary As a Filter, Academic Press , 81–105.

Schuttelaars, H., 1997. Evolution and stability analysis of bottom patterns in a tidal embayment. Ph.D. thesis. Utrecht University.

Schuttelaars, H.M., de Swart, H.E., 1999. Initial formation of channels and shoals in a short tidal embayment. Journal of Fluid Mechanics 386, 15–42.

Schuttelaars, H.M., de Swart, H.E., 2000. Multiple morphodynamic equilibria in tidal embayments. Journal of Geophysical Research 105, 24,105–24,118. doi:10.1029/2000JC900110.

Seminara, G., Turbino, M., 2001. Sand bars in tidal channels. Part 1: Free bars. Journal of Fluid Mechanics 440, 49–74.

Shchepetkin, A.F., McWilliams, J.C., 2005. The regional oceanic modeling system (ROMS): A split-explicit, free-surface, topography following-coordinate oceanic model. Ocean Model. 9(4), 347–404. doi:10.1016/j.ocemod.2004.08.002.

Shellenbarger, G., Wright, S., Shoellhamer, D., 2013. A sediment budget for the southern reach in San Fransisco Bay, CA: Implications for habitat restoration. Mar. Geol. 345, 281–293.

Speer, P.E., Aubrey, D.G., 1985. A Study of Non-Lineair Tidal Propagation in Shallow Inlet/Estuarine Systems, Part ii: Theory. Estuarine, Coastal and Shelf Science 21, 207–224.

Staffleu, J., Maljers, D., Gunnink, J., Menkovic, A., 2011. 3d modelling of the shallow subsurface of Zeeland, The Netherlands. Neth. J. Geosci. 90, 293–310.

Stark, J., Smolders, S., Meire, P., Temmerman, S., 2017. Impact of intertidal area characteristics on estuarine tidal hydrodynamics: A modelling study for the Scheldt Estuary. Est., Coast. and Shelf Sci 198, 138–155. doi:10.1016/j.ecss.2017.09.004.

Stive, M.J.F., Wang, Z.B., 2003. Morphodynamic Modeling of Tidal Basins and Coastal Inlets. Elsevier oceanography series 67, 367–392.

Sutherland, J., Peet, A.H., Soulsby, R.L., 2004. Evaluating the performance of morphological models. Coastal Engineering 51, 917–939. doi:10.1016/j.coastaleng.2004.07.015.

Syvitski, J.P.M., Vörösmarty, C.J., Kettner, A.J., Green, P., 2005. Impact of Humans on the Flux of Terrestrial Sediment to the Global Coastal Ocean. Science 308(5720), 376–380. doi:10.1126/science.1109454.

Taal, M., Kuiper, K., Cleveringa, J., Sas, M., 2013. Historical development of the tide in the Scheldt Estuary and the interaction with dredging works, in: WODCON 2013, Brussels, Belgium.

Tambroni, N., Pittaluga, M.B., Seminara, G., 2005. Laboratory observations of the morphodynamic evolution of tidal channels and tidal inlets. J. Geophys. Res. 110, F04009. doi:10.1029/2004JF000243.

Terwindt, J.H.J., 1967. Mud transport in the Dutch Delta area and along the adjacent coastline. Netherlands Journal of Sea Research 3, 505–531.

Thomas, C.G., Spearman, J.R., Turnbull, M.J., 2002. Historical morphological change in the Mersey Estuary. Continental Shelf Research 22, 1775–1794. doi:10.1016/S0278-4343(02)00037-7.

TNO, 2017. GeoTop subsurface model data, data available at www.dinoloket.nl .

Tolhurst, T., Black, K., Paterson, D., Mitchener, H., Termaat, G., Shayler, S., 2000. A comparison and measurement standardisation of four in situ devices for determining the erosion shear stress of intertidal sediments. Continental Shelf Research 20, 1397 – 1418. doi:10.1016/S0278-4343(00)00029-7.

Tönis, I.E., Stam, J.M.T., van de Graaf, J., 2002. Morphological changes of the Haringvliet estuary after closure in 1970. Coastal Engineering 44, 191–203. doi:10.1016/S0378-3839(01)00026-6.

Townend, I., Wang, Z., Rees, J., 2007. Millennial to annual volume changes in the Humber Estuary. Proc. R. Soc. A 463, 837–854.

Townend, I., Whitehead, P., 2003. A preliminary net sediment budget for the Humber Estuary. Sci. Total Environ. 314-316, 755–767.

Townend, I.H., Dun, R.W., 2000. A diagnostic tool to study long-term changes in estuary morphology, in Coastal and Estuarine Environments, edited by k. pye and j. r. l. allen. Sedimentology, Geomorphology and Geoarchaeology , 75–86.

Van Alphen, J.S.L.J., 1990. A mud balance for Belgium-Dutch coastal waters between 1969 and 1986. Netherlands Journal of Sea Research 25, 19–30.

Van Den Berg, J.H., Jeuken, M.C.J.L., van der Spek, A.J.F., 1996. Hydraulic processes affecting the morphology and evolution of the Westerschelde estuary. Estuarine shores: Evolution, Environments and Human Alterations .

Van der Spek, A.J.F., 1997. Tidal asymmetry and long-term evolution of Holocene tidal basins in the The Netherlands: simulation of paleo-tides in the Schelde estuary. Marine Geology 141, 71–90. doi:10.1016/s0025-3227(97)00064-9.

Van der Wal, D., Pye, K., Neal, A., 2002. Long-term morphological change in the Ribble Estuary, northwest England. Marine Geology 189, 249–266. doi:10.1016/s0025-3227(02)00476-0.

Van der Wegen, M., Jaffe, B., Roelvink, J.A., 2011. Process-based, morphodynamic hindcast of decadal deposition patterns in San Pablo Bay, California. Journal of Geophysical Research 116, 1856–1887.

Van der Wegen, M., Jaffe, B.E., 2013. Towards a probabilistic assessment of process-based, morphodynamic models. Coastal Engineering .

Van der Wegen, M., Roelvink, J.A., 2008. Long-term morphodynamic evolution of a tidal embayment using a two-dimensional, process-based model. Journal of Geophysical Research 114. doi:10.1029/2006jc003983.

Van der Wegen, M., Roelvink, J.A., 2012. Reproduction of estuarine bathymetry by means of a process-based model: Western Scheldt case study, the Netherlands. Geomorphology doi:10.1016/j.geomorph.2012.08.007.

Van der Wegen, M., Wang, Z.B., Savenije, H.H.G., Roelvink, J.A., 2008. Long-term morphodynamic evolution and energy dissipation in a coastal plain, tidal embayment. Journal of Geophysical Research 113. doi:10.1029/2007jf000898.

Van Kessel, T., Vanlede, J., De Kok, J., 2011. Development of a mud transport model for the Scheldt estuary. Continental Shelf Research 31, 165–181. doi:10.1016/j.csr.2010.12.006.

Van Ledden, M., 2003. Sand-mud segregation in estuaries and tidal basins. Ph.D. thesis. Delft University of Technology.

Van Ledden, M., Kesteren, W.G.M., Winterwerp, J.C., 2004a. A conceptual framework for the erosion behaviour of sand-mud mixtures. Continental Shelf Research 24, 1–11. doi:10.1016/j.csr.2003.09.002.

Van Ledden, M., Wang, Z.B., Winterwerp, J.C., De Vriend, H.J., 2004b. Sand-mud morphodynamics in a short tidal basin. Ocean Dynamics 54, 385–391. doi:10.1007/s10236-003-0050-y.

Van Maldegem, D.C., Mulder, H.P.J., Langerak, A., 2003. A cohesive sediment balance for the Scheldt estuary. Netherlands Journal of Aquatic Ecology 27, 247–256.

Van Maren, D., Oost, A., Wang, Z., Vos, P., 2016. The effect of land reclamations and sediment extraction on the suspended sediment concentration in the Ems Estuary. Mar. Geol. 376, 147–157.

Van Prooijen, B.C., Montserrat, F., Herman, P.M., 2011. A process-based model for erosion of Macoma balthica-affected mud beds. Continental Shelf Research 31, 527 – 538. doi:10.1016/j.csr.2010.12.008.

Van Rijn, L.C., 1993. Principles of sediment transport in river, estuaries and coastal seas. Aqua publications, Amsterdam, The Netherlands.

Van Straaten, L.M.J.U., Kuenen, P.H., 1957. Accumulation of Fine Graided Sediment In The Dutch Wadden Sea. Geologie en Mijnbouw 19, 329–354.

Van Veen, J., 1944. Schelderegiem en Schelderegie. (Ed. Pieters, T., reissued (1993), RIKZ, Middelburg, in Dutch available at http://publicaties.minienm.nl/documenten/schelderegiem-en-schelderegie) .

Van Veen, J., 1950. Eb eb vloed scharen in de Nederlandse getij wateren. Journal of the Royal Dutch Geographical Society 67, 303–325 (Engl. transl., Delft Univ. Press, Delft, Netherlands, 2002).

Van Veen, J., der Spek, A.V., Stive, M., Zitman, T., 2005. Ebb and Flood Channel Systems in the Netherlands Tidal Waters. J. Coastal Res. 21, 1107–1120.

Verlaan, P., Donze, M., Kuik, P., 1998. Marine vs fluvial suspended matter in the Scheldt estuary .

Verlaan, P.A.J., 2000. Marine vs Fluvial Bottom Mud in the Scheldt Estuary. Estuarine, Coastal and Shelf Science 50, 627–638. doi:10.1006/ecss.1999.0599.

Vernes, R., Doorn, T.V., 2005. Van Gidslaag naar Hydrogeologische Eenheid – Toelichting op de totstandkoming van de dataset REGIS ii (in Dutch). Netherlands Institute of Applied Geosciences TNO, Report 05-038-B .

Vos, P., 2015. Origin of the Dutch Coastal Landscape, long-term landscape evolution of the Netherlands during the Holocene, described and visualized in national, regional and local peleogeographical map series. Ph.D. thesis. Utrecht University.

Vreugdenhil, C.B., 1994. Numerical methods for shallow-water flow. Kluwer, Dordrecht.

Waeles, B., Hir, P.L., Lesueur, P., Delsinne, N., 2007. Modelling sand/mud transport and morphodynamics in the Seine River mouth (France): an attempt using a process-based approach. Hydrobiologica 588, 69–82.

Wang, H., Bi, N., Saito, Y., Wang, Y., Sun, X., Zhang, J., Yang, Z., 2010. Recent changes in sediment delivery by the Huanghe (Yellow river) to the sea: Causes and environmental implications in its estuary. Journal of Hydrology 391, 302–313. doi:10.1016/j.jhydrol.2010.07.030.

Wang, Z.B., Jeuken, M.C.J.L., Gerritsen, H., Vriend, H.J.D., Kornman, B.A., 2002. Morphology and assymetry of the vertical tide in the Westerschelde estuary. Continental Shelf Research 22, 2599–2609.

Wang, Z.B., Langerak, A., Fokkink, R.J., 1999. Simulation of long-term morphological development in the Western Scheldt. Symposium of the International Association for Hydraulics Research , Genova, Italy.

Wartel, S., 1977. Composition, transport and origin of sediments in the Scheldt estuary. Geol. Mijnbouw 56(3), 219–233.

Widdows, J., Blauw, A., Heip, C., Herman, P., Lucas, C., Middelburg, J., Schmidt, S., Brinsley, M., Twisk, F., Verbeek, H., 2004. Role of physical and biological processes in sediment dynamics of a tidal flat in Westerschelde Estuary, SW Netherlands. Marine Ecology Progress Series 274, 41–56.

Widdows, J., Brinsley, M.D., Salkeld, P.N., Lucas, C.H., 2000. Influence of biota on spatial and temporal variation in sediment erodability and material flux on a tidal flat (Westerschelde, The Netherlands). Marine Ecology Progress Series 194, 23–37.

Winn, P., Young, R., Edwards, A., 2003. Planning for the rising tides: the Humber Estuary Shoreline Management Plan. The Science of The Total Environment 314-316, 13–30. doi:10.1016/s0048-9697(03)00092-5.

Winterwerp, J., Wang, Z., 2013. Man-induced regime shifts in small estuaries-i: theory. Ocean Dynamics 63(11-12), 1279–1292.

Winterwerp, J., Wang, Z., Braeckel, A.V., Holland, G.V., Kösters, F., 2013. Man-induced regime shifts in small estuaries—ii: a comparison of rivers. Ocean Dynamics 63, 1293–1306.

Winterwerp, J.C., Van Kesteren, W.G.M., 2004. Introduction to the physics of cohesive sediment in the marine environment. Developments in Sedimentology, Elsevier, Amsterdam, The Netherlands.

Winterwerp, J.C., Wang, Z.B., Stive, M.J.F., Arends, A., Jeuken, M.C.J.L., Thoolen, P.M.C., 2001. A new morphological schematization of the Western Scheldt Estuary, The Netherlands. Proceedings of the 2nd IAHR Symposium on River, Coastal and Morphodynamics Obihiro, Japan, 525–533.

Wolanski, E., Brinson, M., Cahoon, D., Perillo, G., 2009. Coastal wetlands. a synthesis. In: Coastal Wetlands, An Integrated Ecosystem Approach , 1–62.

Wolanski, E., Williams, D., Hanert, E., 2016. The trapping efficiency of the macro-tidal Daly estuary, tropical australia. Estuarine, Coastal and Shelf Science 69, 291–298.

Woodroffe, C.D., 2002. Coasts: Form, Process and Evolution .

Zhang, Q., Fan, D., Feng, T., Tu, J., Guo, X., 2022. Impacts of land reclamation projects on hydrodynamics and morphodynamics in the highly altered North Branch of the Changjiang Estuary. Anthropocene Coasts 5, 6. doi:10.1007/s44218-022-00006-2.

Zhou, Z., Coco, G., Jimenez, M., Olabarrieta, M., van der Wegen, M., Townend, I., 2014. Morphodynamics of river-influenced back-barrier tidal basins: The role of landscape and hydrodynamic settings. Water Resour. Res. 50, 9514–9535. doi:10.1002/2014WR015891.

A

FINEL2D MODEL

A.1. GOVERNING EQUATIONS WATER MOTION

The model that is used in this research is FINEL2d. FINEL2d is a 2DH numerical model based on the finite elements method and is developed by Svašek Hydraulics (Dam et al., 2007, 2009; Dam and Bliek, 2011). The following sections describe the governing equations of the FINEL2d model.

The depth-integrated shallow water equations are the basis of the flow module. For an overview of shallow water equations see Vreugdenhil (1994).

The model equations are the continuity equation:

$$\frac{\partial H}{\partial t} + \frac{\partial uD}{\partial x} + \frac{\partial vD}{\partial y} = 0 \tag{A.1}$$

the x-momentum balance:

$$\frac{\partial Du}{\partial t} + \frac{\partial Du^2}{\partial x} + \frac{\partial Duv}{\partial y} + f_c Dv + gD\frac{\partial h}{\partial x} - \frac{1}{\rho}\tau_{x,b} + \frac{1}{\rho}\tau_{x,w} + \frac{1}{\rho}\tau_{x,r} = 0 \tag{A.2}$$

the y-momentum balance:

$$\frac{\partial Dv}{\partial t}+\frac{\partial Duv}{\partial x}+\frac{\partial Dv^2}{\partial y}+f_cDu+gD\frac{\partial h}{\partial y} -\frac{1}{\rho}\tau_{y,b}+\frac{1}{\rho}\tau_{y,w}+\frac{1}{\rho}\tau_{y,r}=0 \tag{A.3}$$

In which:

$$H = h+z_b \tag{A.4}$$

where u=depth averaged velocity in x-direction $[m/s]$; v=depth averaged velocity in y-direction $[m/s]$; h=water level $[m]$; z_b=bottom level $[m]$; D=water depth $[m]$; f_c=Coriolis coefficient $[1/s]$; g=gravitational acceleration $[m/s^2]$; ρ=density of water $[kg/m^3]$; τ_b=bottom shear stress $[N/m^2]$; τ_w=wind shear stress $[N/m^2]$; and τ_r=radiation stress $[N/m^2]$.

The discontinuous Galerkin method is adopted to solve for the differential equations. Within this method, the water level and the two horizontal velocity components are taken constant in each element. To apply the discontinuous Galerkin method, the equations of motion, shown in equations A.1, A.2 and A.3, are rewritten as:

$$\frac{\partial}{\partial t}U+\frac{\partial}{\partial x}F_x+\frac{\partial}{\partial y}F_y=S_1+S_2 \tag{A.5}$$

In which:

$$U=\begin{pmatrix} H \\ uH \\ vH \end{pmatrix}, \quad F_x=\begin{pmatrix} uH \\ u^2H+\frac{gH^2}{2} \\ uvH \end{pmatrix}, \quad F_y=\begin{pmatrix} vH \\ uvH \\ v^2H+\frac{gH^2}{2} \end{pmatrix}, \tag{A.6}$$

$$S_1 = \begin{pmatrix} 0 \\ gH\frac{\partial z_b}{\partial x} \\ gH\frac{\partial z_b}{\partial y} \end{pmatrix}, \quad S_2 = \begin{pmatrix} 0 \\ \frac{1}{\rho}\tau_{x,tot} - fv \\ \frac{1}{\rho}\tau_{y,tot} + fu \end{pmatrix} \tag{A.7}$$

For the discontinuous Galerkin method, the rewritten equations of motion are integrated over each element, resulting in:

$$\int_\Omega \frac{\partial}{\partial t} U \, \mathrm{d}\Omega + \int_\Gamma (F_x \cdot n_x + F_y \cdot n_y) \, \mathrm{d}\Gamma = \int_\Omega (S_1 + S_2) \, \mathrm{d}\Omega \tag{A.8}$$

In equations A.8 and A.5, Ω represents the element surface, Γ the element boundary and n the outward pointing unit vector normal to the element contour. Furthermore, F_x and F_y represent the fluxes, and contain the advective terms with the pressure gradient and mass flux. S_1 and S_2 represent the source terms, where S_1 contains the influence of the bottom slope and S_2 contains the external forces, e.g. the Coriolis force and shear stresses.

In addition to the effect of advection and pressure gradients, external forces like the Coriolis force, bottom shear stress, wind shear stress and radiation stress due to surface waves can be taken into account. It is noted that turbulent shear stresses are not taken into account: the application is therefore restricted to advection dominated flows only.

As a solution method, the discontinuous Galerkin method is adopted (Hughes, 1987) in which the flow variables are taken constant in each moment. This method has advantages in dealing with drying elements.

As the momentum equations contain first order derivatives in space, they can be written as:

To solve the local Riemann problem, equation A.5 is rewritten to:

$$\frac{\partial}{\partial t} U + \frac{\partial F_x}{\partial U}\frac{\partial U}{\partial x} + \frac{\partial F_y}{\partial U}\frac{\partial U}{\partial y} = S_1 \tag{A.9}$$

Here, $\frac{\partial F_x}{\partial U}$ and $\frac{\partial F_y}{\partial U}$ represent the flux Jacobians. Neglecting the source term, this can subsequently be rewritten to:

$$\int_\Omega \frac{\partial}{\partial t} U \, \mathrm{d}\Omega + \oint A \left(U_{neighbour} - U\right) \mathrm{d}\Gamma = 0 \tag{A.10}$$

Here, $U_{neighbour}$ represents the flow in the neighbouring element. Matrix A is defined by:

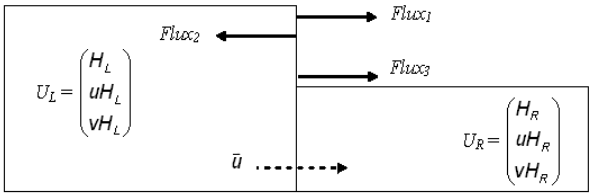

Figure A.1: Discretisation of the mesh

$$A = \left(\frac{\partial F_x}{\partial U}, \frac{\partial F_y}{\partial U} \right) \cdot \vec{n} \tag{A.11}$$

Matrix A, as defined in equation A.11, has three real eigenvalues, which form the characteristics along which the fluxes propagate. The abrupt change in flow variables at every element boundary can be interpreted as two step waves and a shear wave, which, in case of subcritical flow, propagate downstream along two of the characteristics and upstream along one characteristic, as sketched in figure A.1. Every element has tree boundaries on which the three Roe fluxes are determined, by means of the eigenvalues, eigenvectors and wave strengths. These fluxes along the three boundaries together, by adding them to the flow variables of the element, determine the total change of the flow variables in an element in one time step.

In mathematical terms, the Roe solver in FINEL2D is a first order upwind scheme. This scheme does cause some numerical diffusion, but guarantees strict mass and momentum conservation. Furthermore, the explicit integration in time in FINEL2D restricts the time step. The time step is therefore controlled automatically, in order to achieve optimal performance.

A.2. GOVERNING EQUATIONS SEDIMENT TRANSPORT

FINEL2d uses the following sediment balance equation for the evolution of the bed level:

$$\frac{\partial z_b}{\partial t} + \frac{\partial q_x}{\partial x} + \frac{\partial q_y}{\partial y} = 0 \tag{A.12}$$

In which $z_b[m]$ is the bed level and $(q_x, q_y)[m^2/s]$ are the components of the sediment flux in x- and y-direction respectively.

In order to determine the non-cohesive part of the sediment fluxes, the transport formula of Engelund and Hansen formula is used (Engelund and Hansen, 1967). Since most of the sand transport in the Western Scheldt is suspended transport, a time lag effect is introduced in the model according to Galappatti (1983). First a dimensionless equilibrium concentration is calculated:

$$c_e = \frac{S}{D\sqrt{u^2 + v^2}} \tag{A.13}$$

where ce is equilibrium concentration [-] and S the magnitude of the equilibrium sand transport [m2/s] according to Engelund and Hansen (1967).

The concentration c [-] is then calculated according from:

$$\frac{dc}{dt} = \frac{1}{T_A}[c_e(t) - c(t)] \tag{A.14}$$

In which T_A is a characteristic timescale [s].

Equation A.14 shows that if the concentration is lower than the equilibrium concentration erosion will occur ($dc/dt > 0$). If the concentration is higher than the equilibrium concentration sedimentation will occur ($dc/dt < 0$). The coefficient T_A characterises the time needed for the adjustment of the concentration and is defined in A.15

$$T_A = h/w_s \tag{A.15}$$

where w_s [m/s] is the settling velocity of the sand particles. In relative shallow areas the time scale is small and the concentration almost immediately adjusts to the equilibrium concentration.

A

A.3. GOVERNING EQUATIONS SPIRAL FLOW

FINEL2D uses a depth averaged approach to model hydro- and morphodynamics. In many circumstances such approach is appropriate, but for example in sharp bends in rivers or estuaries this assumption is not valid anymore. In sharp bends the flow has a tendency to flow outwards at the surface and inwards at the bed, these secondary currents form a spiral. See Figure 5.1 for a sketch of spiral flow in curved open channel flow.

The influence of spiralflow on waterlevels is small, but because at the bed the direction of secondary flow is always towards the centre of a bend the impact on morphological changes of a bend is large. Spiral flow transports bed material from the outerbend towards the innerbend. The outer bend is getting deeper which leads to increased flow velocities, so this process is increasing itself. FINEL2D calculates depth averaged velocities, therefore normally the influence of 3D spiral flow is not taken into account. But following Kalkwijk and Booij (1986) and Jagers (2003) a parameterised influence on the sediment fluxes can be switched on. Note that the influence of spiralflow in FINEL2D affects sedimentfluxes only, not the water velocities in a bend. The spiral correction is applied to silt and sand (both suspended and bed transport).

To take into account the effects of spiral flow on sediment transport the following parameters need to be determined:

- Radius of the bend Rs (Section A.3.1)
- Intensity of spiralflow (Section A.3.2)
- Adaptation of angle of bottom shear stress towards inner bend (Section A.3.3)

A.3.1. DETERMINATION OF BED RADIUS (R_s)

$$\frac{1}{R_s} = \frac{1}{u_s}\frac{\partial u_n}{\partial s} \tag{A.16}$$

$$\frac{dx}{dy} = \frac{u_y}{u_x} = tan\beta \tag{A.17}$$

$$\begin{bmatrix} s \\ n \end{bmatrix} = \begin{bmatrix} cos\beta & sin\beta \\ -sin\beta & cos\beta \end{bmatrix} \begin{bmatrix} x \\ y \end{bmatrix} \tag{A.18}$$

$$\begin{bmatrix} u_s \\ u_n \end{bmatrix} = \begin{bmatrix} cos\beta & sin\beta \\ -sin\beta & cos\beta \end{bmatrix} \begin{bmatrix} u_x \\ u_y \end{bmatrix} \tag{A.19}$$

Rewriting of A.16 gives:

$$\frac{1}{R_s} = \frac{1}{u_s}\left(\frac{\partial u_n}{\partial x}\frac{\partial x}{\partial s} + \frac{\partial u_n}{\partial y}\frac{\partial y}{\partial s}\right) \tag{A.20}$$

using

$$\frac{dx}{ds} = cos\beta \tag{A.21}$$

$$\frac{dy}{ds} = sin\beta \tag{A.22}$$

in Equation A.20 leads to:

$$\frac{1}{R_s} = \frac{1}{u_s}\left(cos\beta\frac{\partial u_n}{\partial x} + sin\beta\frac{\partial u_n}{\partial y}\right) \tag{A.23}$$

Substitution of Equation A.19 into A.23 results in:

$$\frac{1}{R_s} = \frac{1}{u_x cos\beta + u_y sin\beta}\left(cos\beta\left(-sin\beta\frac{\partial u_x}{\partial x} + cos\beta\frac{\partial u_y}{\partial x}\right) + sin\beta\left(-sin\beta\frac{\partial u_x}{\partial y} + cos\beta\frac{\partial u_y}{\partial y}\right)\right) \tag{A.24}$$

Or:

$$R_s = \frac{u_x cos\beta + u_y sin\beta}{-cos\beta sin\beta\frac{\partial u_x}{\partial x} + cos^2\beta\frac{\partial u_x}{\partial y} + sin\beta cos\beta\frac{\partial u_y}{\partial y}} \tag{A.25}$$

A.3.2. DETERMINATION INTENSITY OF THE SPIRAL FLOW k

Kalkwijk and Booij (1986) developed the following equation of spiral flow intensity:

$$\frac{1-2\alpha}{2\alpha\kappa^2}\frac{D}{\bar{u}_s}\left[\frac{\bar{u}_x}{\bar{u}_s}\frac{\partial k}{\partial x} + \frac{\bar{u}_y}{\bar{u}_s}\frac{\partial k}{\partial y}\right] + k\left[1 + \frac{1-2\alpha}{2\alpha\kappa^2}\frac{R_s}{\bar{u}_s^2}\left(\bar{u}_x\frac{\partial D|\bar{u}_s|/R_s}{\partial x} + \bar{u}_y\frac{\partial D|\bar{u}_s|/R_s}{\partial y}\right)\right] = 1 \tag{A.26}$$

Or:

$$\frac{1-2\alpha}{2\alpha\kappa^2}\frac{D}{\bar{u}_s}\left[\frac{\bar{u}_x}{\bar{u}_s}\frac{\partial k}{\partial x} + \frac{\bar{u}_y}{\bar{u}_s}\frac{\partial k}{\partial y}\right] + k\left[1 + \frac{1-2\alpha}{2\alpha\kappa^2}\frac{R_s}{\bar{u}_s^2}\left(\bar{u}_x\frac{\partial k_{eq}}{\partial x} + \bar{u}_y\frac{\partial k_{eq}}{\partial y}\right)\right] = 1 \tag{A.27}$$

With:

$$\alpha = \frac{\sqrt{g}}{\kappa C} \tag{A.28}$$

$$k_{eq} = \frac{D|U|}{R_s} \tag{A.29}$$

A

D=depth $[m]$
C=Chezy coeffcient $[m^0.5/s]$
κ =0.41 = Von Karman constant $[-]$

In FINEL2d the following equation is used to determine k, based on Jagers (2003)

$$\frac{\partial k}{\partial t} = \frac{\partial k\bar{u}_x}{\partial x} + \frac{\partial k\bar{u}_y}{\partial y} = \frac{k - k_e q}{T} \tag{A.30}$$

with:

$$T = \frac{\left(\frac{1}{2\alpha} - 1\right) D}{\kappa^2 |U|} \tag{A.31}$$

A.3.3. ADAPTATION OF ANGLE OF BOTTOM SHEAR STRESS TOWARDS INNER BEND

Using the spiral flow intensity (k) the normal component of the bottom shear stress in a river bend (directing towards the center) is determined by Kalkwijk and Booij (1986):

$$\tau_n = 2\rho\alpha^2(1-\alpha)|u|k \tag{A.32}$$

Rewriting in:

$$\tau_n = 2\tau_s \frac{1}{\kappa^2}(1-\alpha)\frac{k}{|u|} \tag{A.33}$$

The adaptation of the angle of the bottom shear stress towards the inner bend can be written in x- and y-coordinates by:

$$\tau_x = \tau_s \frac{1}{|u|}\left(u + v\left(\frac{2}{\kappa^2}(1-\alpha)\frac{k}{|u|}\right)\right) \tag{A.34}$$

$$\tau_y = \tau_s \frac{1}{|u|}\left(v - u\left(\frac{2}{\kappa^2}(1-\alpha)\frac{k}{|u|}\right)\right) \tag{A.35}$$

It is assumed that sediment fluxes have the same direction as the bottom shear stress. In FINEL2D the sediment fluxes are calculated using the Roe-fluxes Q at the edges of every triangle. The Roe-fluxes Q consist of a contribution from the velocity ($Q_1 = u_n * H * B_{edge}$) and a contribution from the shock-wave caused by the difference in waterlevel and/or velocity between two adjacent elements ($Q2 \sim c_{wave} * f(\Delta H, \Delta U) * B_{edge}$). To take into account the influence of spiral flow on sediment fluxes, Q1 is corrected using u_{spir}, v_{spir} to calculate

u_n. Q2 is kept the same.
With:

$$u_{spir} = \left(u + v \left(\frac{2}{\kappa^2} (1 - \alpha) \frac{k}{|u|} \right) \right) \tag{A.36}$$

$$v_{spir} = \left(v - u \left(\frac{2}{\kappa^2} (1 - \alpha) \frac{k}{|u|} \right) \right) \tag{A.37}$$

If switched on in FINEL2D the spiral correction is applied to mud and sand (both suspended and bed transport).

B

MEASURED AND MODELED EROSION AND SEDIMENTATION PATTERNS

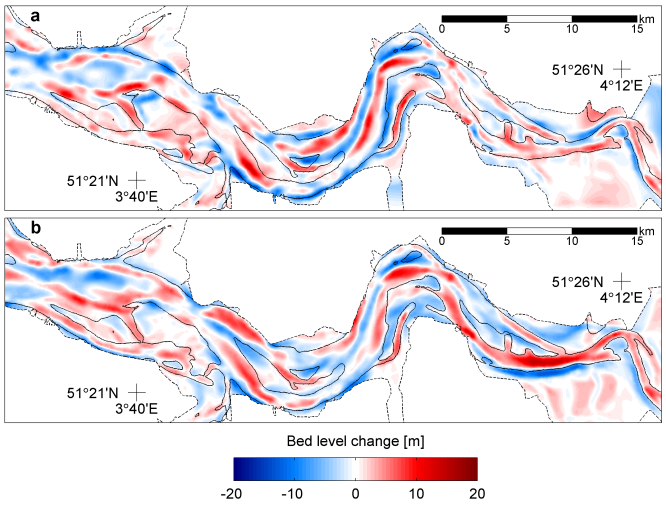

Figure B.1: Erosion and sedimentation patterns over the 1860-1878 period. (a) Measured. (b) Modeled. Black dashed line indicates the 1860 plan form. Black solid line indicates the -5m contour line of the 1860 bed level.

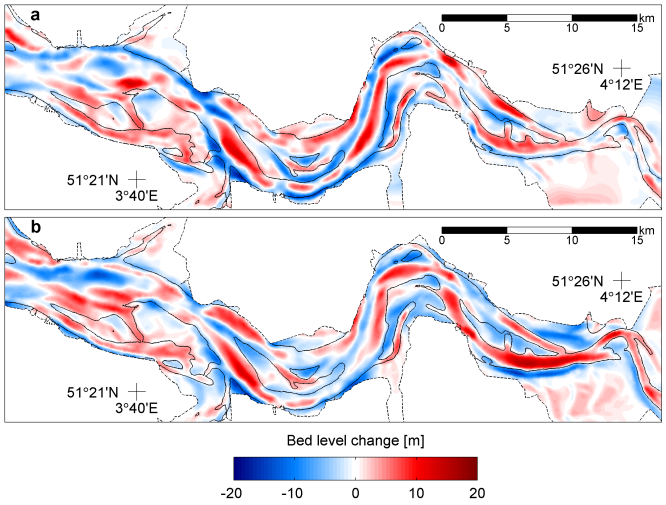

Figure B.2: Erosion and sedimentation patterns over the 1860-1890 period. (a) Measured. (b) Modeled. Black dashed line indicates the 1860 plan form. Black solid line indicates the -5m contour line of the 1860 bed level.

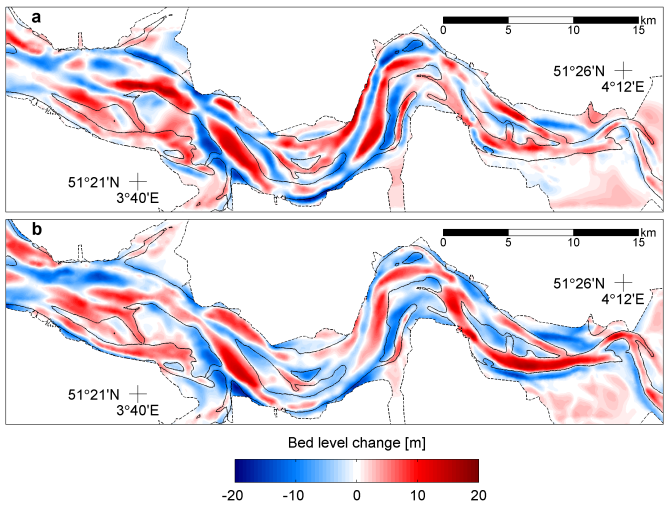

Figure B.3: Erosion and sedimentation patterns over the 1860-1905 period. (a) Measured. (b) Modeled. Black dashed line indicates the 1860 plan form. Black solid line indicates the -5m contour line of the 1860 bed level.

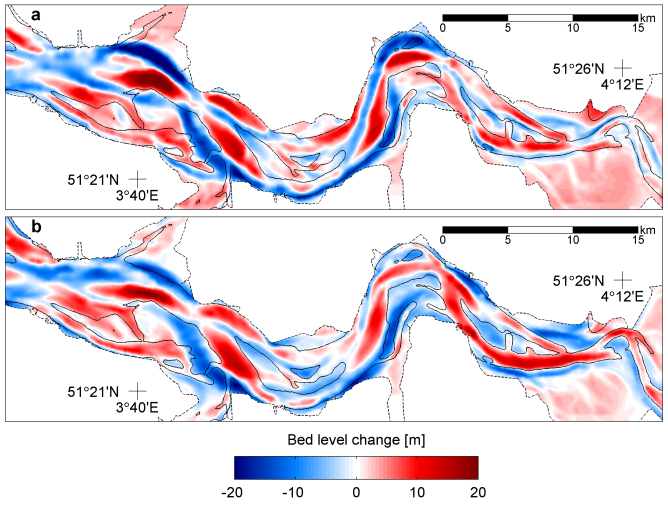

Figure B.4: Erosion and sedimentation patterns over the 1860-1931 period. (a) Measured. (b) Modeled. Black dashed line indicates the 1860 plan form. Black solid line indicates the -5m contour line of the 1860 bed level.

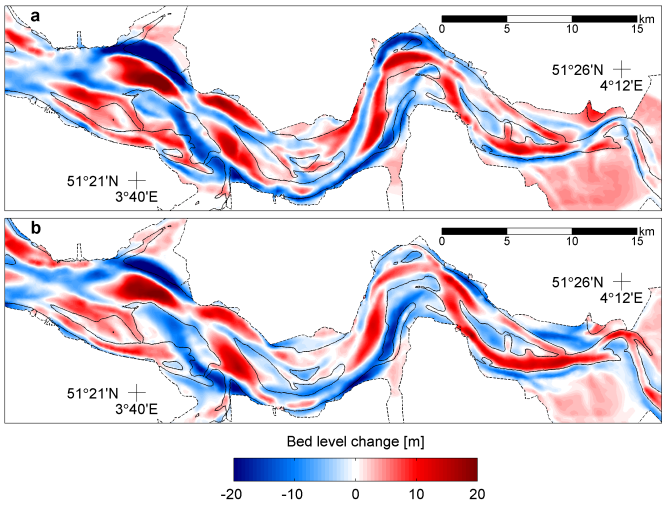

Figure B.5: Erosion and sedimentation patterns over the 1860-1955 period. (a) Measured. (b) Modeled. Black dashed line indicates the 1860 plan form. Black solid line indicates the -5m contour line of the 1860 bed level.

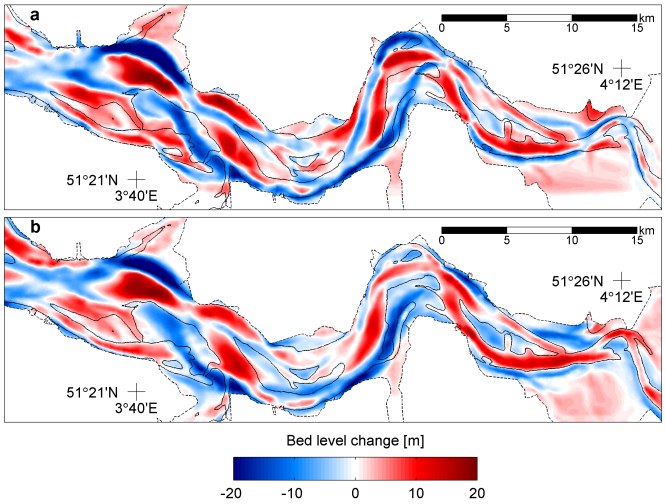

Figure B.6: Erosion and sedimentation patterns over the 1860-1960 period. (a) Measured. (b) Modeled. Black dashed line indicates the 1860 plan form. Black solid line indicates the -5m contour line of the 1860 bed level.

C

MODELLING OF SAND-MUD MIXTURES

(Parts of this chapter are taken from the published peer-reviewed paper Dam and Bliek (2013))

C.1. INTRODUCTION

Process-based morphological models have developed rapidly the last decades. The models are becoming more and more robust tools to predict morphodynamic developments based on physical descriptions and advanced bed update techniques (Van der Wegen and Roelvink, 2012). The focus of most model applications with dynamic bed development is on non-cohesive sediments (sand). Hibma et al. (2003a, 2004a); Marciano et al. (2005); Van der Wegen et al. (2008) and Van der Wegen and Roelvink (2008, 2012) show that it is possible to use process-based models to reproduce channel-shoal formation in a tidal inlet or estuary starting in an idealised way from an initially flat bed. Classically separate models are used for sand (cf. Van Rijn, 1993) and mud (cf. Winterwerp and Van Kesteren, 2004; Van Kessel et al., 2011). However, natural sediment rarely consists of only sand or mud (Mitchener and Torfs, 1996). Sand models have a dynamic coupling between bed level changes and the water motion, whereas mud models generally do not have this coupling (Van Ledden, 2003). The focus of this chapter is on modelling the bed dynamics in an area where both cohesive and non-cohesive sediments are present. This requires not only the integration of 'sand' and 'mud' (non-cohesive and cohesive) processes in one model, but also the interaction between sand and mud.

The biggest problem in developing such a model is in the prediction of the erodability of the cohesive sediment. According to Grabowski et al. (2011) a good comprehensive model for this erodability is still lacking. Grabowski et al. (2011) use two arguments for that: (1)

the strong inter-particle interactions complicates the use of theoretical approaches, and (2) empirical approaches have been limited by the number of sediment properties that influence erodability and a lack of standardised methods for the quantification of erodability and sediment properties. However a concept of such a model is made by Van Ledden (2003) and this concept is used in this research.

C.2. EROSION OF SAND AND MUD

Erosion of sand behaves differently from mud. The erosion of non-cohesive sediments, here termed "sand" with grain size $> 63\mu m$, is dependent on factors such as grain size distribution, the shape and density of individual grains and the forcing. Erosion of sand is generally formulated in terms of a deviation with respect to a specific equilibrium situation. Sand deposition and erosion balance over alluvial beds generating an equilibrium over uniform and stationary situations (Van Ledden et al., 2004a).

Cohesive sediments, here termed "mud" with grain size $< 63\mu m$, have electrochemical forces that bind them together. The clay particles are mainly responsible for this cohesion. Erosion of cohesive sediments are dependent on physical, geochemical and biological parameters like mineral composition, organic content, biological processes, consolidation, the history of the bed, pH, salinity and metal concentrations (Mitchener and Torfs, 1996; Grabowski et al., 2011). Erodability is not determined by any individual property, but is a product of the interactions between multiple properties (Grabowski et al., 2011). Contrary to sand beds, the availability of mud in the bed is often limited for erosion and the flow is far from its transport capacity. An equilibrium between mud deposition and erosion therefore only occurs in highly concentrated mud suspensions (Van Ledden et al., 2004a). A distinction is made between a "Type I" erosion, which is described as a peak in erosion rate which rapidly decreases in time, also known as "benign" erosion and "Type 2" erosion where a high erosion rate is sustained, also known as "chronic" erosion.

A sand-mud mud mixture behaves differently than a pure sand or mud bed. Adding sand to mud, or vice versa, increases the erosion resistance and reduces the erosion rates when the critical shear stress is exceeded (Mitchener and Torfs, 1996; Van Ledden, 2003). Adding a small percentage of mud to a sandy bed has the most significant effect on erosion resistance. According to Mitchener and Torfs (1996) a transition occurs from non-cohesive to cohesive when 3% to 15% of mud (by weight) is added to sand. Van Ledden (2003) uses a 30% mud content in the bed for the transition between non-cohesive to cohesive behaviour.

C.3. INFLUENCE OF BIOTA ON EROSION OF COHESIVE SEDIMENTS

Biota is known to have an effect on the eroding characteristics of the bed (Winterwerp and Van Kesteren, 2004; Borsje et al., 2008). The first class are the 'biostabilisers' which enhance the strength of the bed. Field studies (amongst others in the Western Scheldt) and laboratory expermiments have shown that there is a significant correlation between sediment stability and the content of microphytobentos chlorofyll a which produce EPS (Extracellular Polymeric Substances), which in turn enhances the cohesiveness of the sediments (Widdows et al., 2000, 2004).

The second class are the 'bio-destabilisers' which destabilise the bed by bioturbation. One of the key bioturbators in the Western Scheldt and Humber estuary is the surface deposit feeding clam Macoma balthica. Field studies and controlled laboratory experiments have confirmed a significant relationship between the sediment erodability and the biomass of the Macoma balthica (Widdows et al., 2000, 2004). Van Prooijen et al. (2011) have set up a process-based model to calculate the erosion effect of the Macoma Balthica.

Generally the biological influence has a distinct seasonal scale. In the Western Scheldt a balance shift was observed on the intertidal area 'Molenplaat' between the 'biostabilisers' in the spring and summer to the 'bio-destabilisers' in autumn (Widdows et al., 2004).

A more long-term effect is the growth of vegetation, where they generally lower the velocities and enhance sediment trapping. Also the critical shear stress and erosion rate is affected.

For this research it is not specifically required to model the seasonal scale of mudflats since the focus is on decadal to century scale morphodynamics. If it is possible the model parameters that effect bed erosion will be chosen in such a way that they represent the long-term behaviour over years.

C.4. SAND-MUD SEGREGATION

As the critical shear stress for erosion is higher for sand than non-cohesive mud, sand is generally found in areas where tidal current velocities are high, while mud deposits where velocities are low. Due to a slower settling velocity the mud can travel for a long distance before it settles. Because of these different sediment characteristics there is a horizontal segregation between the sand and mud sediment in the field (Van Ledden, 2003). Furthermore alternating mud and sand layers are found when a vertical profile is taken in the field (Mitchener and Torfs, 1996), amongst other in the Western Scheldt. This is considered to be due to differential settling and sorting of the sediment involved.

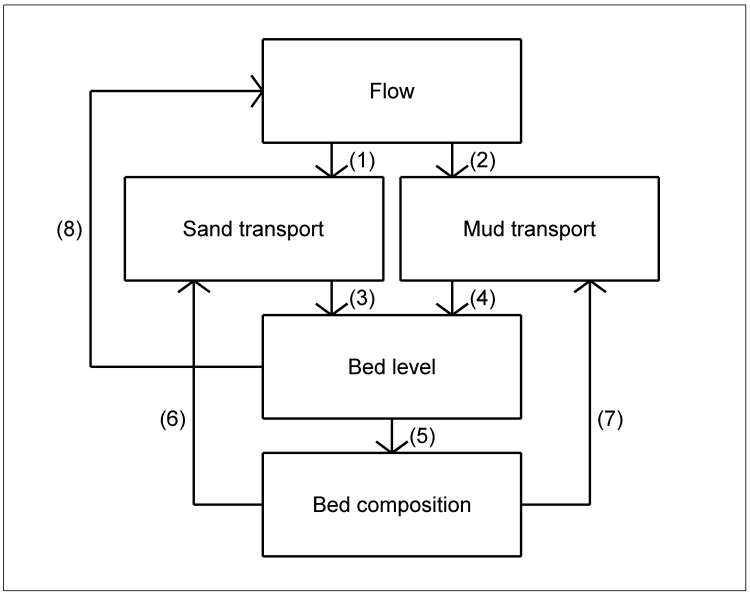

Figure C.1: Set-up of the sand-mud model (after Van Ledden (2003))

C.5. SET-UP OF THE SAND-MUD MODEL

Following Van Ledden et al. (2004a,b) in this research a sand-mud model will be used in which both sand and mud and their interaction contribute to morphological changes. Earlier research with a sand-mud model has been carried out by Van Ledden (2003); Van Ledden et al. (2004b); Paarlberg et al. (2005); Dam et al. (2005); Le Hir et al. (2011); Dam and Bliek (2011). The set-up of this model is shown in Figure C.1. There are a few reasons why this approach has advantages over a classical approach in which sand and mud are treated separately. The first reason is that both sand and mud contribute to morphological change (arrow 3 and 4 in Figure 3) and both fractions have a dynamic coupling with the water motion (arrow 8). The second reason is that the erosion of sediment is limited by the availability of sand or mud in the bed due to the bed module (arrow 6 and 7). The third reason is that the interaction between sand and mud in the bed is taken into account (also arrow 6 and 7). Non-cohesive behaviour of the bed occurs when the mud content in the bed is below a critical mud content. Cohesive behaviour of the bed occurs when the mud content is above this value. Cohesive behaviour will harden the bed, making it more difficult to erode. The two main variables to model the erosional behaviour are the critical erosion shear stress (τ_{cr}) and the erosion coefficient M (Tolhurst et al., 2000). Both the non-cohesive state and cohesive state are described in detail below.

C.5.1. NON-COHESIVE STATE OF THE BED

When the mud content in the bed (p_m) is below the critical mud content ($p_{m,cr}$) the bed layer is treated as non-cohesive. This implies for the sand fraction that the normal sediment transport formula is used, in this case the Engelund-Hansen formula (Engelund and Hansen, 1967). The Engelund-Hansen formula is used to calculate an equilibrium concentration c_e. If the sand concentration in that grid point is below the equilibrium concentration erosion occurs, if above, sedimentation. In this way the vertical flux of sand is described, see Equation C.1. However in case of erosion of sand from the bed the vertical flux is limited by the availability of sand in the bed which is described by the term $(1-p_m)$. Following Van Ledden et al. (2004b) the vertical flux of mud is described by Equation C.2, in which the first part describes the erosion flux (cf. Partheniadis (1965)) and the second part the deposition flux (cf. Krone (1962)).

Vertical sand and mud fluxes between water and non-cohesive bed ($p_m \leq p_{m,cr}$):

$$F_s = (1-p_m)\, w_s c_e - w_s c_s \tag{C.1}$$

$$F_m = p_m M_{nc} \left(\frac{\tau_b}{\tau_{e,nc}} - 1\right) H\left(1 - \frac{\tau_b}{\tau_{e,nc}}\right) - w_m c_m \left(1 - \frac{\tau_b}{\tau_d}\right) H\left(1 - \frac{\tau_b}{\tau_d}\right) \tag{C.2}$$

With:
F_s = vertical flux of sand $[kg/m^2/s]$
F_m = vertical flux of mud $[kg/m^2/s]$
w_s = fall velocity of sand $[m/s]$
w_m = fall velocity of mud $[m/s]$
c_s = sand concentration in the water column $[kg/m^3]$
c_e = equilibrium sand concentration in the water column $[kg/m^3]$
c_m = mud concentration in the water column $[kg/m^3]$
p_m = mud content of the top bed layer $[-]$
$p_{m,cr}$ = critical mud content for cohesive behaviour $[-]$
M_{nc} = erosion coefficient of non-cohesive bed $[kg/m^2/s]$
τ_b = bottom shear stress due to current and waves $[Pa]$
$\tau_{e,nc}$ = critical bottom shear stress for non-cohesive bed $[Pa]$
τ_d = critical shear stress for deposition of mud $[Pa]$
H = heaviside function; equals 0 if argument < 0; equals 1 if argument >= 0

The critical bottom shear stress for erosion $\tau_{e,nc}$ is given by (Van Ledden, 2003):

$$\tau_{e,nc} = \tau_{cr,s}(1+p_m)^{\beta} \; for \; p_m \leq p_{m,cr} \tag{C.3}$$

With:
$\tau_{cr,s}$ = critical bottom shear stress for sand $[Pa]$
β = emprical constant between 0.75 and 1.25 $[-]$

C.5.2. COHESIVE STATE OF THE BED

Cohesive sand-mud mixtures have erosion characteristics that strongly differ from non-cohesive sand-mud mixtures (e.g. Mitchener and Torfs, 1996). Therefore erosion of a cohesive bed is treated differently in the model by a separate erosion coefficient and critical shear stress for a cohesive bed. The key element is that the bed is treated as homogeneous, i.e. the erosion formula for sand and mud is equal, assuming an eroding sand-mud mixture; however the flux is further depending on the availability of sand or mud in the bed module. This is expressed in the first part of Equation C.4 and C.5 which denotes the erosion part (Van Ledden et al., 2004b). The second part of Equation C.4 and C.5 describes the deposition part and is equal to the non-cohesive state (Equation C.1 and C.2).

Vertical sand and mud fluxes between water and cohesive bed ($p_m > p_{m,cr}$)

$$F_s = (1-p_m)M_c\left(\frac{\tau_b}{tau_{e,c}}-1\right)H\left(\frac{\tau_b}{tau_{e,c}}\right) \tag{C.4}$$

$$F_m = p_m M_c\left(\frac{\tau_b}{\tau_{e,c}}-1\right)H\left(1-\frac{\tau_b}{\tau_{e,c}}\right) - w_m c_m\left(1-\frac{\tau_b}{\tau_d}\right)H\left(1-\frac{\tau_b}{\tau_d}\right) \tag{C.5}$$

With:
M_c = erosion coefficient of cohesive bed $[kg/m^2/s]$
$\tau_{e,c}$ = critical bottom shear stress for cohesive bed $[Pa]$

The erosion parameter M_c is obtained by interpolating the erosion parameter for the non-cohesive regime M_{nc} and the erosion parameter for the fully mud regime M_e by:

$$M_c = M_e\left(\frac{M_{nc}}{1-p_{m,cr}}\frac{1}{M_e}\right)^{\frac{1-p_m}{1-p_{m,cr}}} \tag{C.6}$$

The critical bottom shear stress for erosion $\tau_{e,c}$ is also linearly interpolated in the same way:

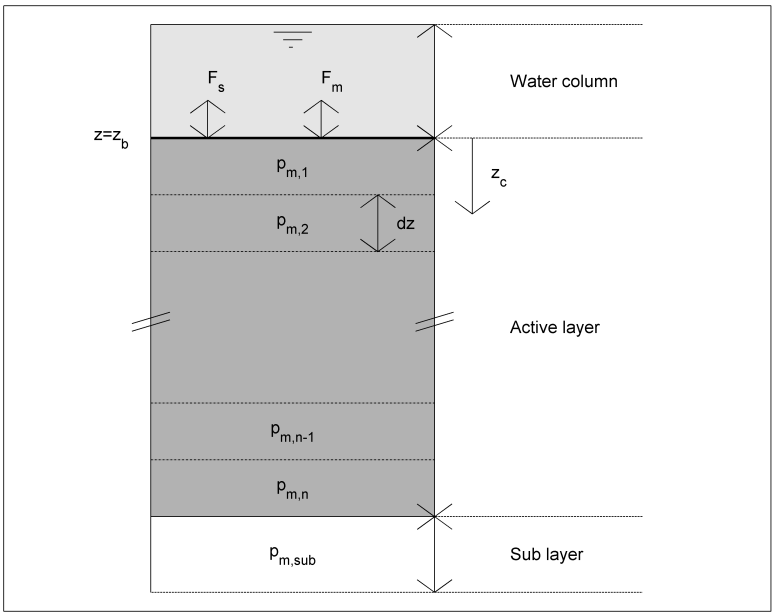

Figure C.2: Bed module (after Van Ledden (2003))

$$\tau_{e,cr} = \left[\frac{\tau_{s,cr}(1-p_{m,cr})^{\beta} - \tau_{m,cr}}{1-p_{m,cr}} \right] (1-p_m) + \tau_{m,cr} \tag{C.7}$$

Although it is not implemented yet in sand/mud models it would be interesting to look at the effect of a hydraulic roughness predictor based on the amount of mud in the bed. Baas et al. (2013) find that ripples generally decrease when the mud content in the bed increase, which effectively means less hydraulic roughness. Van Rijn (1993) finds that the flow over a cohesive bed is generally hydraulically smooth with relatively large Chézy values in the range of 60-100 $m^{0.5}/s$. The effective bed roughness height is in the range of 0.1 to 1mm.

C.5.3. BED MODULE

A bed module consisting of several layers of the sea bed is accounting for the sand/mud content of the bed. In Figure C.2 the bed module is given schematically. A number of layers (n) are defined below the sea bed with thickness dz.

Using a Lagrangian coordinate system the layers move up and down following the bed

level changes while maintaining a fixed thickness dz. The bed composition of the layers varies in time and space, induced by upward and downward fluxes of sand and mud at the bed surface, physical and biological mixing in the sediment layers below. The mud content in the bed is thus described by Formula C.8. A mixing coefficient is introduced to account for the physical and biological mixing. Physical mixing occurs when the bed is stirred by flow and or waves. Biological mixing consists of organisms that move through the bed and mix the sediments (Van Ledden, 2003).

$$\frac{\partial p_m}{\partial t} + \frac{\partial z_b}{\partial t}\frac{\partial p_m}{\partial z_c} - \frac{\partial}{\partial z_c}\left(\Xi \frac{\partial p_m}{\partial z_c}\right) \tag{C.8}$$

With:
z_b = vertical co-ordinate of bed surface $[m]$
Ξ = mixing coefficient $[m^2/s]$
z_c = distance below the bed surface z_b (positive downwards) $[m]$

In the sub-layer a fixed mud percentage ($p_{m,sub}$) must be applied. This mud percentage becomes important in an eroding case. In that case this sub layer mud percentage is introduced in the lowest layers. See for more information of the bed module and the numerical implementation of the bed module Van Ledden (2003).

CURRICULUM VITÆ

Gerrit DAM

05-01-1975	Born in Dokkum, The Netherlands.

EDUCATION

1987–1993	VWO CSG Oostergo, Dokkum, The Netherlands
1993–1998	Civil Engineering & Management Twente University, The Netherlands

AWARDS

2013	Student presentation award, Coastal Dynamics Conference, Archachon, France
2014	Halcrow prize for best publication in Maritime Engineering. Institute of Civil Engineers (ICE), London, United Kingdom

WORK EXPERIENCE

1999–2014	Svašek Hydraulics, Rotterdam, The Netherlands
2014–2018	Dam Engineering, Bergen, Norway
2018–2022	Asplan Viak, Bergen, Norway
2022–present	COWI, Bergen, Norway

List of Publications

Peer reviewed articles

11. **G. Dam, M. van der Wegen** (2024), *Contrasting behavior of sand and mud in a centenial timescale morphodynamic model of the Western Scheldt*, Submitted to Marine Geology.

10. **G. Dam, M. van der Wegen, M. Taal, A. van der Spek** (2022), *Contrasting behaviour of sand and mud in a long-term sediment budget of the Western Scheldt estuary*, Sedimentology, **69**, 3.

9. **G. Dam, M. van der Wegen, R.J. Labeur, D. Roelvink** (2016), *Modeling centuries of estuarine morphodynamics in the Western Scheldt estuary*, Geophysical Research Letters, **43**, pp. 3839-3847.

8. **G. Dam, A.J. Bliek** (2013), *Using a sand-mud model to hindcast the morphology near Waarde, The Netherlands*, Maritime Engineering, **166**, 2, pp. 63-75.

Conference proceedings

7. **G. Dam, M. Van der Wegen, D. Roelvink, R.J. Labeur, A.J. Bliek** (2015), *Simulation of long-term morphodynamics of the Western-Scheldt estuary*, Proceedings of the IAHR Conference, The Hague, The Netherlands.

6. **G. Dam, M. Van der Wegen, D. Roelvink** (2013), *Long-term performance of process-based morphological models in estuaries*, Proceedings of the Coastal Dynamics conference, Arcachon, France.

5. **G. Dam, S.E. Poortman, A.J. Bliek, Y. Plancke** (2013), *Long-term modeling of the impact of dredging strategies on morpho- and hydrodynamic developments in the Western Scheldt*, Proceedings of the 20th WODCON conference, Brussels, Belgium.

4. **G. Dam, A.J. Bliek** (2011), *Hindcasting the morphological impact of 2 dams in the Western Scheldt using a sand-mud model*, Proceedings of the 7th River, Coastal and Estuarine Morphodynamics conference, Bejing, China.

3. **G. Dam, A.J. Bliek, G.J. Nederbragt** (2009), *High resolution long term morphological model of the northern part of the Holland Coast and Texel Inlet*, Proceedings of the 6th River, Coastal and Estuarine Morphodynamics conference, Santa Fe, Argentina.

2. **G. Dam, A.J. Bliek, R.J. Labeur, S. Ides, Y. Plancke** (2009), *Long-term process based morphological model pf the Western Scheldt Estuary*, Proceedings of the 5th River, Coastal and Estuarine Morphodynamics conference, Enschede, The Netherlands.

1. **G. Dam, A.J. Bliek, A.W. Bruens** (2005), *Band width analysis morphological prediction Haringvliet Estuary*, Proceedings of the 4th River, Coastal and Estuarine Morphodynamics conference, Illinois, USA.

IHE DELFT
Institute for Water Education
under the auspices of UNESCO

TU Delft Delft University of Technology

Estuaries are located where freshwater river flow meets ocean saltwater in an environment of channels, shoals, intertidal flats and vegetated area, like salt marshes or mangrove belts. They comprise both unique ecosystems and economic values such as navigational gateways to ports. Estuaries face significant challenges from morphological changes caused by natural and human activities such as land reclamation and dredging. In addition, rising sea levels threaten tidal flats and biodiversity.
This research investigates centennial timescale morphodynamic developments in the Western Scheldt by means of a process-based model (FINEL2d). The model demonstrates good skill in hindcasting morphodynamic changes uniquely observed between 1860 and 1970. Analysis of sub-surface sediment composition and bathymetric data reveals a trend of historic sand export and mud import with the estuary narrowing and deepening over time supported by model results. Model simulations further suggest that, on a centennial timescale, morphodynamic developments evolve towards equilibrium. This study shows that dredging and historic land reclamation have significantly altered morphodynamic evolution of the Western Scheldt estuary. It demonstrates both the significant impact of human interferences and the potential for designing sustainable management strategies to preserve a combination of vital ecosystems and economic values in the face of ongoing climate change.

This book is printed on paper from sustainably managed forests and controlled sources